USGS
science for a changing world

Three-Dimensional Numerical Model of Ground-Water Flow in Northern Utah Valley, Utah County, Utah

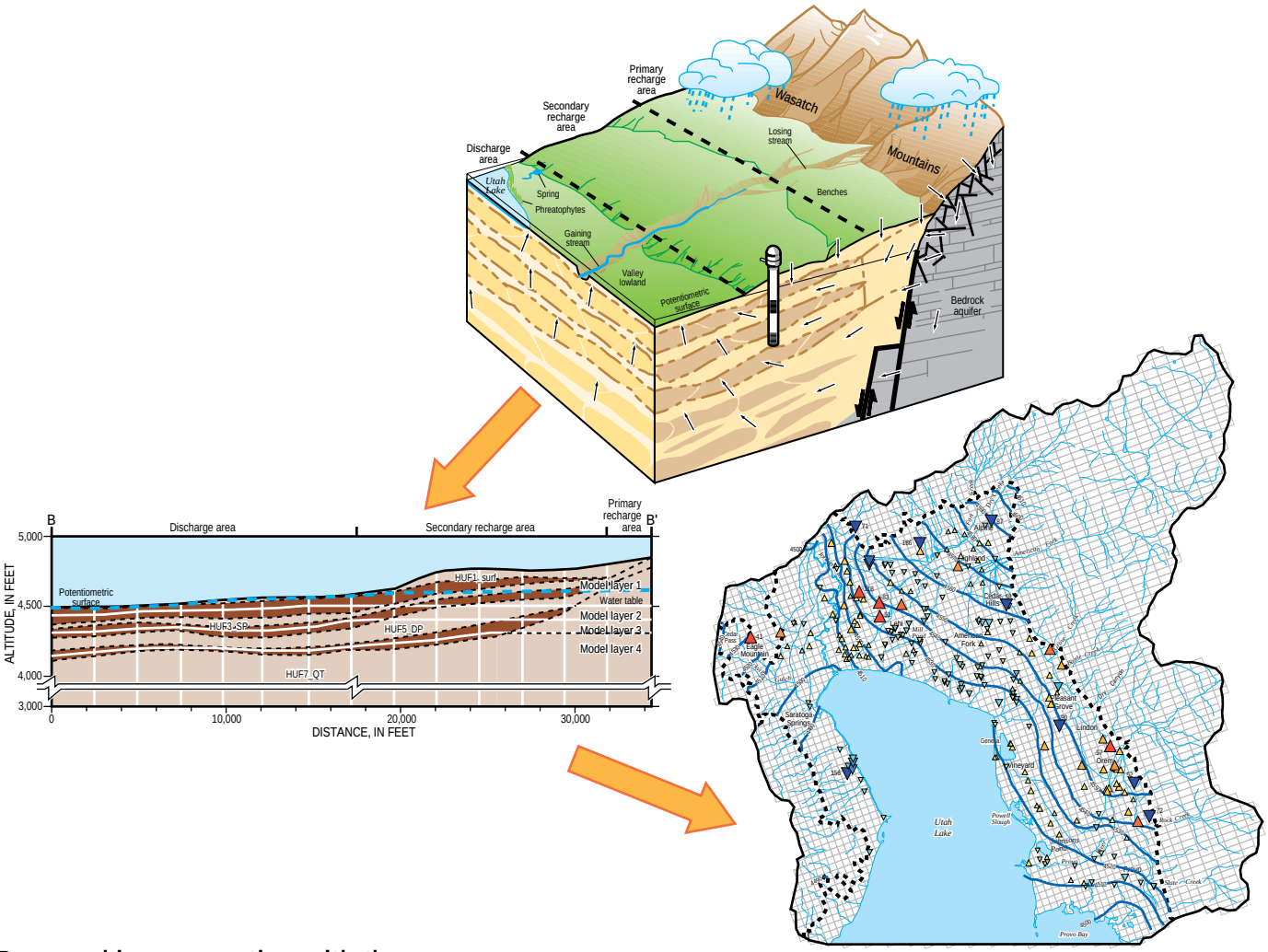

Prepared in cooperation with the
Central Utah Water Conservancy District; Jordan Valley Water Conservancy District representing Draper City; Highland Water Company; Utah Department of Natural Resources, Division of Water Rights; and the municipalities of Alpine, American Fork, Cedar Hills, Eagle Mountain, Highland, Lehi, Lindon, Orem, Pleasant Grove, Provo, Saratoga Springs, and Vineyard

Scientific Investigations Report 2008–5049

Version 2.0, January 2011

U.S. Department of the Interior
U.S. Geological Survey

Three-Dimensional Numerical Model of Ground-Water Flow in Northern Utah Valley, Utah County, Utah

By Philip M. Gardner

Prepared in cooperation with the
Central Utah Water Conservancy District; Jordan Valley Water Conservancy District representing Draper City; Highland Water Company; Utah Department of Natural Resources, Division of Water Rights; and the municipalities of Alpine, American Fork, Cedar Hills, Eagle Mountain, Highland, Lehi, Lindon, Orem, Pleasant Grove, Provo, Saratoga Springs, and Vineyard

Scientific Investigations Report 2008–5049
Version 2.0, January 2011

U.S. Department of the Interior
U.S. Geological Survey

U.S. Department of the Interior
DIRK KEMPTHORNE, Secretary

U.S. Geological Survey
Mark D. Myers, Director

U.S. Geological Survey, Reston, Virginia: 2009
Version 2.0, January 2011

For additional information write to:
U.S. Geological Survey
Director, Utah Water Science Center
2329 W. Orton Circle
Salt Lake City, UT 84119-2047
Email: GS-W-UTpublic-info@usgs.gov
URL: http://ut.water.usgs.gov/

For more information about the USGS and its products:
Telephone: 1-888-ASK-USGS
World Wide Web: http://www.usgs.gov/

Suggested citation:

Gardner, P.M., 2009, Three-dimensional numerical model of ground-water flow in northern Utah Valley, Utah County, Utah: U.S. Geological Survey Scientific Investigations Report 2008–5049, 95 p.

Contents

Figures

Tables

Conversion Factors and Datums

Multiply	By	To obtain
Length		
foot (ft)	0.3048	meter (m)
mile (mi)	1.609	kilometer (km)
Area		
acre	0.004047	square kilometer (km^2)
square mile (mi^2)	2.590	square kilometer (km^2)
Volume		
acre-foot (acre-ft)	1,233	cubic meter (m^3)
Flow rate		
acre-foot per year (acre-ft/yr)	1,233	cubic meter per year (m^3/yr)
foot per day (ft/d)	0.3048	meter per day (m/d)
gallon per minute (gal/min)	0.06309	liter per second (L/s)
inch per year (in/yr)	25.4	millimeter per year (mm/yr)
Hydraulic conductivity		
foot per day (ft/day)	0.3048	meter per day (m/d)

Temperature in degrees Celsius (°C) may be converted to degrees Fahrenheit (°F) as follows:

$$°F=(1.8×°C)+32.$$

Temperature in degrees Fahrenheit (°F) may be converted to degrees Celsius (°C) as follows:

$$°C=(°F-32)/1.8.$$

Vertical coordinate information is referenced to the North American Vertical Datum of 1988 (NAVD 88). Altitude, as used in this report, refers to distance above the vertical datum. Horizontal coordinate information is referenced to the North American Datum of 1983 (NAD 83).

The system of numbering wells, springs, and other hydrologic-data sites in Utah is based on the cadastral land-survey system of the U.S. Government. The number, in addition to designating the site, describes its position in the land net. By the land-survey system, the State is divided into four quadrants by the Salt Lake Base Line and the Salt Lake Meridian. These quadrants are designated by the uppercase letters A, B, C, and D, indicating the northeast, northwest, southwest, and southeast quadrants, respectively. Numbers designating the township and range, in that order, follow the quadrant letter, and all three are enclosed in parentheses. The number after the parentheses indicates the section and is followed by three letters indicating the quarter section, the quarter-quarter section, and the quarter-quarter-quarter section — generally 10 acres for regular sections[1]. The lowercase letters a, b, c, and d indicate, respectively, the northeast, northwest, southwest, and southeast quarters of each subdivision. The number after the letters is the serial number of the site within the 10-acre tract. The letter S preceding the serial number designates a spring. Thus, (C-5-1)25cdc-1 designates the first well constructed or visited in the southwest 1/4 of the southeast 1/4 of section 25, T. 5 S., R. 1 W. The numbering system is illustrated below.

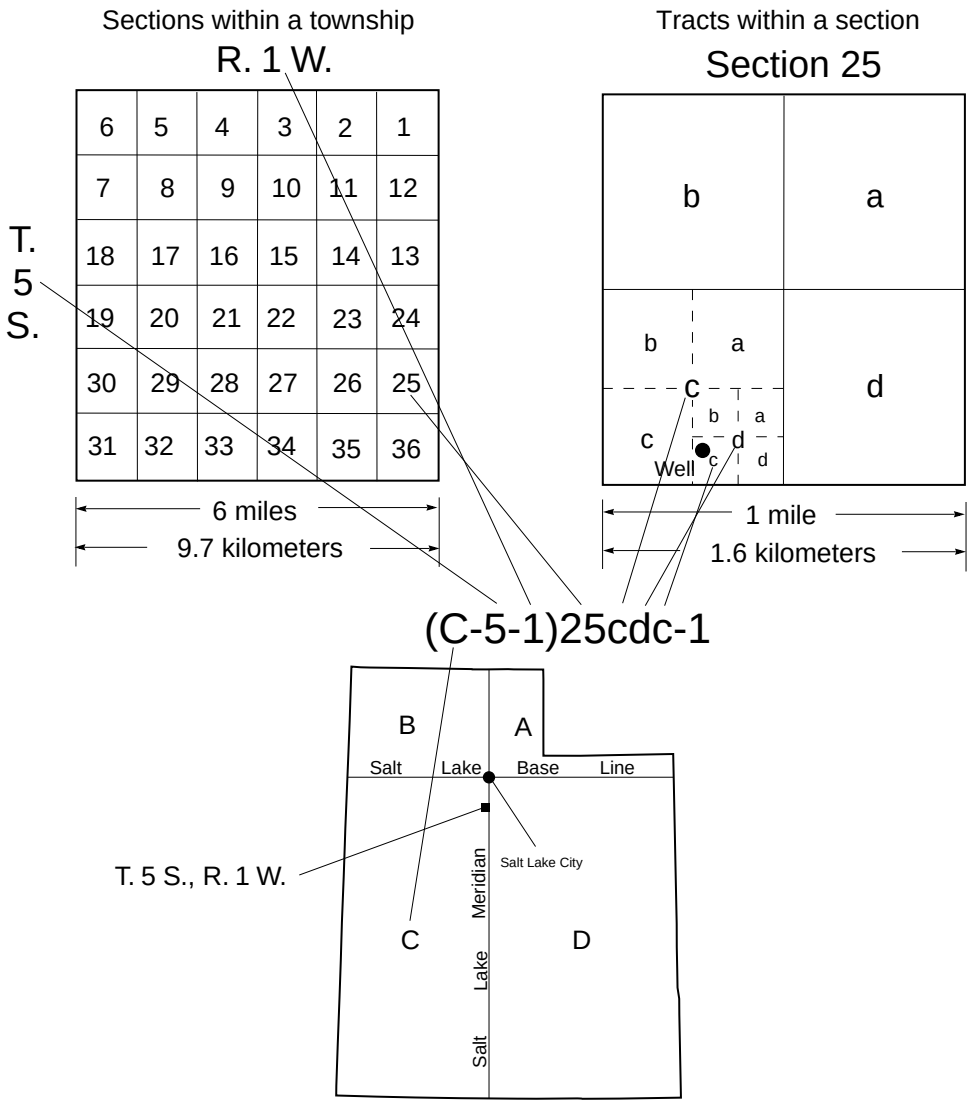

[1]Although the basic land unit, the section, is theoretically 1 square mile, many sections are irregular. Such sections are subdivided into 10-acre tracts, generally beginning at the southeast corner, and the surplus or shortage is taken up in the tracts along the north and west sides of the section.

Three-Dimensional Numerical Model of Ground-Water Flow in Northern Utah Valley, Utah County, Utah

By Philip M. Gardner

Abstract

A three-dimensional, finite-difference, numerical model was developed to simulate ground-water flow in northern Utah Valley, Utah. The model includes expanded areal boundaries as compared to a previous ground-water flow model of the valley and incorporates more than 20 years of additional hydrologic data. The model boundary was generally expanded to include the bedrock in the surrounding mountain block as far as the surface-water divide. New wells have been drilled in basin-fill deposits near the consolidated-rock boundary. Simulating the hydrologic conditions within the bedrock allows for improved simulation of the effect of withdrawal from these wells. The inclusion of bedrock also allowed for the use of a recharge model that provided an alternative method for spatially distributing areal recharge over the mountains.

The model was calibrated to steady- and transient-state conditions. The steady-state simulation was developed and calibrated by using hydrologic data that represented average conditions for 1947. The transient-state simulation was developed and calibrated by using hydrologic data collected from 1947 to 2004. Areally, the model grid is 79 rows by 70 columns, with variable cell size. Cells throughout most of the model domain represent 0.3 mile on each side. The largest cells are rectangular with dimensions of about 0.3 by 0.6 mile. The largest cells represent the mountain block on the eastern edge of the model domain where the least hydrologic data are available. Vertically, the aquifer system is divided into 4 layers which incorporate 11 hydrogeologic units. The model simulates recharge to the ground-water flow system as (1) infiltration of precipitation over the mountain block, (2) infiltration of precipitation over the valley floor, (3) infiltration of unconsumed irrigation water from fields, lawns, and gardens, (4) seepage from streams and canals, and (5) subsurface inflow from Cedar Valley. Discharge of ground water is simulated by the model to (1) flowing and pumping wells, (2) drains and springs, (3) evapotranspiration, (4) Utah Lake, (5) the Jordan River and mountain streams, and (6) Salt Lake Valley by subsurface outflow through the Jordan Narrows.

During steady-state calibration, variables were adjusted within probable ranges to minimize differences between model-computed and measured water levels as well as between model-computed and independently estimated flows that include: recharge by seepage from individual streams and canals, discharge by seepage to individual streams and the Jordan River, discharge to Utah Lake, discharge to drains and springs, discharge by evapotranspiration, and subsurface flows into and out of northern Utah Valley from Cedar Valley and to Salt Lake Valley, respectively. The transient-state simulation was calibrated to measured water levels and water-level changes with consideration given to annual changes in the flows listed above.

Introduction

Northern Utah Valley is located on the west side of the Wasatch Mountains along the Wasatch Front in north-central Utah, about 30 mi south of Salt Lake City (fig. 1). The 428 mi^2 study area includes about 250 mi^2 of unconsolidated basin-fill deposits in the northern half of Utah Valley surrounded by the contributing mountain watersheds. The valley is experiencing a period of rapid population growth and an associated change from agricultural to urban and residential land uses. Ground water is the primary source of municipal water within northern Utah Valley. The increased population growth coupled with recent drought conditions has increased the demand for municipal and industrial supplies from ground-water resources. Water levels generally declined in northern Utah Valley from March 1975 to March 2005 and this is likely a response to increased ground-water withdrawals (Burden, 2004, p. 38). Understanding the effects of natural and anthropogenic stresses on the ground-water system is essential for water managers to maintain adequate supplies of water suitable for domestic use while minimizing the adverse effects of drawdown throughout the valley. State and other water-management officials require detailed information regarding the sources and subsurface pathways of ground water to anticipate potential changes in water quality and supply and to best manage the development of the ground-water system.

In July of 2003, the U.S. Geological Survey (USGS), in cooperation with the Central Utah Water Conservancy District;

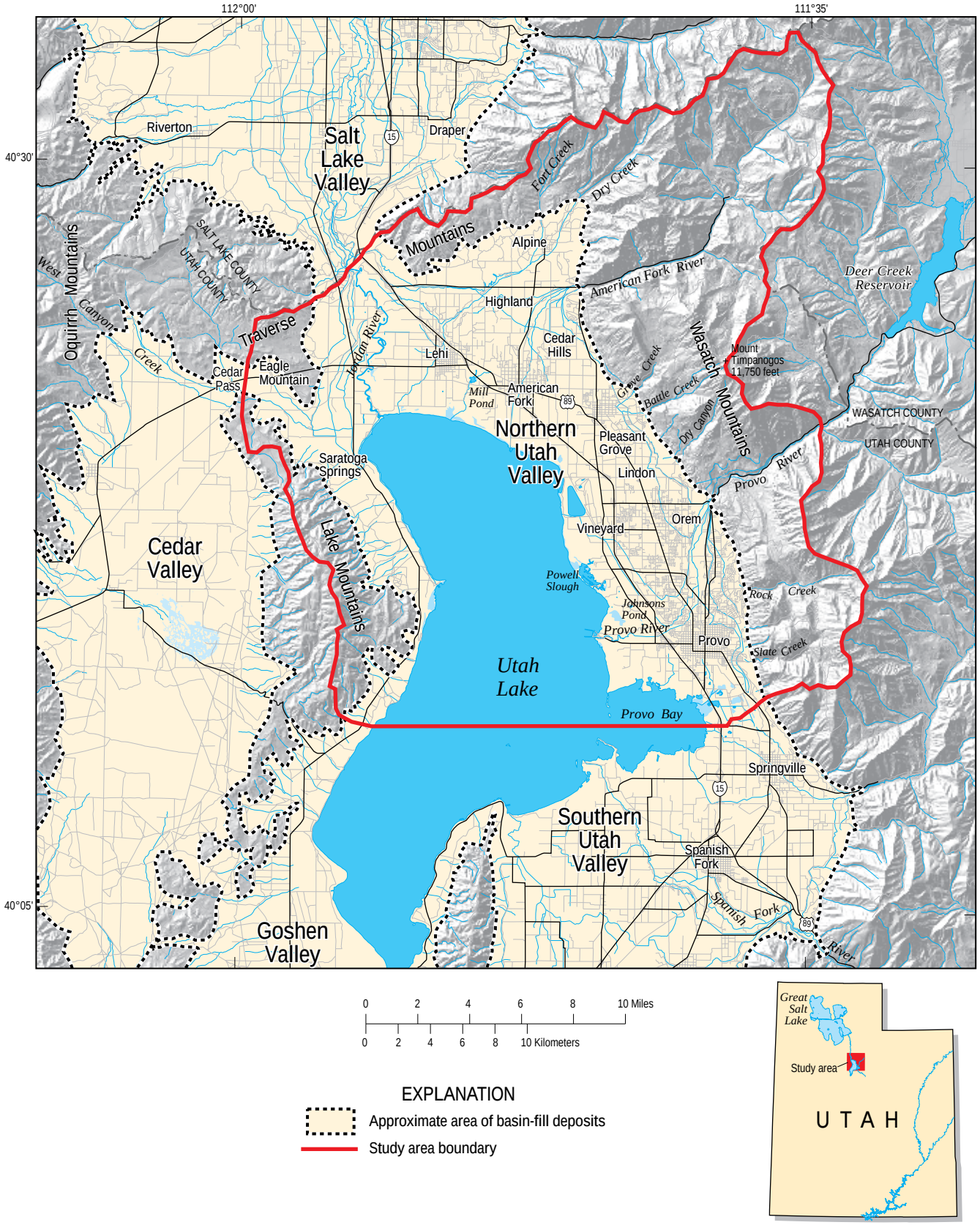

Figure 1. Location of northern Utah Valley study area, Utah County, Utah.

Jordan Valley Water Conservancy District representing Draper City; Highland Water Company; Utah Department of Natural Resources, Division of Water Rights; and the municipalities of Alpine, American Fork, Cedar Hills, Eagle Mountain, Highland, Lehi, Lindon, Orem, Pleasant Grove, Provo, Saratoga Springs, and Vineyard began a study of the ground-water flow system in northern Utah Valley. The objectives of the study were to (1) develop an improved understanding of the ground-water flow system and its relation to ground water in adjacent areas of bedrock and to Utah Lake and (2) provide water managers, State and local governments, and other interested parties with information and tools to help refine the water budget of the ground-water system, and to estimate what effects future ground-water development and management may have on water levels, water quality, and ground-water discharge in northern Utah Valley. Meeting the objectives of the study required the development and calibration of a new three-dimensional ground-water flow model of northern Utah Valley. This report documents the development and calibration of that model. A previous numerical ground-water flow model for northern Utah Valley was based largely on data collected by Appel and others (1982) for 1981 and 1982, a period of greater-than-normal precipitation, and calibrated to water levels from 1947 to 1981 (Clark, 1984). The updated and aerially expanded numerical model that is described in this report incorporates more than 20 years of additional hydrologic data and is based on an updated conceptual model presented by Cederberg and others (2009).

Purpose and Scope

This report documents the development and calibration of a three-dimensional, finite-difference, numerical model to simulate ground-water flow in basin-fill deposits in northern Utah Valley and the surrounding bedrock mountain block (fig. 1). The ground-water flow model described in this report can be used to evaluate the movement of ground water, the effects of water use on ground-water levels, and changes to the ground-water budget. This report describes the numerical ground-water flow model in conjunction with a report by Cederberg and others (2009) which describes the hydrogeology of northern Utah Valley, including recent data collection, data interpretation, and conceptual model development. This report also includes assessments of the ability of the numerical model to sufficiently reproduce observed hydrologic conditions and limitations of the model as an accurate representation of the ground-water flow system.

Hydrogeology

The hydrogeology of northern Utah Valley has been previously described in detail by Hunt and others (1953), Cordova and Subitzky (1965), and Clark and Appel (1985). Brooks and Stolp (1995) evaluated and modeled the ground-water system of southern Utah and Goshen Valleys to the south and Feltis (1967) evaluated the ground-water system of Cedar Valley to the west of the northern Utah Valley model area boundary. A detailed description of the current understanding of the hydrogeology of northern Utah Valley is presented in Cederberg and others (2009). The following is a summary based mainly on information from that report.

Northern Utah Valley is a north-south trending structural graben located along the eastern edge of the Basin and Range Physiographic Province. The center of the valley is occupied by Utah Lake, a large (about 150 mi^2), shallow (9.5 ft average depth) natural freshwater lake that covers about 69 of the 240 mi^2 of basin-fill deposits in the northern Utah Valley study area (fig. 2). The Jordan River is the natural outlet for Utah Lake and carries water from the northwestern end of the lake through the Jordan Narrows and into Salt Lake Valley. The valley is bounded by the Wasatch Mountains on the east, the Traverse Mountains on the north and the Lake Mountains on the west (fig. 2). Sediment eroded from the surrounding mountains is the source of the Tertiary- and Quaternary-age deposits that fill the basin and form the valley floor. The Wasatch Fault zone forms the eastern boundary between the valley and uplifted mountain block. The transition from basin-fill deposits in the valley to bedrock in the mountain block is abrupt across this zone of normal faults (figs. 2 and 3). Wells drilled in basin-fill deposits near the Wasatch Fault zone rarely encounter bedrock, even at depths of more than 1,000 ft. The maximum thickness of basin fill in northern Utah Valley is unknown; however, multiple wells that are finished in fill north and east of Utah Lake have been drilled to depths of 1,000 to 1,600 ft. The deepest well in Utah Valley is an oil test well near Spanish Fork (in southern Utah Valley) that is completed in Tertiary-age sediments at a depth of about 13,000 ft (Dustin and Merritt, 1980, p. 15). The west side of the valley is separated from the east side by a broad zone of north-south trending normal faults that have been mapped beneath Utah Lake (Hecker, 1993; Beik, 2005) and distinguished by areas of much shallower bedrock (figs. 2 and 3) (Cederberg and others, 2009). Wells drilled in basin-fill deposits between the Lake Mountains and the west side of Utah Lake have encountered fractured limestone at depths between 150 and 300 ft.

Current ground-water resources in northern Utah Valley consist of aquifers in both bedrock and unconsolidated basin-fill deposits. Productive bedrock aquifers exist in highly fractured limestone and quartzite in the surrounding mountains and beneath basin–fill deposits in the northern and western parts of the valley. Bedrock aquifers are increasingly being developed as sources of ground water for irrigation, industrial, and municipal supply near the Jordan Narrows and west of the Jordan River where they exist at shallow to moderate depths (as much as several hundred feet) beneath basin-fill deposits.

The principal ground-water system in northern Utah Valley is in the basin-fill deposits and is characterized by coarse-grained sediments (boulders, cobbles, gravel, and sand) near the mountain front that grade into predominantly finer-grained material (silt and clay) near the center of the valley. Fine-grained clays and silts are mostly absent near the

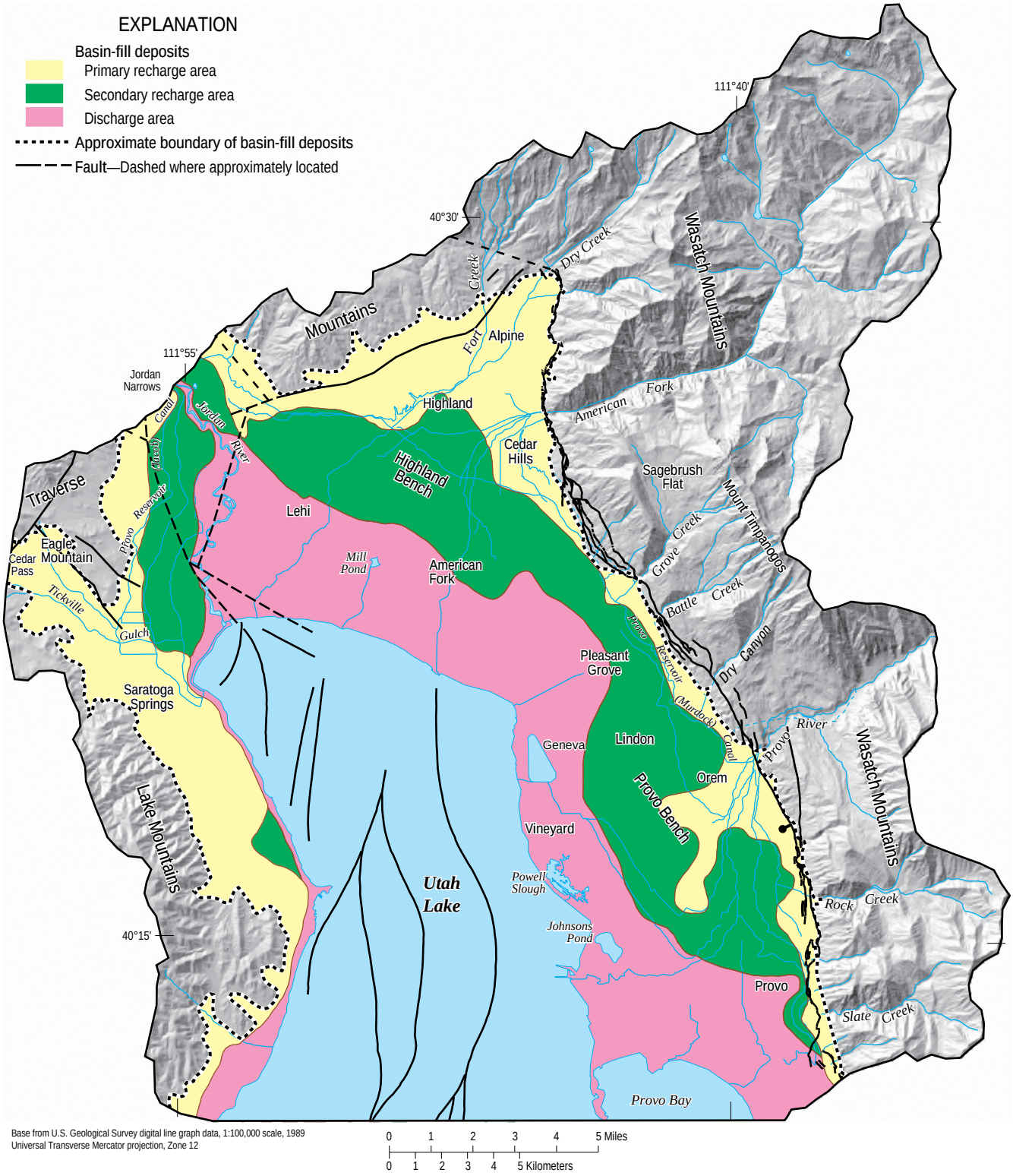

Figure 2. Location of important conceptual components of the ground-water flow system used to construct the ground-water flow model of northern Utah Valley, Utah.

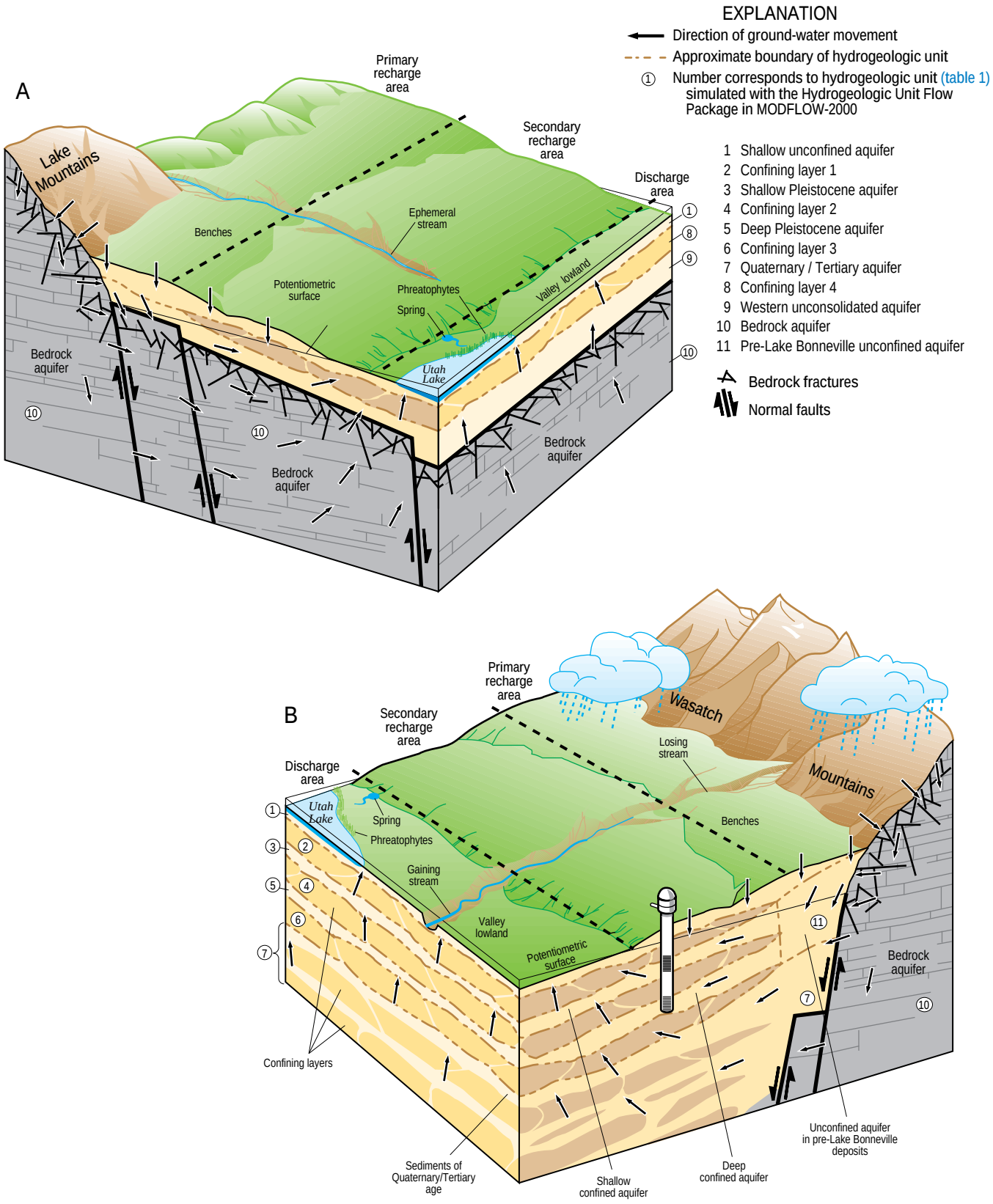

Figure 3. Conceptual components of the ground-water flow system on the (A) western and (B) eastern parts of the valley used to construct the ground-water flow model of northern Utah Valley, Utah.

valley margins, allowing water from streams flowing out of the mountains to infiltrate through the coarse sediments and recharge the aquifer. Large lakes, including Lake Bonneville, have intermittently covered much of northern Utah Valley during the Quaternary and Tertiary Periods. During periods when lakes covered the valley, fine-grained lacustrine sediments were deposited throughout the basin. When lakes receded or dried, lacustrine sediments were subject to erosion from streams and coarser-grained material was deposited in alluvial fans and stream channels emanating from the adjacent mountains. This repeated sequence of depositional environments resulted in the interlayered lacustrine and alluvial sediments that fill the valley today (fig. 3).

Richardson (1906) was the first to recognize separate confined aquifers in northern Utah Valley when he noticed different water levels in nearby wells that were completed at different depths. Hunt and others (1953) distinguished three confined aquifers in the basin-fill deposits on the eastern side of northern Utah Valley on the basis of relative depth and suspected age. The naming convention applied to these aquifers from shallow to deep is as follows: the shallow confined aquifer in deposits of Pleistocene age (SP aquifer), the deep confined aquifer in deposits of Pleistocene age (DP aquifer), and the confined aquifer in deposits of Quaternary/Tertiary age (QT aquifer). For the purposes of this report, the confining units that separate these aquifers are referred to as confining units 1 through 3 (CF1 – CF3) (fig. 3). All three of the confined aquifers are lateral extensions of an unconfined aquifer near the mountain front that consists mostly of deposits that predate Lake Bonneville and is referred to as the unconfined aquifer in Pre-Lake Bonneville deposits (PLB aquifer) (fig. 3b).

A shallow unconfined aquifer overlies the shallow confining layer across most of the valley. The aquifer is composed mostly of fine-grained sediments deposited during and after the time of Lake Bonneville and in some areas cannot be differentiated from the underlying confining layer. Ground water is perched in areas where the water level in the underlying aquifer is below the bottom of the shallow confining layer and an unsaturated zone exists between the water table in the underlying aquifer and the body of perched water above it. Although these areas of perched ground water occasionally yield small amounts of water used for local irrigation, they are not used for municipal or industrial purposes and are not simulated with the numerical ground-water model.

Wells located west of the Jordan River indicate a somewhat different system of valley aquifers in that area. Because of differences in lithologic characteristics and water quality west of the faulted area beneath Utah Lake and near the Jordan River, basin-fill aquifers on the west side of the valley are designated separately (Cederberg and others, 2009). One confining layer (CF4), generally present at less than 50 ft below land surface, separates the shallow unconfined aquifer from the underlying western unconsolidated (WU) aquifer (fig. 3a). The unconsolidated basin-fill deposits on the western side of the valley form the WU aquifer that is confined near Utah Lake and the Jordan River and unconfined near the Traverse and Lake Mountains and in the Cedar Pass area to the west. The WU aquifer overlies a fractured-limestone bedrock aquifer at depths of around 150 to 300 ft between the north end of the Lake Mountains and the western shore of Utah Lake. Relatively few wells with lithologic data were available west of the Jordan River at the time of this study. As a result, little is known about the extent of this bedrock aquifer and its connection to the overlying WU aquifer. The boundary between the WU/bedrock aquifers on the west and the SP/DP/QT aquifer system to the east is uncertain, but is interpreted to coincide with the faulted zone beneath Utah Lake that extends north to the Jordan Narrows (fig. 2). Although faulting may be the primary mechanism separating the WU aquifer from those on the east side of the valley, different parent materials sourced from mountains on opposite sides of the basin also may be a factor.

Anderson and others (1994) divided the valley into a primary recharge area, a secondary recharge area, and a discharge area (figs. 2 and 3). Most ground-water recharge to the basin-fill aquifers occurs in the primary recharge area along the valley margins near the mountain front where the unsaturated zone is generally hundreds of feet thick and confining layers are absent. The secondary recharge area, farther from the mountains, is where confining layers are present but a downward hydraulic gradient exists between the upper unconfined and the lower confined aquifers (fig. 3). The discharge area is located near the valley center, where hydraulic heads in the confined aquifers are generally above the altitude of the land surface and vertical hydraulic gradients are generally upward.

Recharge to the ground-water flow system primarily is from infiltration of precipitation over the mountains and on the valley floor, seepage from streams and canals, infiltration of unconsumed water from irrigated fields, lawns, and gardens, and subsurface inflow from Cedar Valley. Some of the recharge that originates as infiltration of precipitation over the mountain block is discharged as base flow in perennial mountain streams and springs, and the remainder enters the basin-fill aquifer system as subsurface inflow. Infiltration of precipitation on the valley floor, seepage from streams and canals, and infiltration of unconsumed irrigation water is not simulated in regions outside of the primary recharge area where fine-grained material impedes the downward movement of water. Ground water in the basin-fill aquifer system moves from the deep unconfined aquifer in the primary recharge areas near the valley margins toward the discharge area surrounding Utah Lake and the Jordan River (figs. 2 and 3). As ground water moves laterally toward the center of the valley from all directions, substantial upward vertical hydraulic gradients are developed within the confined aquifers. In the discharge area, ground water moves upward through overlying confining layers. Discharge from the basin-fill aquifer system occurs through drains and springs surrounding Utah Lake, through wells, by evapotranspiration (ET) and upward seepage into Utah Lake and the Jordan River, and by subsurface outflow through the Jordan Narrows.

Modeling Approach

The ground-water flow model was developed using MODFLOW-2000 (Harbaugh and others, 2000; and Hill and others, 2000) to simulate the regional flow system in the basin-fill deposits and surrounding bedrock in northern Utah Valley, Utah. Development of the model included compilation and examination of water-level, streamflow, and ground-water withdrawal data and estimation of the spatial distribution of recharge, discharge, hydraulic conductivity, specific storage, and specific yield. The modular design of MODFLOW-2000 uses packages to represent the various components of the ground-water flow system, such as recharge, well withdrawal, and interactions between the aquifer and surface-water bodies. The "Model Construction" section of this report discusses the details of discretization, boundary conditions, and model parameters. The "Model Calibration" section discusses how the model was changed to match measured water levels, streamflow, and drain and spring discharge data, and how adequately the model simulates the ground-water system. The terms "observed" and "observation" are used to define water-level and discharge data used as observations in the ground-water flow model (Hill and others, 2000, p. 23).

The model was calibrated to steady-state and transient-state conditions. Steady-state conditions exist when the volume of water flowing into the system is equal to the volume flowing out. The steady-state simulation was developed using data from 1947, a year when the ground-water system was assumed to be approximately at steady state. Water levels generally rose during 1935–46 and then remained relatively stable until 1952 (Clark and Appel, 1985, fig. 38). Precipitation, streamflow, and lake-level data all indicate that hydrologic conditions were near the 1947–2004 average during 1947 (fig. 4). Ground-water withdrawals prior to 1947 primarily were from flowing wells in the center of the valley. Annual ground-water discharge from wells is assumed to have been about 30,000 acre-ft in 1947 according to flowing well measurements made during 1938–40 (Hunt and others, 1953, p. 73) and 1981–82 (Clark and Appel, 1985, p. 71).

The transient-state simulation was developed by using hydrologic data for 1947–2004. The results of the steady-state calibration were used as initial conditions for the transient-state simulation. The transient-state simulation incorporates annual variations in recharge from different sources, withdrawals by pumpage, and changing lake levels at Utah Lake. During the calibration, model-simulated water levels were compared to measured water levels for each stress period and simulated flow rates at model boundaries were compared to measured or independently estimated components of the conceptual ground-water budget.

Model Construction

Construction of the ground-water flow model was accomplished by discretizing the conceptual ground-water system; establishing model boundaries that represent conceptual hydrologic boundaries; determining recharge, ground-water withdrawal, and natural discharge rates for the steady-state simulation and each stress period of the transient simulation; and assigning model parameters to recharge, discharge, and aquifer characteristics. The model described in this report uses parameters (Harbaugh and others, 2000, p. 4) to define much of the input data. A parameter is a single value that is given a name and determines the value of a variable in the finite-difference ground-water flow equation at one or more model cells. When parameters are used, the data value for a cell is calculated as the product of the parameter value, which might apply to many cells, and a cell multiplier, which applies only to that cell (Harbaugh and others, 2000, p. 13). Zone arrays are also defined in order to allow only some of the cells in a model layer to be associated with a particular parameter (Harbaugh and others, 2000, p. 15). Sensitivity analysis (Hill and others, 2000, p. 98) was used to guide model construction and calibration.

Hydrogeologic Units

A three-dimensional hydrogeologic framework model was developed by Cederberg and others (2009) for the area within the basin-fill boundary in northern Utah Valley (figs. 5 and 6). This model, constructed from lithologic and drillers' logs for more than 900 wells, grouped the lithology into 11 hydrogeologic units (table 1). A hydrogeologic unit is a layer or section of sediment or rock assumed to have common hydrologic properties. Hydrogeologic units in northern Utah Valley have variable thickness and do not span the entire extent of the valley because of faulting (figs. 5 and 6). This complex system consists of multiple unconfined and confined aquifers in both basin-fill deposits and bedrock and each aquifer is designated as a separate hydrogeologic unit within the model.

In order to accurately represent the discontinuous hydrogeologic units with variable thickness and elevation, the Hydrogeologic-Unit Flow (HUF) Package of MODFLOW-2000 was used. The HUF package calculates effective hydrologic properties for each model cell based on the hydrologic properties of hydrogeologic units that intersect the cell, which are defined using parameters (Anderman and Hill, 2000, p. 7–10). This gives the user the flexibility to change the flow-model grid geometry without having to manually resample the hydrostratigraphic framework model. Each hydrogeologic unit is represented within the model domain (the three-dimensional extent of the model grid or simulated area) by the altitude of its top and its thickness. During model construction, the hydrogeologic framework was defined as a series of vertically stacked hydrogeologic units that all span

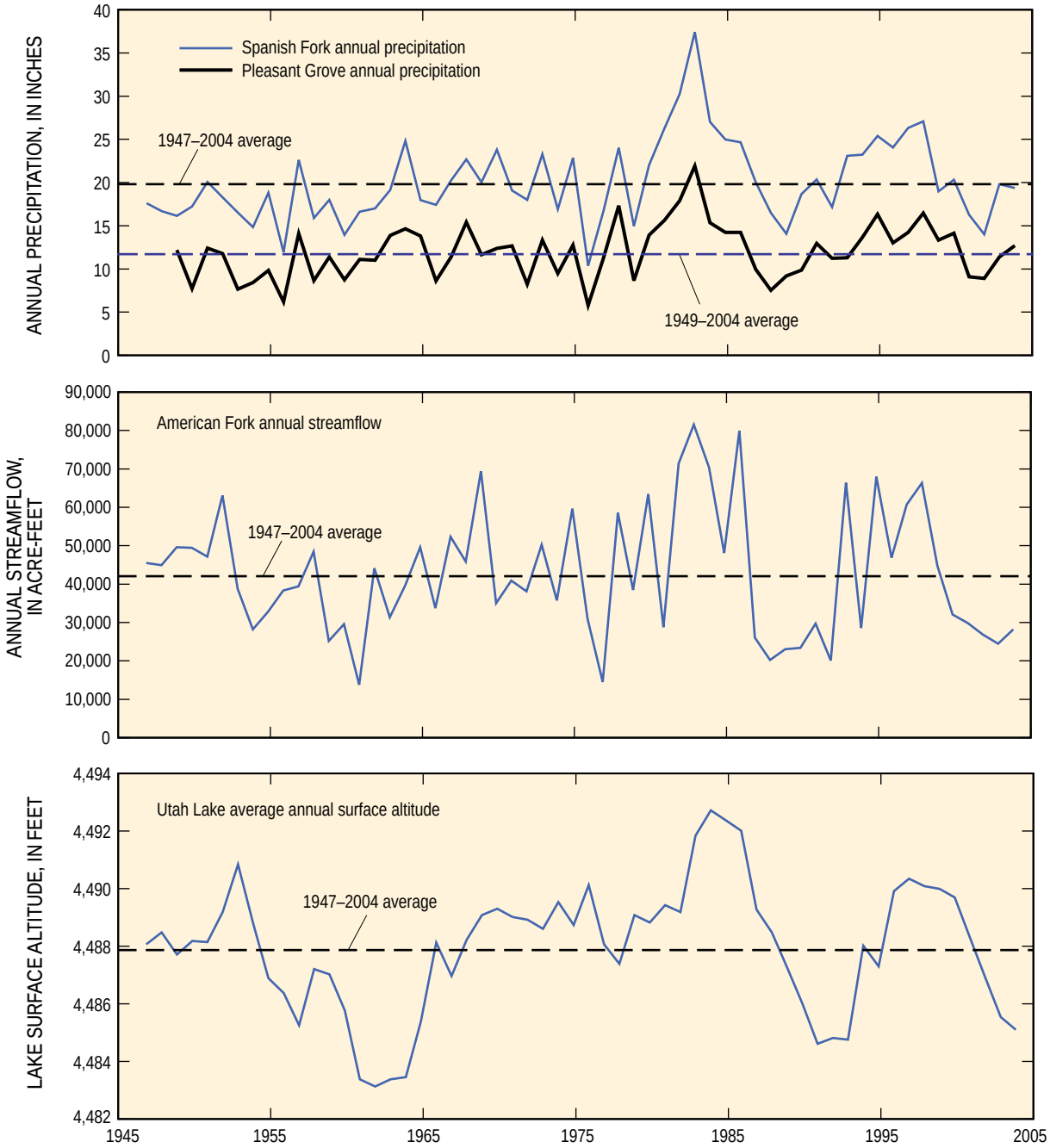

Figure 4. Annual precipitation at Spanish Fork and Pleasant Grove, annual streamflow in American Fork, and average annual surface altitude of Utah Lake, northern Utah Valley, Utah, 1947–2004.

the entire model domain. Hydrogeologic units were assigned a thickness of zero in areas where they do not physically exist and, in subsequent figures, are shown only where they have a thickness greater than zero. Information provided in table 1 and illustrated in figures 3, 5, and 6 describes the hydrogeologic framework used with the HUF package in the ground-water flow model.

An areally extensive, shallow unconfined aquifer exists at the surface across most of the valley and is designated as the shallowest hydrogeologic unit, HUF1_Surf, in the HUF package (fig. 5a). In areas high on the benches where the layers of fine-grained sediments that form the base of this aquifer are discontinuous, small perched aquifers that are not simulated may be present. Near the eastern margin of the valley, a deeper unconfined aquifer is present in pre-Lake Bonneville deposits. This is the PLB aquifer, designated as hydrogeologic unit HUF11_PLB, which underlies any perched ground water in HUF1_Surf and is the water-table aquifer where coarse-grained sediments are unconfined in the primary recharge area along the mountain front (fig. 5k). In the model, HUF11_PLB

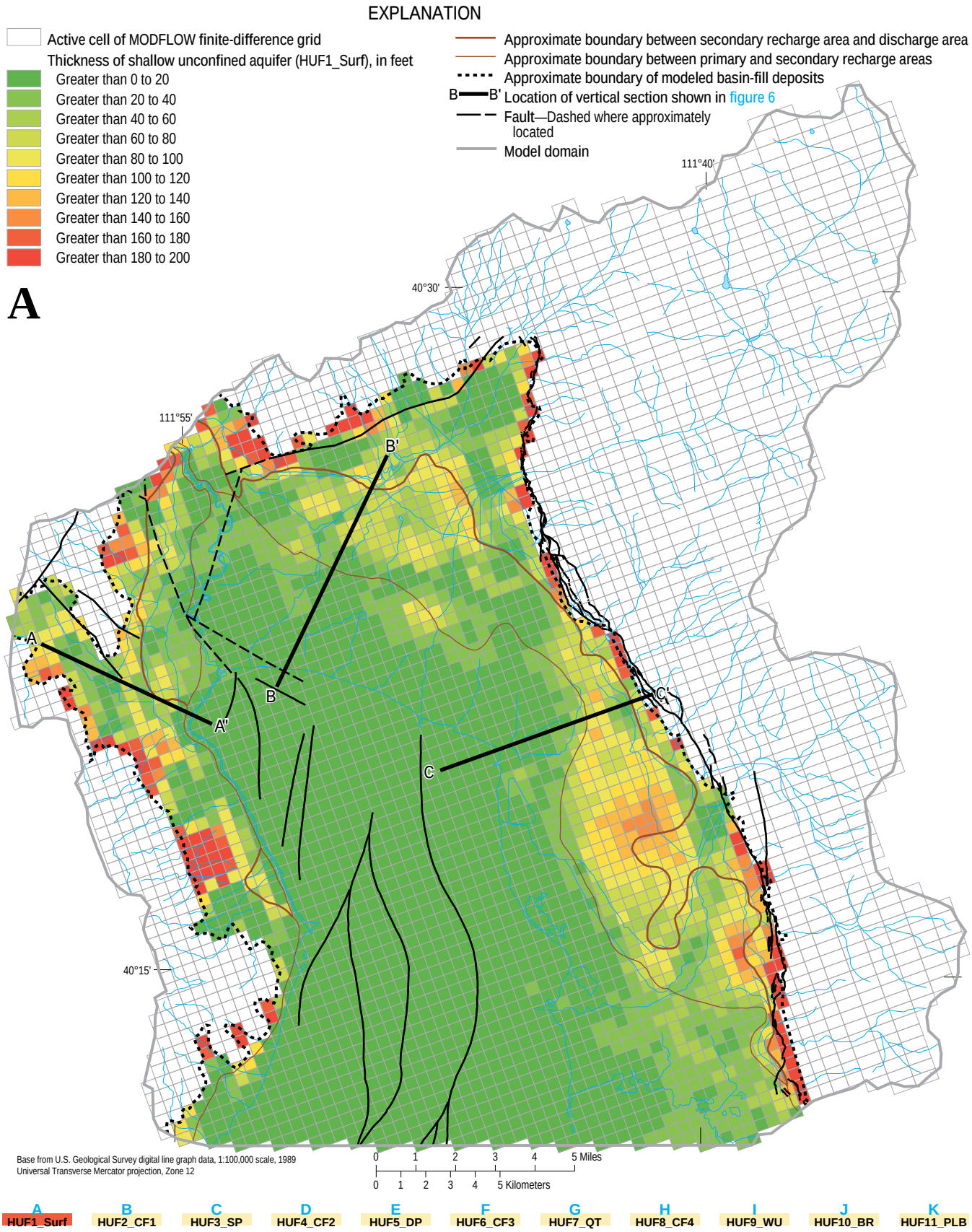

Figure 5. Interactive map showing thickness and areal extent of all hydrogeologic units (data layers A–K) within the basin-fill boundary simulated with the Hydrogeologic Unit Flow Package in MODFLOW-2000, northern Utah Valley, Utah.

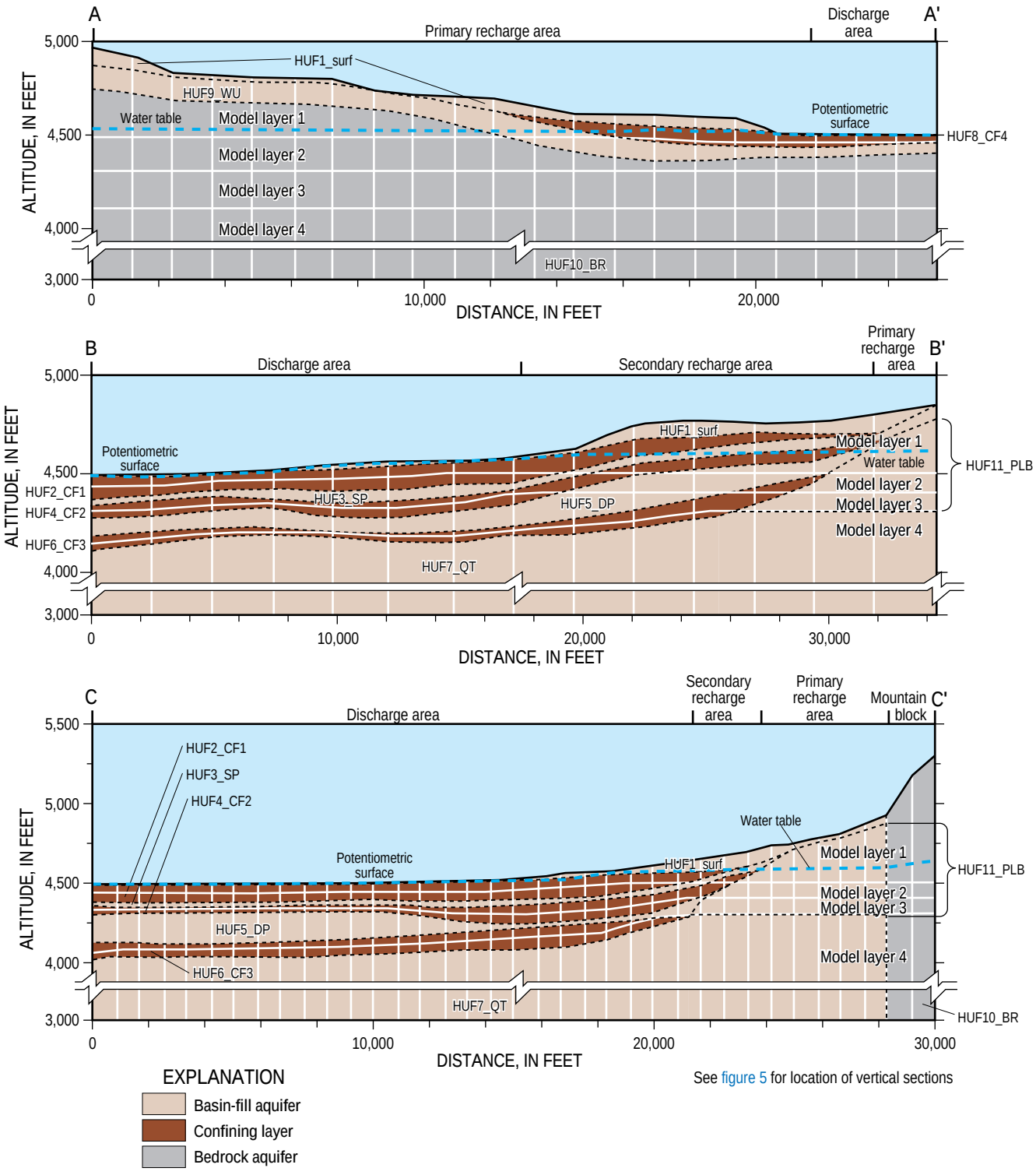

Figure 6. Vertical sections showing the relation of hydrogeologic units to model layers in the ground-water flow model of northern Utah Valley, Utah.

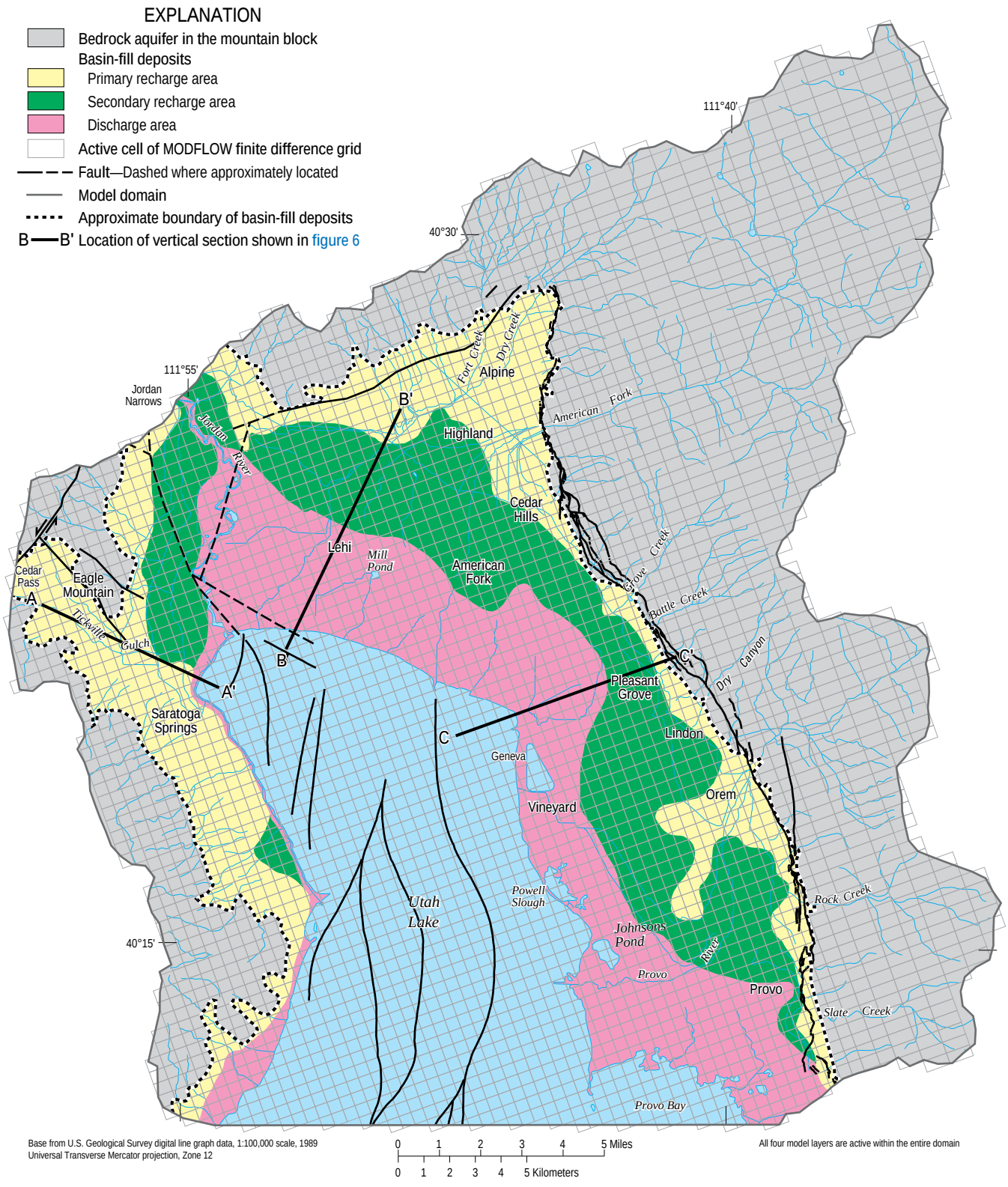

Figure 7. Active cells in model layers 1 through 4 in the ground-water flow model and location of vertical sections used in this report, northern Utah Valley, Utah.

Table 1. Description of each of the 11 hydrogeologic units simulated with the Hydrogeologic-Unit Flow package in MODFLOW-2000 in the ground-water flow model of northern Utah Valley, Utah.

Hydrogeologic unit number	Hydrogeologic unit name	Feature Description
1	HUF1_Surf	*Shallow unconfined aquifer*: generally present across all of northern Utah Valley, sometimes containing perched aquifers that are not simulated.
2	HUF2_CF1	*Confining layer 1*: shallowest of three modeled confining layers on the eastern side of northern Utah Valley.
3	HUF3_SP	*Shallow Pleistocene (SP) aquifer*: shallowest of three modeled confined aquifers on the eastern side of northern Utah Valley, this aquifer is a lateral continuation of the pre-Lake Bonneville unconfined aquifer near the mountain front.
4	HUF4_CF2	*Confining layer 2*: middle of three modeled confining layers on the eastern side of northern Utah Valley.
5	HUF5_DP	*Deep Pleistocene (DP) aquifer*: middle of three modeled confined aquifers on the eastern side of northern Utah Valley, this aquifer is a lateral continuation of the pre-Lake Bonneville unconfined aquifer near the mountain front.
6	HUF6_CF3	*Confining layer 3*: deepest of three modeled confining layers on the eastern side of northern Utah Valley.
7	HUF7_QT	*Quaternary/Tertiary (QT) aquifer*: deepest of three modeled confined aquifers on the eastern side of northern Utah Valley; although this aquifer underlies the pre-Lake Bonneville unconfined aquifer near mountain front, it is simulated as confined everywhere.
8	HUF8_CF4	*Confining layer 4*: shallow modeled confining layer on the western side of northern Utah Valley, separated from HUF2_CF1 by a fault zone underlying Utah Lake and the area near the Jordan River.
9	HUF9_WU	*West-side unconsolidated (WU) aquifer*: shallow, unconsolidated, aquifer on the western side of northern Utah Valley. Confined where it underlies HUF8_CF4 and unconfined near the western valley margin.
10	HUF10_BR	*Bedrock*: all consolidated-rock aquifers, including the mountain block and the fractured rock aquifer underlying HUF9_WU on the west side of valley. Bedrock hydraulic properties are differentiated by a zone array.
11	HUF_11PLB	*Pre-Lake Bonneville unconfined (PLB) aquifer*: aquifer composed of generally coarse-grained sediment that is present between the eastern extent of the confining layers and the western extent of the Wasatch Mountains.

also is the unconfined eastern extension of the confined SP and DP aquifers (fig. 6, sections *B-B′* and *C-C′*).

Closer to Utah Lake, the ground-water system is divided into a vertical series of confining units and confined aquifers. Model hydrogeologic units underlying HUF1_Surf are, in order from top to bottom, confining unit 1 (HUF2_CF1, fig. 5b), the SP aquifer (HUF3_SP, fig. 5c), confining unit 2 (HUF4_CF2, fig. 5d), the DP aquifer (HUF5_DP, fig. 5e), confining unit 3 (HUF6_CF3, fig. 5f), and the QT aquifer (HUF7_QT, fig. 5g). HUF7_QT extends from the fault zone beneath the west side of Utah Lake below HUF11_PLB all the way to the mountain block on the eastern half of the valley (fig. 6, section *C-C′*).

Because of the variations in lithologic characteristics and water quality, separate hydrogeologic units were designated below HUF1_Surf for the area west of Utah Lake and the Jordan River. The boundary between the eastern and western hydrogeologic units is uncertain, but for the purposes of the model, the specified boundary coincides with the western edge of a series of north-south trending normal faults that have been mapped by Hecker (1993) and Beik (2003) in basin-fill deposits beneath Utah Lake and near the Jordan River (fig. 7). Model hydrogeologic units underlying HUF1_Surf west of Utah Lake and the Jordan River are, in order from top to bottom, confining unit 4 (HUF8_CF4, fig. 5h), the WU aquifer (HUF9_WU, fig. 5i), and a fractured bedrock aquifer (HUF10_BR, fig. 5j). HUF8_CF4 is the only confining unit evident in well logs west of the Jordan River and is often present at depths of about 50 ft (fig. 6, section *A-A′*). HUF9_WU is mostly unconfined near the western margin of the valley and becomes confined where it underlies HUF8_CF4 closer to Utah Lake (fig. 6, section *A-A′*). All bedrock in the model is represented by HUF10_BR. This hydrogeologic unit is divided into five zones that simulate variations in hydrologic properties as discussed in the “Hydrologic Properties” section of this report. The modeled thickness of HUF10_BR where it underlies basin fill is shown in figure 5j. The thickness of HUF10_BR was specified at 8,500 ft everywhere in the mountain block (outside the basin-fill boundary) in order to encompass the entire range of altitudes present within the model domain. This

ensured that HUF10_BR encompassed all model layers in the mountain block regardless of changes in model layer thickness that occurred during model construction and calibration.

Horizontal and Vertical Discretization

A finite-difference grid of 79 rows by 70 columns with variable cell sizes is used to represent the northern Utah Valley ground-water flow system (fig. 7). The model grid is rotated about 20 degrees counterclockwise from north to minimize the number of inactive cells. Cells throughout most of the model domain are 0.3 mi on a side in the horizontal dimension. The largest cells are rectangular with horizontal dimensions of about 0.3 by 0.6 mi, and occur in the mountain block on the eastern edge of the model domain where the least hydrologic data are available. This model cell size is considered adequate. Trial simulations that used a uniform cell size as small as 1,000 ft (0.19 mi) on a side yielded nearly identical results while increasing the total number of active model cells by a factor of 3 (from 15,936 to 46,972 cells) and the model execution time by a factor of 7.

The boundary of active cells of the simulated ground-water system generally corresponds with the surface-water divide along the eastern, northern, and western boundaries of the model domain. Two exceptions are at the Jordan Narrows on the northern boundary and Cedar Pass on the western boundary, and both are discussed in the "General Head Boundary Package" subsection of this report. The southern boundary of the model is an east-west line that bisects Provo Bay and Utah Lake (fig. 7). This boundary, similar to the one used for numerical ground-water models by Clark (1984) for northern Utah Valley and Brooks and Stolp (1995) for southern Utah Valley, is considered a ground-water divide.

Vertically, the aquifer system is divided into four model layers of variable thickness that incorporate the 11 hydrogeologic units (figs. 3 and 6). All four model layers are active throughout the entire model domain. Vertical discretization was used in the model to enable the simulation of known vertical hydraulic gradients, particularly between confined aquifers in the discharge area in the center of the valley. Although the HUF package allows model-layer boundaries to be defined independently of hydrogeologic units, specifying model-layer boundaries that coincide with or are parallel to hydrogeologic-unit boundaries is useful. However, this was not possible for discontinuous hydrogeologic units in northern Utah Valley, for example where confining layers pinch out near the primary recharge area and where basin-fill aquifers abut bedrock (fig. 6). Within the basin fill it was possible to specify model-layer boundaries subparallel to hydrogeologic unit boundaries by generally bisecting overlying and underlying confining layers where they exist (fig. 6). The advantage of this is that, in areas where aquifers are confined, model results closely approximate what is occurring within a particular confined aquifer. For example, simulated hydraulic heads in a particular cell in model layers 2, 3, and 4 in the discharge area represent the hydraulic heads at that location in the SP, DP, and QT aquifers, respectively. This design was applied nearly everywhere in the discharge and secondary recharge areas of the valley for the SP, DP, QT, and WU aquifers where the largest vertical hydraulic gradients exist. However, the spatial variability of the hydrogeologic units prohibited applying this design in all basin-fill locations.

The top of model layer 1 is specified as land-surface altitude everywhere in the model domain. The altitude of the bottom of model layer 1 varies from about 4,400 ft in the middle of Utah Lake to 4,500 ft below the primary recharge area in the eastern part of the valley and beneath the mountain block. The thickness of model layer 1 varies from as little as 20–50 ft near the shores of Utah Lake to more than 6,500 ft beneath the tallest peaks in the Wasatch Mountains. In the center of the valley, model layer 1 contains the shallow unconfined aquifer (HUF1_Surf) and the upper half of the underlying confining units (HUF2_CF1 and HUF8_CF4). Along the valley margins, model layer 1 contains the shallow unconfined aquifer (HUF1_Surf) and a portion of the PLB unconfined aquifer (HUF11_PLB) on the east and the uppermost portions of the WU aquifer (HUF9_WU) where it is unconfined on the west. Outside of the basin-fill boundary, in the mountain block, all four model layers contain only bedrock (HUF10_BR).

Model layer 2 varies from 100 to 200 ft in thickness across the model domain. In the center of the valley, east of the dividing fault zone, model layer 2 contains the SP aquifer (HUF3_SP) and fractions of the overlying and underlying confining units (HUF2_CF1 and HUF4_CF2). In the center of the valley, west of the dividing fault zone, model layer 2 contains the lower portion of the WU aquifer (HUF9_WU) where it is confined and fractions of the overlying confining unit (HUF8_CF4) and underlying bedrock aquifer (HUF10_BR). Along the valley margins, model layer 2 contains part of the PLB unconfined aquifer (HUF11_PLB) on the east and mostly bedrock (HUF10_BR) where it underlies basin-fill deposits on the west.

Model layer 3 varies from 100 to about 310 ft in thickness across the model domain. The thickest portion of model layer 3 occurs near the Jordan Narrows along the northern model boundary. In the center of the valley, east of the dividing fault zone, model layer 3 contains the DP aquifer (HUF5_DP) and fractions of the overlying and underlying confining units (HUF4_CF2 and HUF6_CF3). West of the dividing fault zone, model layer 3 contains only bedrock (HUF10_BR). Along the eastern valley margin, model layer 3 contains only the pre-Lake Bonneville unconfined aquifer (HUF11_PLB).

Model layer 4 varies from 1,020 to about 1,300 ft in thickness across the model domain. The altitude of the bottom of model layer 4 (the bottom of the model) was specified at 3,000 ft. Thus, the simulated thickness of the flow system near Utah Lake is about 1,500 ft. East of the dividing fault zone, model layer 4 contains the QT aquifer (HUF7_QT) and a fraction of the overlying confining unit (HUF6_CF3). West of the dividing fault zone, model layer 4 contains only bedrock (HUF10_BR). Because of the spatial variability of

the hydrogeologic units, the above descriptions are somewhat generalized and do not accurately describe the intersection of the model layers with hydrogeologic units at all points in the model.

Model layer 1 was designated as a convertible layer in MODFLOW-2000. This allows the layer to be simulated as confined if the simulated water level is above the top of the layer (as it is in the center of the valley) and unconfined if the simulated water level is below the top of the layer (as it is in the mountains and along the valley margins).

Temporal Discretization

The model simulates both steady-state and transient conditions; a separate model does not exist for steady-state conditions. MODFLOW-2000 allows the first period in a transient simulation to be steady-state and the simulated water levels from that stress period to be used as the initial conditions for the transient simulation. The steady-state period simulates recharge and discharge in 1947 and is referred to throughout this report as the steady-state simulation. The transient period was designed to simulate annual water-level fluctuations and changes in ground-water storage for 58 yearly stress periods from 1947 to 2004 and is referred to throughout this report as the transient simulation. Five time steps were simulated for each of the stress periods. A time-step multiplier of 1.4 was used to increase the length of each successive time step so that the first time step of each stress period (when new stresses are applied) is about 1 month long and the final time step is about 4 months long.

Hydrologic Properties

The distribution of hydrologic properties in the basin-fill and bedrock aquifers of northern Utah Valley is variable and all model parameters defining the hydrologic properties of aquifer material were considered to be calibration variables. When possible, initial estimates and ranges of probable values for these parameters were determined on the basis of information obtained during the recent study of northern Utah Valley reported by Cederberg and others (2009) and on the results of previous studies, including a previously calibrated numerical model (Clark, 1984) that covers a portion of the area modeled in the study. In parts of the valley, hydraulic-conductivity values are near the upper end of published ranges for natural aquifer materials and wells yield several thousand gallons per minute with relatively little drawdown. The aquifer also contains large zones of fine-grained, low-permeability deposits. Few data are available from which to estimate vertical hydraulic conductivity and the spatial distribution of specific yield and specific storage in both the basin-fill deposits and bedrock aquifers. As a result, initially a uniform distribution of these parameters was specified in the numerical model and variability was incorporated as parameter distributions were adjusted during the calibration process.

Horizontal Hydraulic Conductivity

Estimates of horizontal hydraulic conductivity (HK) in northern Utah Valley are derived from multiple-well aquifer tests, specific-capacity data, and an earlier calibrated numerical model of the ground-water flow system. Horizontal hydraulic-conductivity estimates for 24 wells (8 from specific-capacity data and 16 from multiple-well aquifer tests) were reported by Clark and Appel (1985, table 9) and an additional 30 estimates from specific-capacity tests were collected during this study. Multiple-well aquifer tests are designed to quantify the characteristics of an aquifer and yield aquifer properties that represent larger areas better than those derived from specific-capacity tests in a single well. Specific-capacity data, however, often are more abundant.

Specific capacity is the ratio of the pumping rate to the drawdown in a well after a given duration of pumping. Values of HK were estimated from specific-capacity data by first deriving transmissivity with a method described by Theis and others (1963) and then dividing by the open interval of the well. The open screen interval of a well does not always represent the entire saturated thickness of the contributing aquifer. Thus, HK derived from a specific-capacity test is likely a maximum value. Furthermore, the rate and duration of pumping can be highly variable from one specific-capacity test to another, and HK values derived from specific-capacity tests typically have more error associated with them than those derived from multiple-well aquifer tests. With these limitations in mind, the available data do provide reasonable estimates of HK and were used to guide model development.

Hydraulic-property data are most abundant in the historically populated areas on the eastern side of northern Utah Valley. Horizontal hydraulic-conductivity estimates from specific-capacity tests and multiple-well aquifer tests in the basin fill range from 1 to more than 1,000 ft/d (fig. 8) and the highest values extend basinward from the mouths of American Fork and Provo Canyons. Ground-water resources west of the Jordan River are presently being developed. However, few hydraulic-property data were available for this area at the time of this study. Specific-capacity tests in wells in fractured limestone west of the Jordan River yielded no reliable estimate of HK because of the lack of measured drawdown during pumping, and no test data were available to estimate hydrologic properties of the bedrock in the mountain block. Where data were not available, hydrologic properties were assumed to be similar to those in areas with analogous aquifer material and were considered model-calibration variables. During calibration, the confining unit (HUF8_CF4) and underlying aquifer (HUF9_WU) west of the Jordan River were assumed to have HK values within the same range as the shallow confining unit (HUF2_CF1) and underlying aquifer (HUF3_SP) east of the Jordan River. HK values of bedrock aquifers were assumed to fall within the range of values published by Domenico and Schwartz (1998, table 3.2, p. 39) for similar rock types (fig. 9).

Horizontal hydraulic conductivity is defined in the model by using 15 HK parameters (hk_rock2, hk_rock3, hk_rock4,

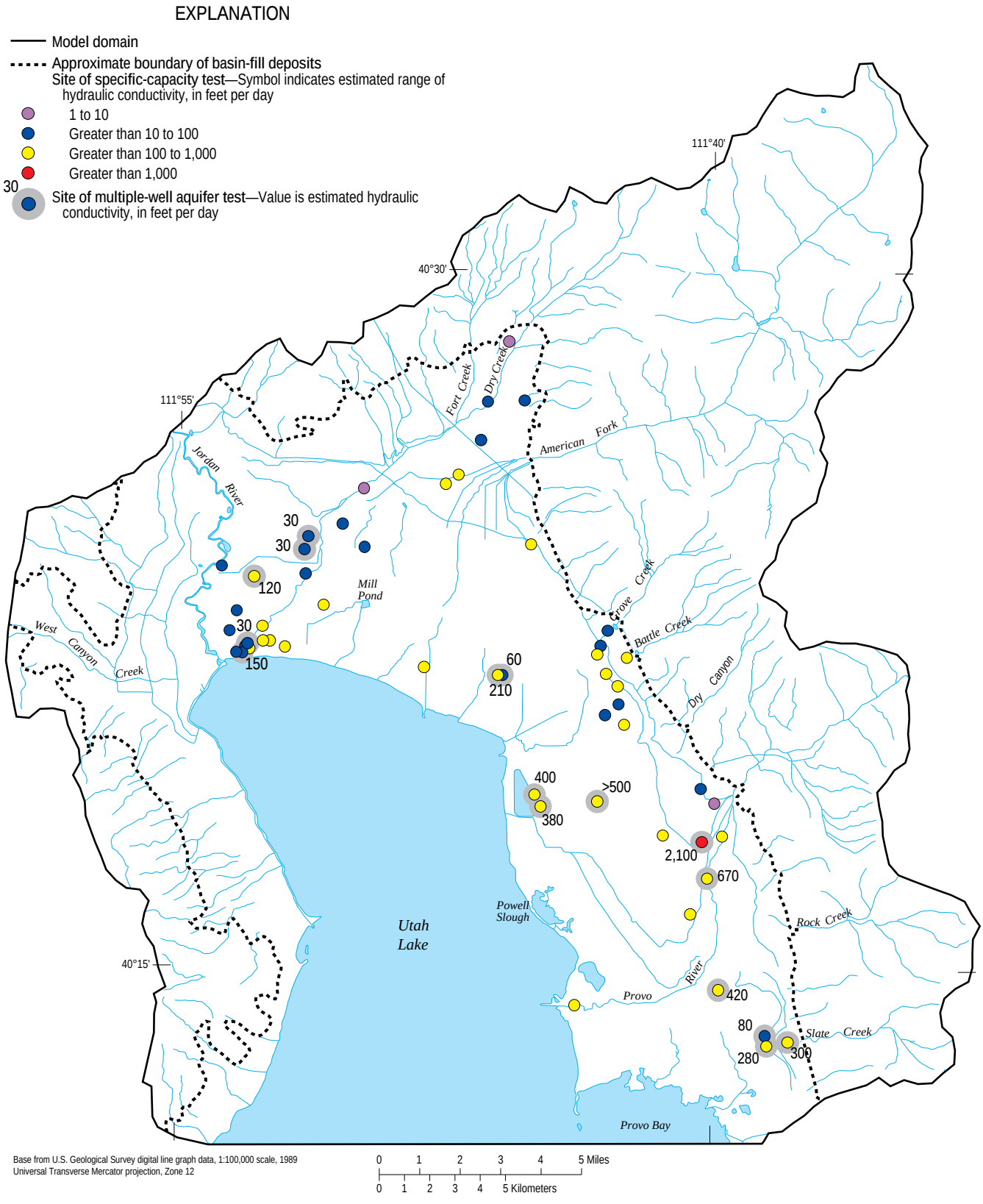

Figure 8. Distribution of selected specific-capacity and multiple-well aquifer test data, northern Utah Valley, Utah.

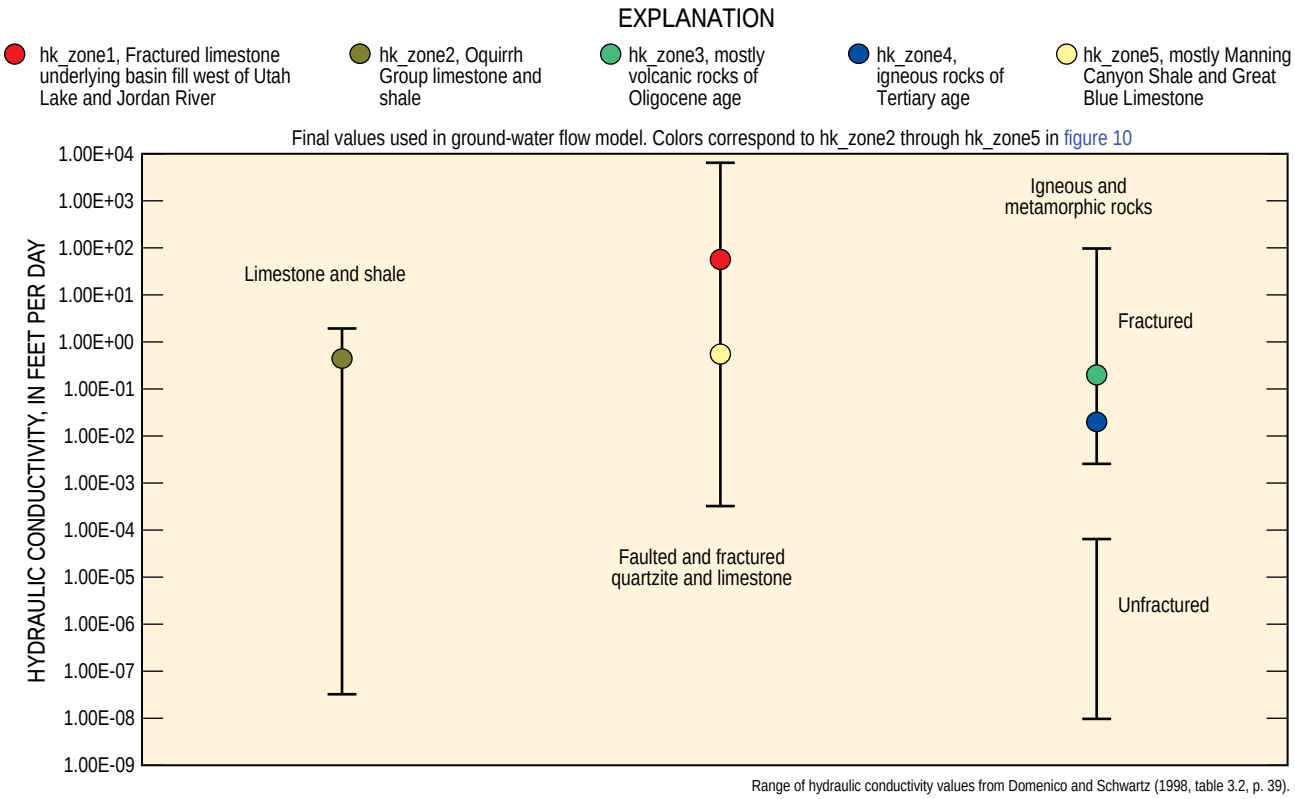

Figure 9. Typical range of hydraulic-conductivity values for the types of bedrock present in northern Utah Valley, and final values used to simulate bedrock horizontal hydraulic conductivity in the ground-water flow model of northern Utah Valley, Utah.

hk_rock5, hk_WBR, hk_surf, hk_CF1, hk_CF2, hk_CF3, hk_CF4, hk_SP, hk_DP, hk_QT, hk_PLB, hk_WU). In the model, HK parameters are assigned to hydrogeologic units and the spatial distribution of the resulting data values (in this case the actual simulated values of horizontal hydraulic conductivity) are defined by using zone and multiplier arrays (table 2). As previously described, zone arrays determine which model cells in a model layer or hydrogeologic unit are associated with a particular parameter and multiplier arrays allow the simulated values of particular data types to vary spatially across a zone.

In mountain areas (hk_zones 2-5), the HK values corresponding to bedrock are zoned according to major hydrogeologic facies changes (fig. 10). The spatial variation of HK in basin-fill deposits is represented in a more complex manner, using multiplier arrays, where it is justified by data from the multiple-well aquifer tests, specific-capacity well tests, and the earlier numerical model of northern Utah Valley (fig. 11). In lieu of a detailed description of the relation between each HK parameter and its associated hydrogeologic unit, zone array, and multiplier array, the following examples are provided to illustrate how these components are related to yield the final distribution and simulated values of horizontal hydraulic conductivity. The parameter hk_WBR has a value of 50 and is used to describe the horizontal hydraulic conductivity of fractured limestone underlying areas of basin-fill deposits west of Utah Lake (table 2). This parameter is assigned to the hydrogeologic unit HUF10_BR, which represents bedrock everywhere in the model, but only in hk_zone1, which represents the area of bedrock underlying basin-fill deposits in the western part of the valley. Because there is no multiplier array associated with this parameter, the final value of horizontal hydraulic conductivity is equal to the parameter value (50 ft/d) everywhere that HUF10_BR and hk_zone1 intersect (fig. 11j). The parameter HK_rock2 has a value of 0.44 and is used to describe the horizontal hydraulic conductivity of predominantly Oquirrh Group limestone and shale in mountain block areas (table 2). This parameter also is assigned to the hydrogeologic unit HUF10_BR, but only in hk_zone2, which represents the areas of bedrock in the mountain block (outside of the basin-fill boundary) that are composed of predominantly Oquirrh Group limestone and shale (fig. 10). Because there is no multiplier array associated with this parameter, the final value of horizontal hydraulic conductivity is equal to the parameter value (0.44 ft/d) everywhere that HUF10_BR and hk_zone2 intersect (fig. 10). As a final example, hk_SP has a value 2.5 and is used to describe the horizontal hydraulic conductivity of the SP aquifer (table 2). This parameter is assigned to the hydrogeologic unit HUF3_SP, which represents the SP aquifer only in the eastern two-thirds of the basin-fill deposits, and is assigned to the existing hk_zone1. It was not necessary to assign this parameter to a new zone because HUF3_SP exists only in hk_zone1. The parameter hk_SP is

Table 2. Description of MODFLOW-2000 parameters showing applicable hydrogeologic units, and zone and multiplier arrays used in the ground-water flow model of northern Utah Valley, Utah.

[HUF, Hydrogeologic Unit Flow package; —, not associated with model parameter]

Parameter number	Parameter name	Modflow parameter type	Parameter description	Applicable hydrogeologic units (if HUF parameter)	Zone array, zone	Multiplier array	Calibrated parameter value
1	rock1_rch	RCH	Recharge flux from precipitation over most of the mountain block	—	mbr_zone, 1	MtnPrcpRch[1]	1
2	rock2_rch	RCH	Recharge flux from precipitation over the American Fork drainage in the mountain block	—	mbr_zone, 2	MtnPrcpRch[1]	2.8
3	valley_rch	RCH	Recharge flux from precipitation over the primary recharge area	—	—	VlyPrcpRch[2]	1.9
4	irr_rch	RCH	Recharge flux by seepage from irrigated fields within the primary recharge area	—	—	IrrRch1966, IrrRch1980, IrrRch1988, IrrRch1995, IrrRch2002[3]	0.78
5	base_et	EVT	Maximum evapotranspiration flux that occurs in the discharge area	—	—	ET	1.4
6	PumpWell	Q	Multiplier to withdrawal rates from individual wells	—	—	—	1
7	CdrSubSrf	GHB	Hydraulic conductance of general head boundary in layers 2, 3, and 4 that simulates subsurface inflow from Cedar Valley	—	—	—	1.1
8	JdnSubSrf	GHB	Hydraulic conductance of general head boundary in model layers 2 and 3 that simulates subsurface outflow to Salt Lake Valley	—	—	—	0.35
9	STR_MTN	STR	Streambed hydraulic conductivity in mountain streams	—	—	—	0.44
10	STR_VAL	STR	Multiplier to streambed hydraulic conductivity in most valley stream segments	—	—	—	0.63
11	STR_PvoVal	STR	Multiplier to streambed hydraulic conductivity in valley segments of the Provo River	—	—	—	1.5
12	STR_Jrdn	STR	Multiplier to streambed hydraulic conductivity in the Jordan River	—	—	—	0.04
13	STR_Murdck	STR	Multiplier to streambed hydraulic conductivity in Provo Reservoir (Murdock) Canal	—	—	—	1.2
14	STR_EstCnl	STR	Multiplier to streambed hydraulic conductivity in irrigation canals east of the Jordan River	—	—	—	0.35
15	STR_WstCnl	STR	Multiplier to streambed hydraulic conductivity in irrigation canals west of the Jordan River	—	—	—	1
16	DRN_SARATOGA	DRN	Drain hydraulic conductance for simulated drains and springs near Utah Lake at Saratoga Springs	—	—	—	0.01
17	DRN_DRYCRK	DRN	Drain hydraulic conductance for simulated drains and springs near the mouth of Dry Creek	—	—	—	0.01
18	DRN_BYU_G1	DRN	Drain hydraulic conductance for simulated drains and springs near Utah Lake between Dry Creek and Mill Pond	—	—	—	0.0005
19	DRN_MILPND	DRN	Drain hydraulic conductance for simulated drains and springs near Mill Pond	—	—	—	0.05
20	DRN_BYU_G2	DRN	Drain hydraulic conductance for simulated drains and springs near Utah Lake between Mill Pond and Geneva	—	—	—	0.0003
21	DRN_BYU_G3	DRN	Drain hydraulic conductance for simulated drains and springs near Utah Lake between Mill Pond and Geneva	—	—	—	0.01
22	DRN_BYU_G4	DRN	Drain hydraulic conductance for simulated drains and springs near Utah Lake between Geneva and Powell Slough	—	—	—	0.0005
23	DRN_GENEVA	DRN	Drain hydraulic conductance for simulated drains and springs near Utah Lake at Geneva	—	—	—	0.001
24	DRN_POWELL	DRN	Drain hydraulic conductance for simulated drains and springs near Powell Slough	—	—	—	0.005
25	DRN_JOHNSON	DRN	Drain hydraulic conductance for simulated drains and springs near Johnsons Pond	—	—	—	0.0005
26	DRN_BGDRCK	DRN	Drain hydraulic conductance for simulated drains and springs near Big Dry Creek north of Provo Bay	—	—	—	0.0002
27	DRN_SSPRGS	DRN	Drain hydraulic conductance for Spring Creek and simulated drains and springs east of Provo Bay	—	—	—	0.05
28	FloWel	DRN	Drain conductance for flowing wells in model layers 2 and 3 in discharge area simulated with the drain package	—	—	—	9.00E-05
29	hk_rock2	HK	Horizontal hydraulic conductivity of predominantly Oquirrh Group limestone and shale	HUF10_BR	hk_zone, 2	—	0.44

[1] Recharge flux from precipitation that falls over the mountain block is scaled annually (1) according to the deviation from 1970 to 2004 average annual streamflow for American Fork prior to 1970, and (2) according to annual results of the transient Basin Characterization Model for total in-place recharge from 1970 to 2004. Average precipitation scaler equals 1.00.

[2] Recharge flux from precipitation that falls over the primary recharge area in the valley is scaled annually according to the deviation from 1971 to 2000 annual average total precipitation at Pleasant Grove, Utah.

[3] In order to account for changes in recharge from changing irrigation patterns in the Primary Recharge Area over time, the following multiplier arrays were applied to stress periods corresponding to the years indicated: IrrRch1966 = 1948-1973, IrrRch1980 = 1974-1983, IrrRch1988 = 1984-1991, IrrRch1995 = 1992-1998, and IrrRch2002 = 1998-2004.

Table 2. Description of MODFLOW-2000 parameters showing applicable hydrogeologic units, and zone and multiplier arrays used in the ground-water flow model of northern Utah Valley, Utah—Continued.

Parameter number	Parameter name	Modflow parameter type	Parameter description	Applicable hydrogeologic units (if HUF parameter)	Zone array, zone	Multiplier array	Calibrated parameter value
30	hk_rock3	HK	Horizontal hydraulic conductivity of Oligocene volcanic rocks underlain by fractured quartzite	HUF10_BR	hk_zone, 3	—	0.2
31	hk_rock4	HK	Horizontal hydraulic conductivity of Tertiary igneous rocks	HUF10_BR	hk_zone, 4	—	0.02
32	hk_rock5	HK	Horizontal hydraulic conductivity of faulted and fractured limestone and quartzite	HUF10_BR	hk_zone, 5	—	0.55
33	hk_WBR	HK	Horizontal hydraulic conductivity of fractured limestone underlying areas of basin fill west of Utah Lake	HUF10_BR	hk_zone, 1	—	50
34	vani_rock	VANI	Vertical anisotropy of all bedrock hydrogeologic units	HUF10_BR	—	—	1
35	hk_surf	HK	Horizontal hydraulic conductivity of surficial basin-fill deposits	HUF1_surf	hk_zone, 1	hk_surface	1
36	vani_surf	VANI	Vertical anisotropy of of surficial basin-fill deposits	HUF1_surf	hk_zone, 1	—	100
37	hk_CF1	HK	Horizontal hydraulic conductivity of shallow confining layer on the east side of the valley	HUF2_cf1	hk_zone, 1	hk_surface	0.05
38	vani_CF1	VANI	Vertical anisotropy of shallow confining layer on the east side of the valley	HUF2_cf1	hk_zone, 1	—	46
39	hk_CF2	HK	Horizontal hydraulic conductivity of middle confining layer on the east side of the valley	HUF4_cf2	hk_zone, 1	hk_cf1	0.1
40	vani_CF2	VANI	Vertical anisotropy of middle confining layer on the east side of the valley	HUF4_cf2	hk_zone, 1	—	322
41	hk_CF3	HK	Horizontal hydraulic conductivity of deep confining layer on the east side of the valley	HUF6_cf3	hk_zone, 1	hk_cf2	0.1
42	vani_CF3	VANI	Vertical anisotropy of deep confining layer on the east side of the valley	HUF6_cf3	hk_zone, 1	—	100
43	hk_CF4	HK	Horizontal hydraulic conductivity of shallow confining layer on the west side of the valley	HUF8_cf4	hk_zone, 1	hk_cf3	1
44	vani_CF4	VANI	Vertical anisotropy of shallow confining layer on the west side of the valley	HUF8_cf4	hk_zone, 1	—	100
45	hk_SP	HK	Horizontal hydraulic conductivity of shallow confined aquifer (SP) on the east side of the valley	HUF3_SP	hk_zone, 1	hk_SP	2.5
46	hk_DP	HK	Horizontal hydraulic conductivity of middle confined aquifer (DP) on the east side of the valley	HUF5_DP	hk_zone, 1	hk_DP	1
47	hk_QT	HK	Horizontal hydraulic conductivity of deep confined aquifer (QT) on the east side of the valley	HUF7_QT	hk_zone, 1	hk_QT	0.7
48	hk_PLB	HK	Horizontal hydraulic conductivity of generally coarse-grained basin-fill that borders the eastern mountain front	HUF11_PLB	hk_zone, 1	hk_PLB	1
49	hk_WU	HK	Horizontal hydraulic conductivity of the unconsolidated confined aquifer on the west side of the valley	HUF9_WU	hk_zone, 1	hk_WU	1
50	vani_aquif	VANI	Vertical anisotropy of all basin-fill aquifer material except for the shallow unconfined aquifer	HUF3, 5, 7, 9, 11	hk_zone, 1	—	2
51	SY_Valley	SY	Specific yield of all basin-fill aquifer material in layer 1	HUF1, 2, 3, 4, 5, 6, 7, 8, 9, 11	hk_zone, 1	—	0.01
52	SY_Mtn	SY	Specific yield of all bedrock in layer 1	HUF10_BR	hk_zone, 1, 2, 3, 4, 5	—	0.005
53	SS_Valley	SS	Specific storage of all basin-fill aquifer material exclusive of the deep QT aquifer	HUF1, 2, 3, 4, 5, 6, 8, 9, 11	hk_zone, 1	—	4.00E-05
54	SS_Mtn	SS	Specific storage of mountain bedrock in all layers	HUF10_BR	hk_zone, 2, 3, 4, 5	—	7.00E-07
55	SS_QT	SS	Specific storage of all basin-fill in the deep QT aquifer	HUF7_QT	hk_zone, 1	—	1.35E-05

[1] Recharge flux from precipitation that falls over the mountain block is scaled annually (1) according to the deviation from 1970 to 2004 average annual streamflow for American Fork prior to 1970, and (2) according to annual results of the transient Basin Characterization Model for total in-place recharge from 1970 to 2004. Average precipitation scaler equals 1.00.

[2] Recharge flux from precipitation that falls over the primary recharge area in the valley is scaled annually according to the deviation from 1971 to 2000 annual average total precipitation at Pleasant Grove, Utah.

[3] In order to account for changes in recharge from changing irrigation patterns in the Primary Recharge Area over time, the following multiplier arrays were applied to stress periods corresponding to the years indicated: IrrRch1966 = 1948-1973, IrrRch1980 = 1974-1983, IrrRch1988 = 1984-1991, IrrRch1995 = 1992-1998, and IrrRch2002 = 1998-2004.

associated with a multiplier array, also named hk_SP, which has values ranging from 1 to 250 (not shown). The final distribution of horizontal hydraulic conductivity in the SP aquifer is equal to the product of the parameter value (2.5) and the cell-by-cell value of the multiplier array (1 to 250) everywhere that HUF3_SP exists. This results in values of horizontal hydraulic conductivity in the SP aquifer ranging from 2.5 to 625 ft/d (fig. 11c).

Vertical Hydraulic Conductivity

Water-level measurements in many wells indicate substantial vertical-head gradients in some areas of northern Utah Valley, especially between, but also within, confined aquifers in the discharge area near Utah Lake. In order for the model to simulate the measured vertical-head gradients, it is necessary for vertical hydraulic conductivity to be less than horizontal hydraulic conductivity in those areas. Vertical hydraulic

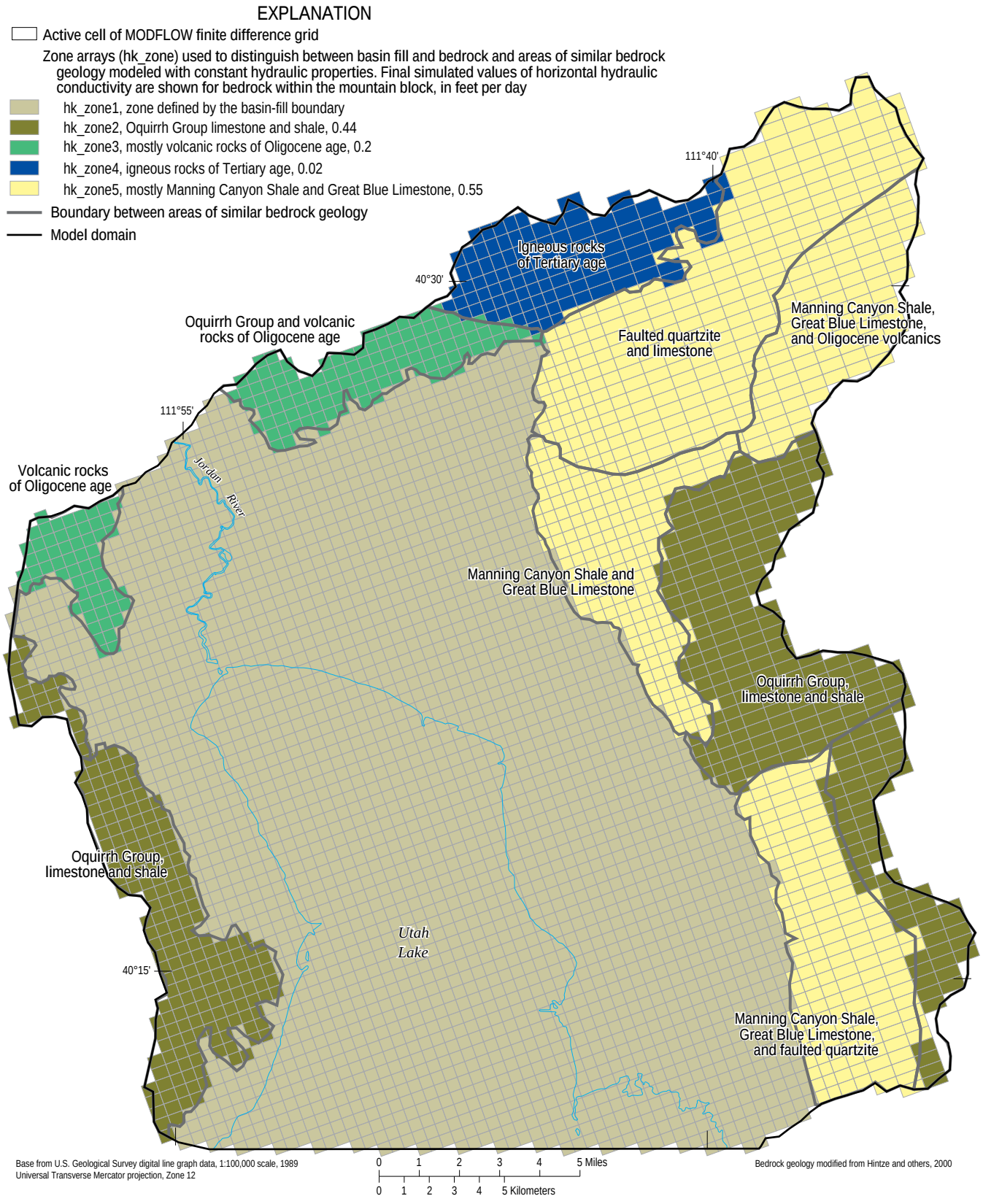

Figure 10. Hydraulic-conductivity zones (hk_zone) in model layers 1 through 4 and simulated values of horizontal hydraulic conductivity for bedrock within the mountain block in the ground-water flow model of northern Utah Valley, Utah.

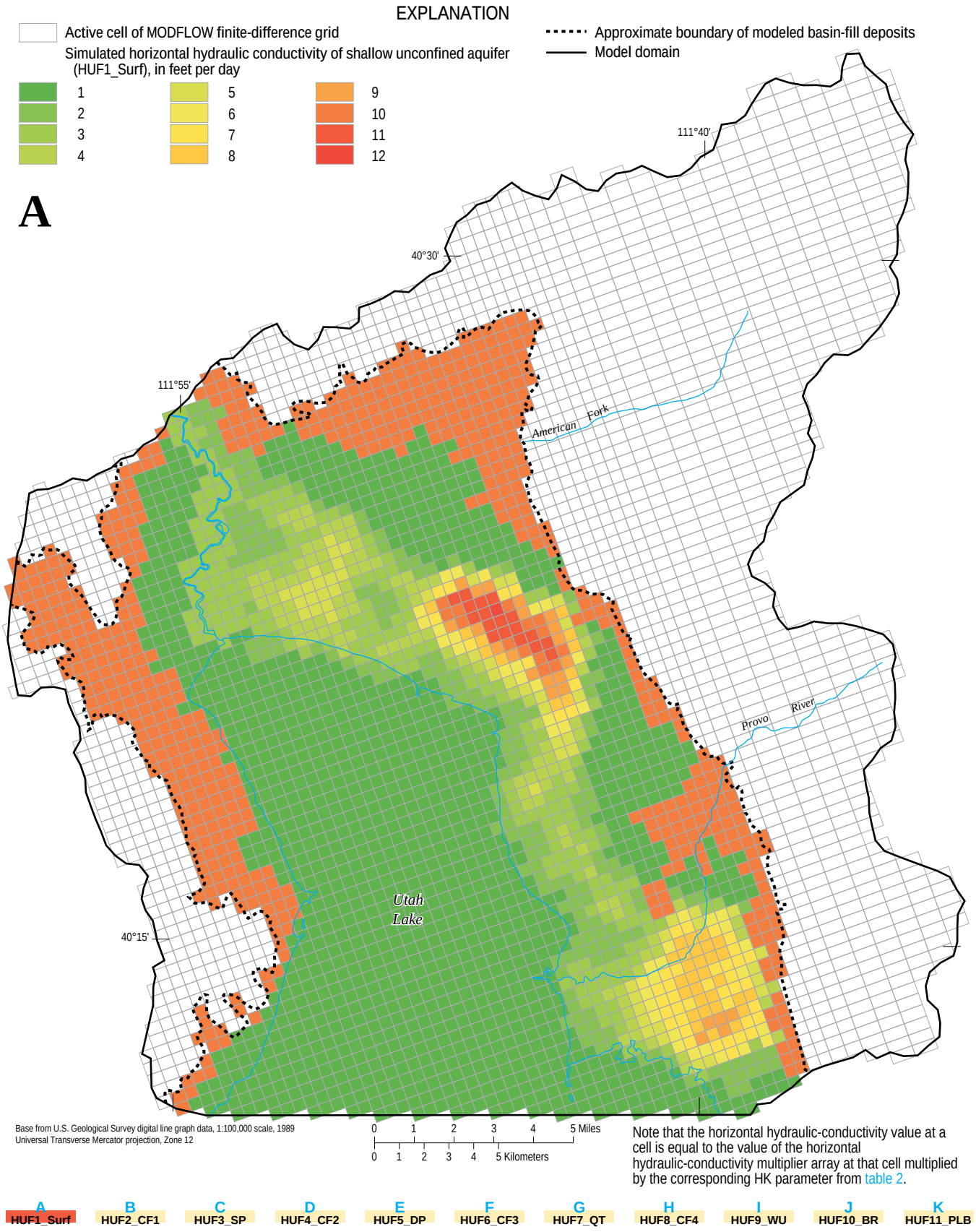

Figure 11. Interactive map showing simulated horizontal hydraulic conductivity of all hydrogeologic units (data layers A–K) simulated with the Hydrogeologic Unit Flow Package in the ground-water flow model of northern Utah Valley, Utah.

conductivity is simulated with the model by assigning vertical anisotropy (VANI) parameters to hydrogeologic units using zone arrays. Because few data are available from which to estimate the spatial distribution of vertical hydraulic conductivity, multiplier arrays are not used and VANI parameters are constant everywhere within the hydrogeologic unit and zone where they are defined. In MODFLOW-2000, VANI parameters are entered as the ratio of horizontal to vertical hydraulic conductivity, for example a VANI of 100 indicates that vertical hydraulic conductivity is 100 times smaller than horizontal hydraulic conductivity. Seven VANI parameters (vani_rock, vani_surf, vani_CF1, vani_CF2, vani_CF3, vani_CF4, and vani_aquif) are used to simulate vertical anisotropy in all HUF units (table 2). Bedrock (HUF10_BR) is assumed to be isotropic and assigned a VANI value equal to one (vani_rock) everywhere in the model. Most basin-fill aquifers are composed of sand and gravel with interbedded lenses of finer-grained material. HUF units representing these aquifers (HUF3_SP, HUF5_DP, HUF7_QT, HUF9_WU, and HUF11_PLB) are assumed to have minimal anisotropy and are assigned a VANI value equal to two (vani_aquif) everywhere that they exist.

Confining units and much of the shallow unconfined aquifer in the center of the valley are composed of lacustrine silts and clays. These layers are the primary control on vertical hydraulic gradients and vertical ground-water movement in the system and, where they are continuous or overlapping, they are much less permeable than the sand and gravel that makes up much of the basin-fill aquifers. Clark and Appel (1985, p. 47) report a value for vertical hydraulic conductivity of 0.001 ft/d for the confining layer above the QT aquifer from an aquifer test performed in the Lehi area. Thiros (1992, table 12) reported a range of vertical hydraulic conductivity for shallow silt and clay in nearby Salt Lake Valley from 5.1 $x10^{-5}$ to 0.02 ft/d determined from laboratory tests on 35 core samples. Horizontal hydraulic conductivity in these silts and clays is often two to three orders of magnitude larger than vertical hydraulic conductivity owing to hydraulically connected coarse-grained paleo-stream channel deposits that interfinger with the confining units. HUF units used to simulate these layers (HUF1_Surf, HUF2_CF1, HUF4_CF2, HUF6_CF3, and HUF8_CF4) have VANI values ranging from 46 to 322 (parameters vani_surf, vani_CF1, vani_CF2, vani_CF3, and vani_CF4 in table 2) that yield vertical hydraulic-conductivity values (HK/VANI) ranging from 5.0 $x10^{-4}$ to 0.12 ft/d, which generally agree with the values observed in the low-permeability materials described above. The smallest simulated values of vertical hydraulic conductivity in the confining hydrogeologic units occur near or beneath Utah Lake. The largest values, determined through model calibration, occur where confining hydrogeologic units are thought to be discontinuous below areas where ground water is known to discharge from springs at the surface.

Specific Yield and Specific Storage

Specific yield is used in areas where MODFLOW simulates unconfined conditions. Values of specific yield represent the ratio of the volume of water that a given mass of saturated rock or soil will yield by gravity to the volume of that mass, stated as a percentage and are typically orders of magnitude larger than values of specific storage—the volume of water that a confined aquifer releases or takes into storage per unit volume per unit change in head. Specific storage is a function of porosity, and fluid and matrix compressibility. The specific storage (L^{-1}) is equivalent to the storage coefficient (dimensionless) divided by the thickness of the aquifer system. Storage coefficients obtained from aquifer tests for the confined aquifers in northern Utah Valley range from 6.1 $x10^{-6}$ to 2.6 $x10^{-2}$ (Clark and Appel, 1985, table 9). Thus, these values are equivalent to a specific storage range of 2.0 $x10^{-8}$ to 5.2 $x10^{-4}$ ft^{-1} for typical 50- to 300-ft thick confined basin-fill aquifers. Specific yield and specific storage were assumed to be smaller in bedrock than in the unconsolidated basin fill because consolidated rocks typically have smaller porosities and smaller matrix compressibilities than unconsolidated rocks.

Sensitivity analyses of early versions of the model, where individual parameters defined specific storage for each hydrogeologic unit, indicated that a simple spatial representation of specific yield and specific storage was adequate to define these aquifer properties. Specific yield and specific storage were simulated by using five MODFLOW parameters (SY_Valley, SY_Mtn, SS_Valley, SS_Mtn, SS_QT) (table 2). The values of the parameters used are the actual simulated values; no multiplier arrays are used. SY_Valley defines the specific yield for all basin-fill hydrogeologic units and SY_Mtn defines the specific yield for all bedrock hydrogeologic units, including the bedrock aquifer that underlies basin-fill deposits west of Utah Lake. Because specific-yield parameters are used by the model only in layers designated as convertible, they affect hydrogeologic units that intersect model layer 1. However, specific-yield parameters are specified for all hydrogeologic units in the event that future simulations require other model layers to be designated as convertible. Specific storage for all basin-fill hydrogeologic units except for HUF7_QT was defined by the parameter SS_Valley. The specific storage of HUF7_QT is less than that for shallower basin-fill hydrogeologic units and is defined by a separate parameter, SS_QT. All bedrock in the model (HUF10_BR) has a specific-storage value defined by the parameter SS_Mtn. The final values of specific yield and specific storage parameters listed in table 2 were determined during calibration and are discussed further in the “Model Calibration” section of this report.

Boundary Conditions and Implementation of MODFLOW Packages

Mathematical boundaries used to represent hydrologic boundaries in the model include specified-flux and head-dependent flux boundaries. These boundaries define the physical limits of the model and simulate recharge to and discharge from the ground-water system. Specified-flux boundaries allow a specified rate of water through the cell and are used to simulate much of the recharge in the model. Head-dependent flux boundaries simulate flow across the boundary proportional to the difference in heads across the boundary and are used to simulate most discharge and some recharge in the model.

No-flow boundaries are specified-flux boundaries with flux equal to zero—no ground-water flow is simulated across them. No-flow boundaries are specified on the bottom of the model domain and along all sides except in two locations where subsurface flow is exchanged with other basins. The altitude of the bottom of the model domain is 3,000 ft, which allows a simulated thickness of about 1,500 ft below Utah Lake. Although basin-fill sediments are present at greater depths in parts of Utah Valley, no active wells exist below the simulated depth, where it is assumed that the ground-water flow system is relatively inactive. All other boundary conditions are represented in the model using MODFLOW packages and are described in the following subsections.

Recharge Package

The Recharge Package was used to simulate annual recharge from infiltration of precipitation, and seepage of unconsumed irrigation to fields, lawns, and gardens. Recharge is applied as a specified flux to the uppermost active cell at the beginning of each stress period (Harbaugh and others, 2000, p. 67). Four parameters are used with this package: the parameters rock1_rch and rock2_rch simulate recharge over the mountain block, and valley_rch and irr_rch simulate recharge in the primary recharge area over the basin fill (table 2).

Average annual recharge to the mountain block from the infiltration of precipitation is estimated to range from 46,900 to 91,600 acre-ft or from about 17 to 33 percent of the 1971–2000 average annual precipitation of 280,000 acre-ft (Cederberg and others, 2009, table 11). The areal distribution of recharge from precipitation over the mountain block was simulated by using a multiplier and zone array with two zones based on the results of a Geographic Information Systems (GIS)-based basin characterization model of net infiltration (Flint and others, 2004; and Hevesi and others, 2003). Net infiltration is the flux of water that occurs at a depth below which ET ceases to affect the downward movement of water. The basin characterization model (BCM) incorporates spatial estimates of monthly precipitation, monthly air temperature, monthly potential ET, soil water storage, and bedrock permeability to simulate water available for net-infiltration. Depending on soil and bedrock permeability, water available for net-infiltration is partitioned as either (1) in-place recharge or (2) runoff that can potentially become mountain-front recharge where streams cross from the mountain block into the basin fill (Flint and others, 2004). The transient BCM yielded 35 grids of annual in-place recharge for the period 1970–2004, inclusive. Examination of the BCM results showed that annually, though the total in-place recharge over the mountains varied significantly, the spatial variation of in-place recharge changed very little. On the basis of the BCM results, a single grid representing the 1970–2004 average in-place recharge was used as the multiplier array (MtnPrcpRch) that represented the areal distribution of recharge over the mountain block (fig. 12).

Annual variation in recharge over the mountain block was simulated by applying a multiplication factor for each stress period that scaled the entire multiplier array (MtnPrcpRch) (table 3). From 1970 to 2004, this factor was derived by normalizing the sum of the in-place recharge over the mountain block for each year (derived from the BCM) by the 1970–2004 average recharge over the mountain block. Prior to 1970, no BCM results were available and recharge over the mountain block was assumed to vary by the same proportion as annual streamflow recorded at the USGS streamflow-gaging station 10164500, American Fork above upper power plant near American Fork, Utah (fig. 13).

During calibration of the ground-water flow model, it was necessary to increase recharge in the American Fork drainage basin as described in Cederberg and others (2009). This was accomplished through the addition of a zone array (mbr_zone) that allowed recharge over the American Fork drainage basin to be controlled by one parameter (rock2_rch, in mbr_zone2) while recharge over the rest of the mountain block was controlled by another parameter (rock1_rch, in mbr_zone1) during calibration (table 2, fig. 12). During the transient simulation, recharge from precipitation over the mountain block varied from a minimum of about 11,200 acre-ft in 1976 to a maximum of about 152,900 acre-ft in 1982 (table 3).

Studies of ground-water recharge processes in the Great Basin during the past two decades indicate that little recharge originates from precipitation that falls on valley floors (Harrill and Prudic, 1998, p. A23). The BCM, used to distribute recharge from precipitation over mountain blocks in the ground-water flow model, was used to simulate the entire study area and simulated no recharge at valley altitudes for most years. However, the primary recharge area in northern Utah Valley is located adjacent to the Wasatch Mountains—one of the wettest mountain ranges in the Great Basin—and consists of extensive areas of permeable sediments. For these reasons, it is thought that some amount of in-place recharge results from precipitation that falls on the valley floor in the primary recharge area. Areal recharge in the valley is simulated only over the primary recharge area. The fraction of infiltration that reaches the principal aquifer in the secondary recharge area is unknown and probably low because of the relative abundance of confining layers and shallow perched

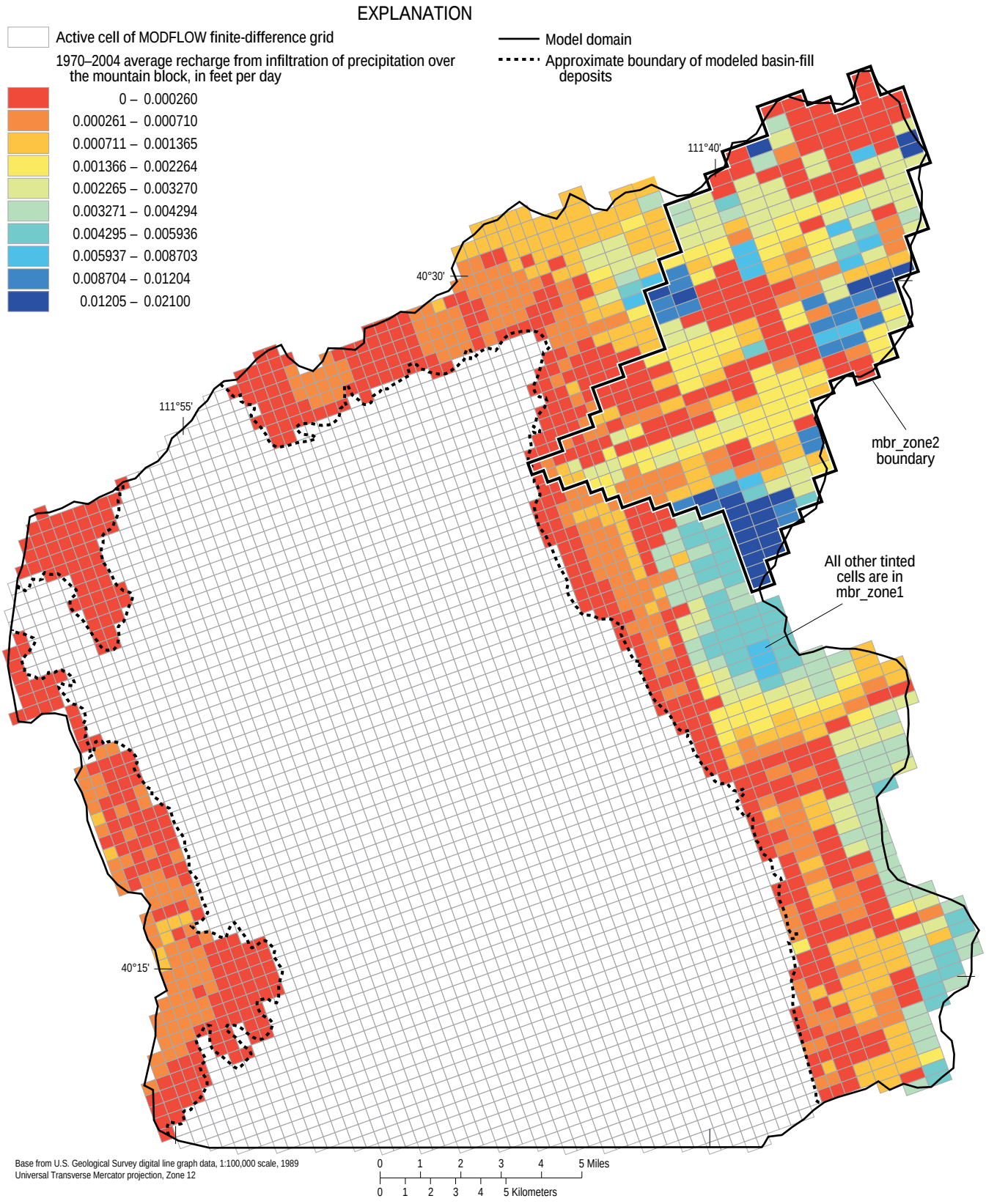

Figure 12. Zone boundaries and average recharge from precipitation over the mountain block in the ground-water flow model of northern Utah Valley, Utah, 1970–2004.

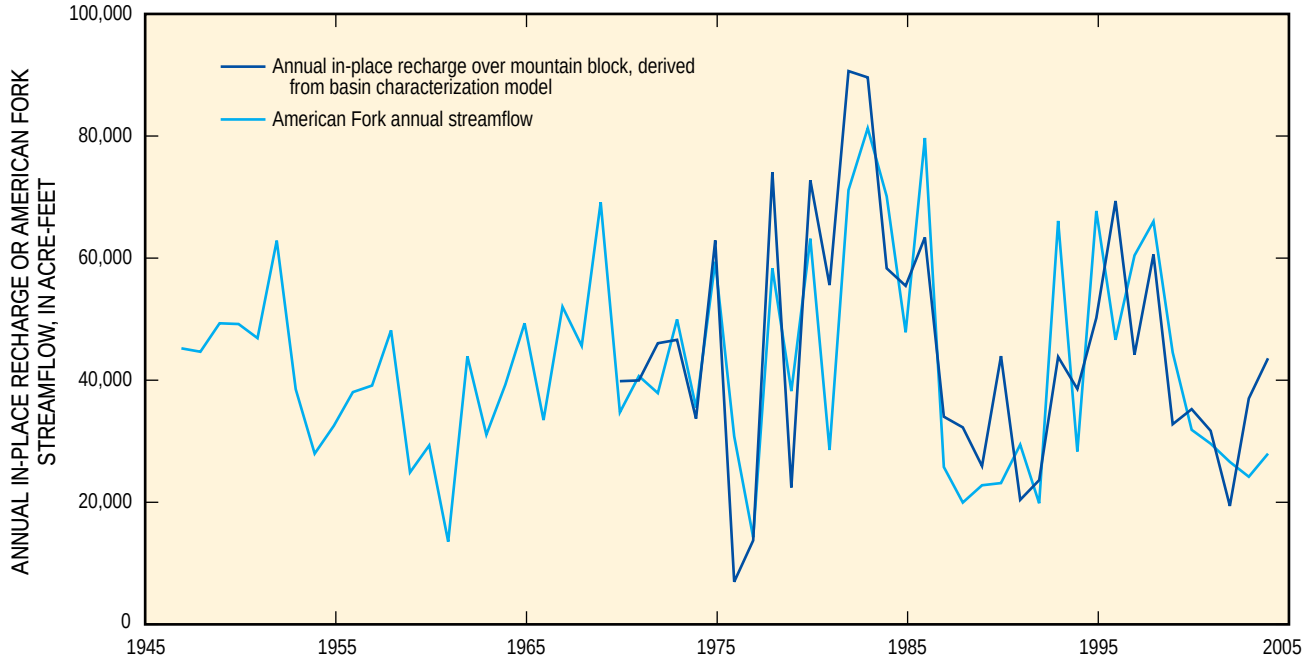

Figure 13. Annual in-place recharge over the mountain block for 1970–2004 (derived from the basin characterization model) and American Fork streamflow for 1947–2004 used to construct the multiplication factor that was applied to vary annual recharge from precipitation over the mountains prior to 1970 in the ground-water flow model of northern Utah Valley, Utah.

aquifers. Areal recharge from precipitation over the valley is estimated to range from 1,400 to 5,000 acre-ft/yr or from about 3 to 10 percent of the 1971–2000 average annual precipitation of 45,000 acre-ft/yr over the primary recharge area (Cederberg and others, 2009, table 8; Clark and Appel, 1985, p. 31). These estimates are based on methods that derive recharge directly as a fraction of precipitation (Harrill and Prudic, 1998, p. A25; Brooks and Stolp, 1995, p. 26; Clark and Appel, 1985, p. 31; Maxey and Eakin, 1949). One parameter (valley_rch) is used in conjunction with a multiplier array (VlyPrcpRch) in the Recharge Package to areally distribute recharge from precipitation across the primary recharge area of northern Utah Valley (table 2, fig. 14). The multiplier array VlyPrcpRch was constructed by using 30-year average PRISM precipitation contours for 1971–2000 (Spatial Climate Analysis Service, 2006). Annual variation in recharge from precipitation over the primary recharge area was simulated by applying a multiplication factor for each stress period that scaled the entire multiplier array (VlyPrcpRch) and resulted in this component of recharge varying from a minimum of about 800 acre-ft in 1976 to a maximum of about 2,700 acre-ft in 1983 (table 3). This factor was derived by normalizing the annual precipitation at Pleasant Grove (fig. 4) by the 1971–2000 average precipitation from the same station.

Recharge of unconsumed irrigation water by infiltration from irrigated fields, lawns, and gardens was applied over the primary recharge area in the valley. Minimal infiltration is thought to occur in the secondary recharge area for reasons described above and the upward hydraulic gradient in the discharge area prevents any unconsumed irrigation water from recharging the underlying confined aquifers. Even if the

Table 3. Multiplication factor used to vary annual recharge and final values of annual recharge from precipitation over the mountains and primary recharge area in the ground-water flow model of northern Utah Valley, Utah.

Stress period	Year	Multiplication factor used to vary recharge over the mountain block	Areal recharge simulated over the mountain block, in acre-feet	Multiplication factor used to vary recharge over the primary recharge area	Areal recharge simulated over the primary recharge area, in acre-feet
1	1947	1.05	78,322	1.00	1,616
2	1948	1.05	78,322	1.00	1,616
3	1949	1.15	85,781	0.95	1,535
4	1950	1.15	85,781	0.65	1,050
5	1951	1.10	82,051	0.95	1,535
6	1952	1.45	108,158	0.90	1,454
7	1953	0.90	67,133	0.65	1,050
8	1954	0.65	48,485	0.70	1,131
9	1955	0.75	55,944	0.80	1,293
10	1956	0.90	67,133	0.55	889
11	1957	0.90	67,133	1.10	1,778
12	1958	1.10	82,051	0.70	1,131
13	1959	0.60	44,755	0.90	1,454
14	1960	0.70	52,214	0.70	1,131
15	1961	0.30	22,378	0.90	1,454
16	1962	1.00	74,592	0.85	1,374
17	1963	0.70	52,214	1.05	1,697
18	1964	0.90	67,133	1.10	1,778
19	1965	1.15	85,781	1.05	1,697

Table 3. Multiplication factor used to vary annual recharge and final values of annual recharge from precipitation over the mountains and primary recharge area in the ground-water flow model of northern Utah Valley, Utah—Continued.

Stress period	Year	Multiplication factor used to vary recharge over the mountain block	Areal recharge simulated over the mountain block, in acre-feet	Multiplication factor used to vary recharge over the primary recharge area	Areal recharge simulated over the primary recharge area, in acre-feet
20	1966	0.80	59,674	0.70	1,131
21	1967	1.20	89,510	0.90	1,454
22	1968	1.05	78,322	1.20	1,939
23	1969	1.60	119,347	0.90	1,454
24	1970	0.90	67,133	0.95	1,535
25	1971	0.90	67,133	1.00	1,616
26	1972	1.05	78,322	0.70	1,131
27	1973	1.05	78,322	1.05	1,697
28	1974	0.75	55,944	0.75	1,212
29	1975	1.40	104,429	1.00	1,616
30	1976	0.15	11,189	0.50	808
31	1977	0.30	22,378	0.90	1,454
32	1978	1.65	123,077	1.30	2,101
33	1979	0.50	37,296	0.70	1,131
34	1980	1.65	123,077	1.05	1,697
35	1981	1.25	93,240	1.20	1,939
36	1982	2.05	152,913	1.35	2,182
37	1983	2.00	149,184	1.65	2,666
38	1984	1.30	96,970	1.15	1,858
39	1985	1.25	93,240	1.10	1,778
40	1986	1.45	108,158	1.10	1,778
41	1987	0.75	55,944	0.80	1,293
42	1988	0.70	52,214	0.65	1,050
43	1989	0.60	44,755	0.75	1,212
44	1990	1.00	74,592	0.80	1,293
45	1991	0.45	33,566	1.00	1,616
46	1992	0.55	41,026	0.90	1,454
47	1993	1.00	74,592	0.90	1,454
48	1994	0.85	63,403	1.05	1,697
49	1995	1.15	85,781	1.25	2,020
50	1996	1.55	115,617	1.00	1,616
51	1997	1.00	74,592	1.10	1,778
52	1998	1.35	74,592	1.25	2,020
53	1999	0.75	55,944	1.05	1,697
54	2000	0.80	59,674	1.10	1,778
55	2001	0.70	52,214	0.75	1,212
56	2002	0.45	33,566	0.70	1,131
57	2003	0.85	63,403	0.90	1,454
58	2004	1.00	74,592	1.00	1,616

hydraulic gradient were reversed, the shallow soils have high fractions of silt and clay and would not likely permit recharge to occur in this area. The distribution of irrigation recharge in the primary recharge area in the valley is based on water-related land-use surveys made in 1966, 1980, 1988, 1995, and 2002 (Utah Department of Natural Resources, 2004). Four categories of land use were delineated (flood irrigated agriculture, line-sprinkler irrigated agriculture, center-pivot irrigated agriculture, and urban/residential irrigation of lawns and gardens) and a multiplier array was constructed for each survey. The recharge rate applied to each of the categories was calculated as a percentage of the average water applied annually to the area representing each category as described by Cederberg and others (2009). One parameter (irr_rch) is applied to the five multiplier arrays (IrrRch1966, IrrRch1980, IrrRch1988, IrrRch1995, and IrrRch2002) in order to simulate changes in land use through time. Only one of these multiplier arrays is used at a time (IrrRch1966 from 1947 to 1973, IrrRch1980 from 1974 to 1983, IrrRch1988 from 1984 to 1991, IrrRch1995 from 1992 to 1998, and IrrRch2002 from 1999 to 2004) to simulate recharge fluxes in feet per day (figs. 15a through 15d).

Simulated recharge caused by the infiltration of unconsumed irrigation water from fields, lawns, and gardens was about 9,000 acre-ft/yr in the early stress periods of the model. This component of recharge decreased to about 6,000 acre-ft/yr during the mid-1990s as agricultural land was converted for urban or residential use and was about 5,600 acre-ft/yr by the final stress periods as land that was previously irrigated became developed.

Evapotranspiration Package

The Evapotranspiration Package (Harbaugh and others, 2000, p. 73) was used to simulate ET in model layer 1. The rate of ET simulated depends on the maximum ET rate, the depth below land surface at which transpiration stops (extinction depth), and the simulated ground-water level (McDonald and Harbaugh, 1988, fig. 42). Data required for the Evapotranspiration Package are the altitude of the ET surface, the extinction depth, and the maximum ET rate. The altitude of the ET surface was estimated as land surface from USGS 1:24,000-scale topographic maps and 10-m resolution Digital Elevation Models (National Center for Earth Resources Observation & Science, 1999). In most areas of ET, the error associated with the altitude estimate is 5–10 ft because the topographic map contour interval is either 10 or 20 ft. An extinction depth of 15 ft was used for all areas of ET. The boundary of ET cells used in the model (fig. 16) was defined by including generalized areas of native vegetation, irrigated land, and open pasture determined from land-use data (Utah Department of Natural Resources, 2004) within the discharge area surrounding Utah Lake.

The maximum rate of ET in the model is the product of the parameter base_et and the ET multiplier array which represents the boundary of active ET cells (table 2). The ET

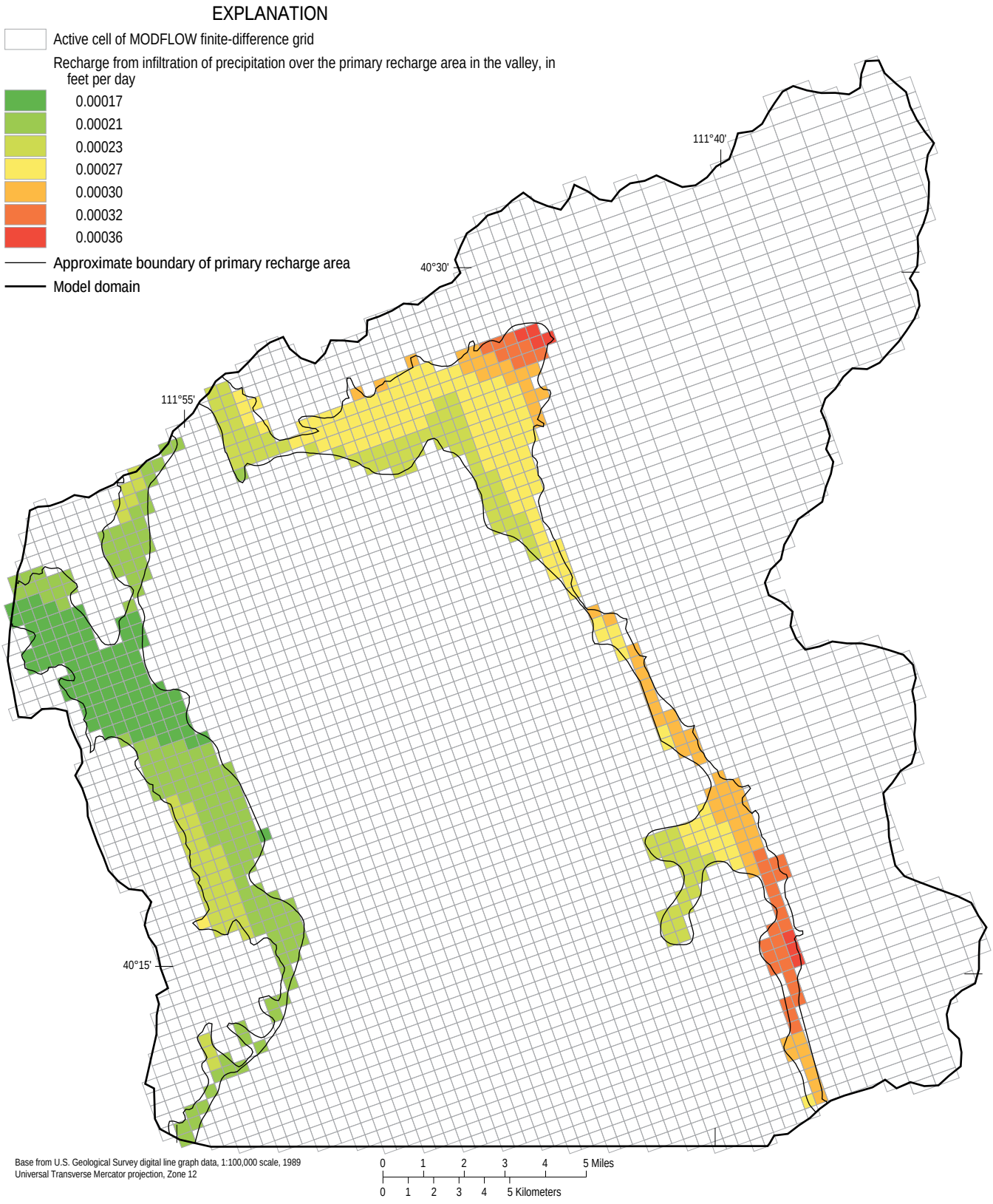

Figure 14. Average areal recharge from precipitation over the primary recharge area in the valley in the ground-water flow model of northern Utah Valley, Utah, 1971–2004.

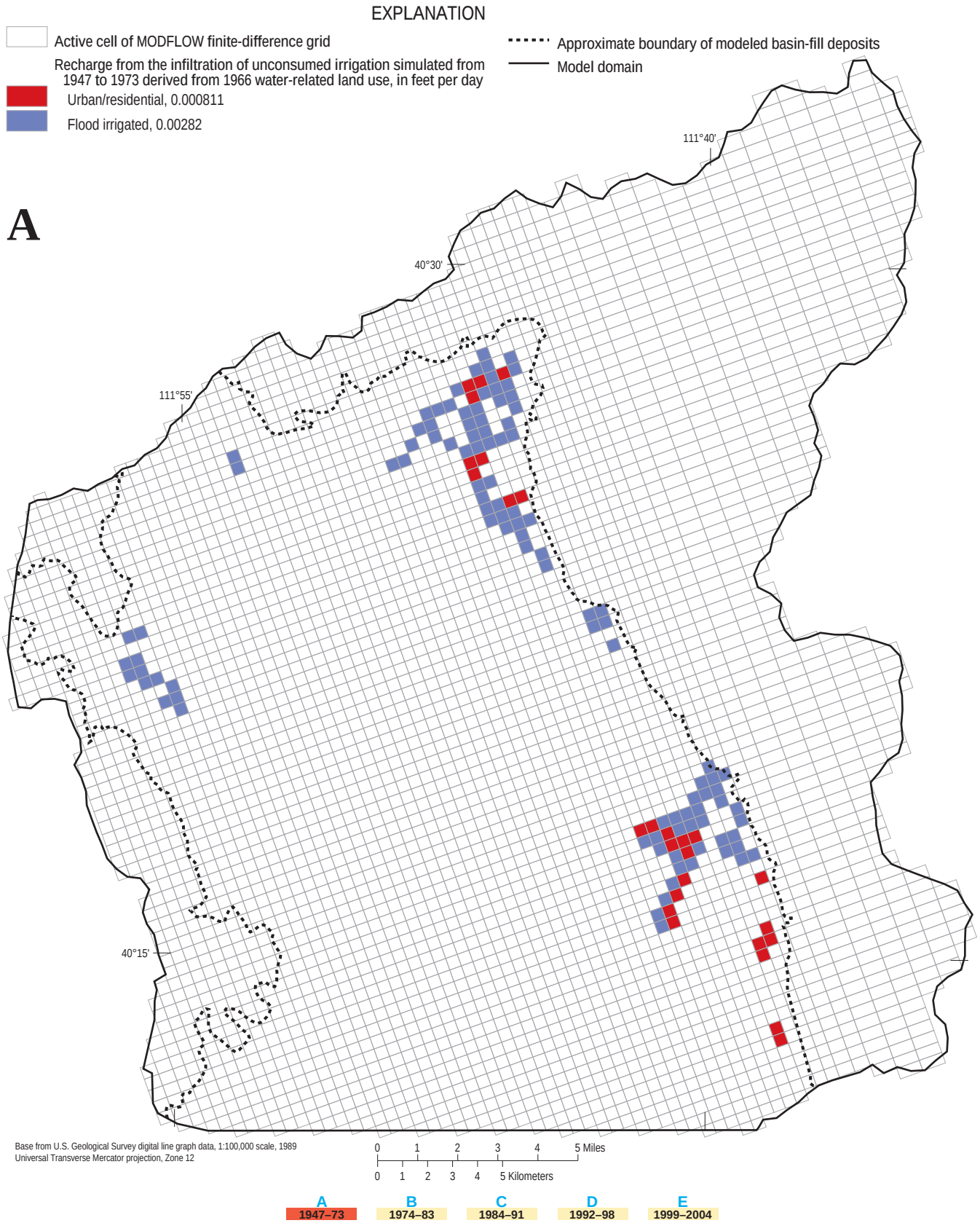

Figure 15. Interactive map showing simulated recharge as seepage from irrigated fields, lawns, and gardens over the primary valley recharge area during five time periods (A, 1947–73; B, 1974–83; C, 1984–91; D, 1992–98; and E, 1999–2004) in the ground-water flow model of northern Utah Valley, Utah, 1947–2004.

multiplier array does not vary spatially. The initial maximum rate of ET was set by giving the multiplier array a constant value of 0.001 ft/d and the parameter base_et a value of 1. The parameter value was then adjusted during calibration until the total discharge of ground water by ET during the steady-state simulation approximately matched the 8,000 acre-ft/yr estimated by Clark and Appel (1985, p. 83). Input to the Evapotranspiration Package was not changed during the transient simulation, but the rate of ET varies from a maximum of about 9,200 acre-ft/yr in 1984 to a minimum of about 7,200 acre-ft/yr in 2003 as simulated water levels vary.

General Head Boundary Package

Subsurface inflow through basin-fill deposits and bedrock from Cedar Valley north of the Lake Mountains has been estimated to be between 7,000 and 14,000 acre-ft/yr (Cederberg and others, 2009; Feltis, 1967). Subsurface outflow to Salt Lake Valley through basin-fill deposits in the Jordan Narrows has been estimated to be between 2,000 and 3,000 acre-ft/yr (Cederberg and others, 2009; Clark and Appel, 1985). Both of these estimates are based on limited data and the true subsurface flows are likely variable through time. The General Head Boundary Package (Harbaugh and others, 2000, p. 76) was used to represent this conceptualization because it allows flow across the boundaries to vary as the water-level difference across the boundary changes. The package was applied to five cells each in layers 2, 3, and 4, at Cedar Pass to represent where subsurface inflow moves through basin fill and underlying fractured limestone, and to five cells each in layers 2 and 3 to represent where subsurface outflow moves through basin fill at the Jordan Narrows (fig. 16). Ground-water flow into or out of each cell (Q_b) is computed as

$$Q_b = C_b(h_b - h_a), \quad (1)$$

where:

C_b is the boundary conductance (L^2T^{-1}),
h_b is the hydraulic head on the outside of the model boundary (L), and
h_a is the hydraulic head in the model cell (L).

The hydraulic head on the outside of the Cedar Pass general head boundary, h_b, was estimated from 1966 water-level contours in Cedar Valley (Feltis, 1967). The hydraulic head on the outside of the Jordan Narrows boundary was estimated from 1992 simulated and measured water levels in Salt Lake Valley (Lambert, 1995, fig. 25) and 1981 and 2004 measured water levels in northern Utah Valley (Cederberg and others, 2009, fig. 19; Clark and Appel, 1985, fig. 24). These values remain constant throughout the transient simulation. Although this assumption may introduce some error in future simulations if the true head outside of each boundary changes, it is considered reasonable for the calibration period because the head at Cedar Pass is in a deep, fractured-rock aquifer that was not heavily pumped until recently and the heads near the Jordan Narrows were similar for 1981, 1992, and 2004. The conductance (C_b) at the general head boundaries were specified by two parameters (CdrSubSrf, JdnSubSrf) that were adjusted during calibration so that the total flow at each general head boundary approximated the estimates of subsurface flow described above during the steady-state simulation. Input to the General Head Boundary Package was not changed during the transient simulation, but the simulated subsurface inflows vary between about 8,300 acre-ft/yr in 1983 and 9,800 acre-ft/yr in 2004 from Cedar Valley and the simulated subsurface outflows vary between about 2,700 acre-ft/yr in 1984 and 1,800 acre-ft/yr in 2004 at the Jordan Narrows as simulated water levels within the model domain vary.

Well Package

Discharge to pumping wells is simulated in all model layers with the Well Package (Harbaugh and others, 2000, p. 69). The Well Package simulates a specified-flux boundary in each cell to which a well is assigned. Data required for the Well Package are the withdrawal rate for each well or groups of pumping wells for each model cell containing the well or wells, and for each model layer. The distribution of withdrawal among layers in each well was determined prior to input into MODFLOW-2000 by assuming that the fraction of withdrawal from each model layer was equal to the fraction of the open well interval within that layer.

Ground-water withdrawal for individual pumped wells is needed for the steady-state simulation and for each annual stress period in the transient simulation. Annual withdrawal data from 1947 to 2004 were obtained from the Utah Department of Natural Resources, Division of Water Rights, for public-supply and industrial wells and from unpublished records of the U.S. Geological Survey for irrigation wells. In some cases, records for particular wells from the Division of Water Rights were incomplete and annual withdrawal values were assumed to remain unchanged from the previous year or to be the average of surrounding years, depending on which estimate was more appropriate for the particular well. Total annual ground-water withdrawals from pumping wells range from about 1,200 acre-ft in 1947 to a maximum of about 56,000 acre-ft in 2001 (fig. 17). Discharge to domestic pumping wells is not simulated because the withdrawals are small (totaling less than 700 acre-ft/yr) and distributed across large parts of the valley in both the SP and DP aquifers. Sensitivity analysis indicates that this amount of annual withdrawal distributed across a representative area has no significant effect on simulated water levels.

One MODFLOW-2000 parameter (PumpWell) was defined for discharge to wells and acts as a multiplier by which all well discharge can be scaled. The parameter was not changed during calibration because the well discharge rates are not a calibration variable. Rather, the parameter was used for the purpose of including pumping-well withdrawal, as a whole, in sensitivity analysis using the Sensitivity Process of MODFLOW-2000.

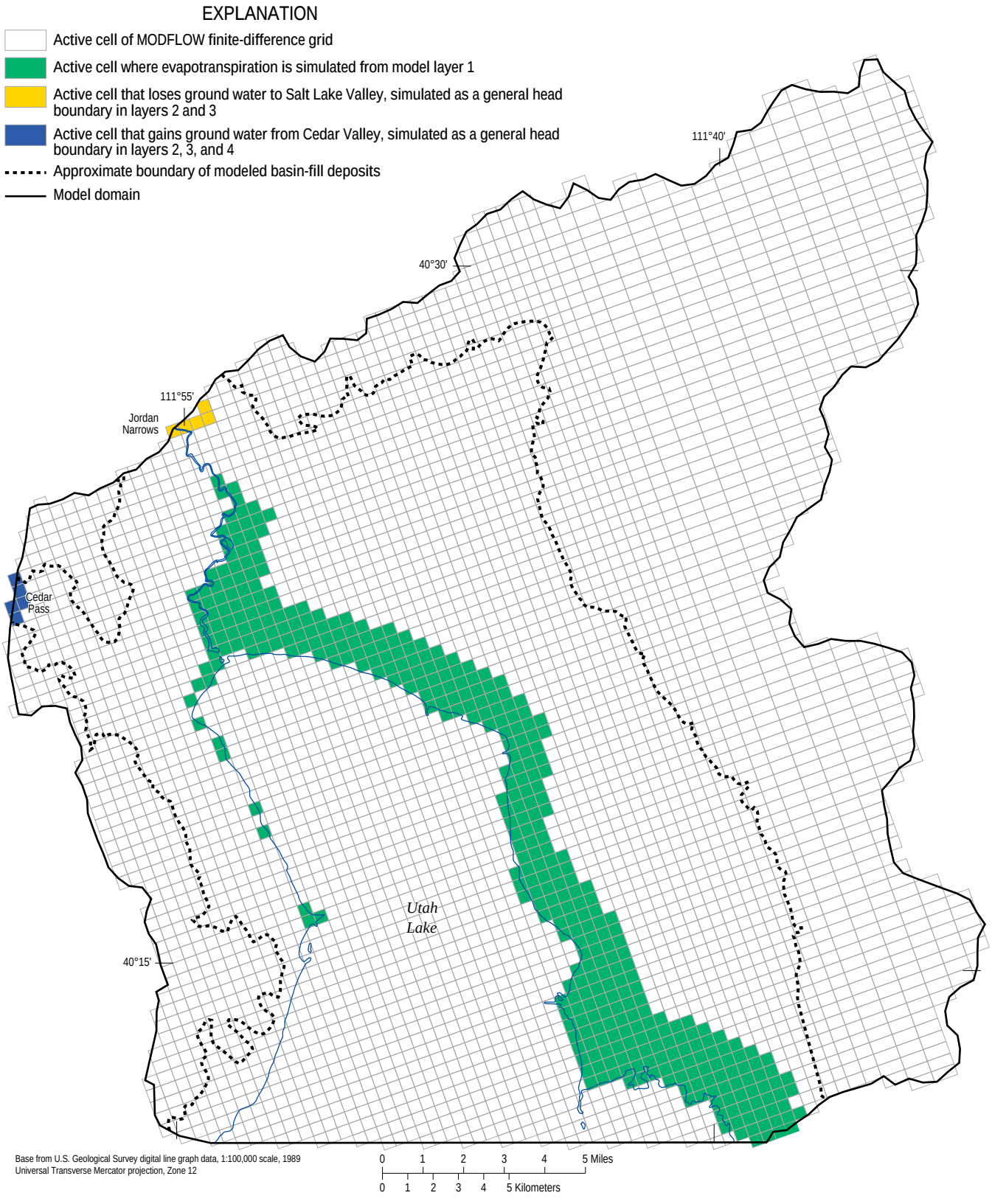

Figure 16. Model cells used to define head-dependent flux boundaries that simulate ground-water evapotranspiration and exchange of ground water with neighboring basins in the ground-water flow model of northern Utah Valley, Utah.

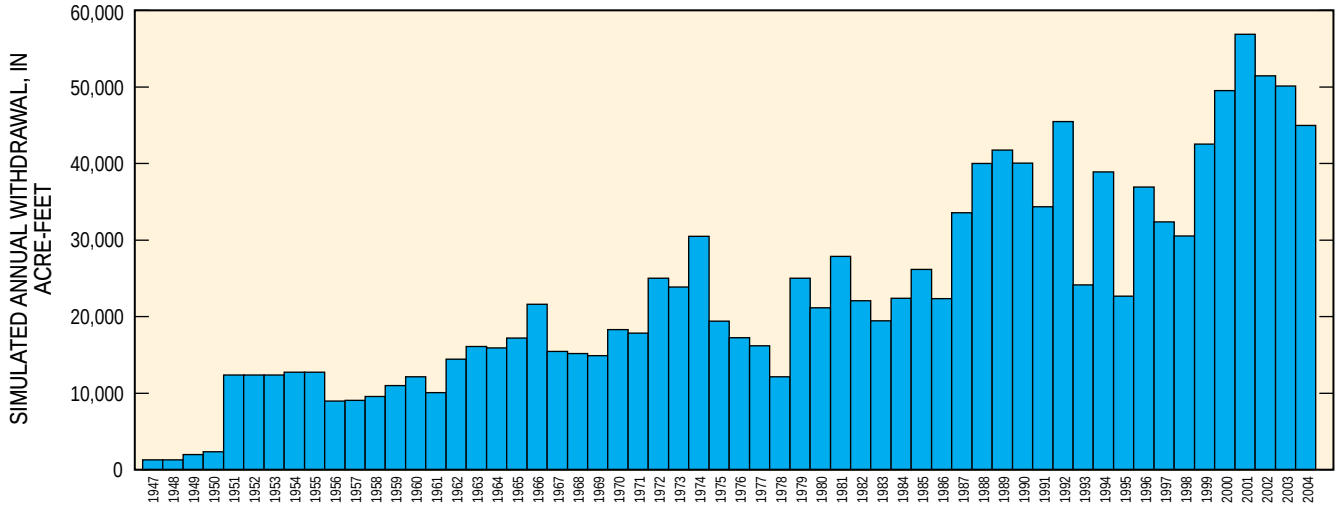

Figure 17. Annual withdrawal of ground water by public supply, irrigation, and industrial pumping wells simulated in the ground-water flow model of northern Utah Valley, Utah, 1947–2004.

Stream Package

Major streams and canals within the model domain were simulated as head-dependent flux boundaries by using the Stream Package (Prudic, 1989). In addition to simulating stream-aquifer interaction, the Stream Package has the capability to route surface water through a network of streams, tributaries, and diversions. Data needed for the Stream Package included streambed altitude, stream width, Manning's roughness coefficients, and streambed conductance. It was impractical, at the scale of this model, to obtain and use detailed measurements to describe the geometry and characteristics of streams. Instead, values were estimated and adjustments were made during model calibration. Streambed altitude was estimated from USGS 1:24,000-scale topographic maps and 10-m resolution Digital Elevation Models (National Center for Earth Resources Observation & Science, 1999). Most streams were assumed to be 10 ft wide and selected segments of larger streams (the Jordan, American Fork, and Provo Rivers) were assumed to be 15–20 ft wide. Typical values of Manning's roughness coefficients for natural channels were used (Chow, 1959). These values ranged from 0.02 for the rivers and canals with the lowest gradient and least obstructions (such as the Jordan River and Provo Reservoir Canal) to 0.06 for mountain streams with irregular and obstructed channels. Streambed conductance was adjusted during calibration.

MODFLOW-2000 allows streambed conductance to be defined as the product of a conductance multiplier for each stream segment and a streambed hydraulic conductivity parameter that can apply to multiple streams or stream segments. During calibration, adjustments were made to both the conductance multipliers and the streambed hydraulic-conductivity parameters. Making changes to the conductance multipliers allows the conductance of a streambed to vary along its length where the physical character of the streambed (or rates of stream loss or gain) might actually vary. Making changes to the hydraulic-conductivity parameter evenly scales the streambed conductance up or down for all streams or segments that the parameter applies to. The inclusion of parameters allowed for the use of sensitivity analyses to investigate the importance of fluxes through groups of streams that are similar in their location or physical character. Seven MODFLOW parameters (STR_MTN, STR_VAL, STR_PvoVal, STR_Jrdn, STR_Murdck, STR_EstCnl, STR_WstCnl) were used to modify streambed conductance in cells that simulate mountain streams and valley streams and canals in northern Utah Valley (table 2, fig. 18).

Ground-water discharge to streams in the mountains was simulated to provide some method of judging the accuracy of the model in areas where flow through bedrock is simulated. Mountain streams and their tributaries, associated with the parameter STR_MTN, are simulated in the following areas: Tickville Gulch, the Traverse Mountains, Fort Creek Canyon, Dry Creek Canyon, American Fork Canyon, Grove Canyon, Battle Canyon, Dry Canyon, Provo Canyon, Rock Canyon, and Slate Canyon (fig. 18). Comparisons of simulated gain in mountain streams to estimates of actual base flow were used to constrain bedrock hydraulic conductivity in the mountains. It was determined that only streams in the deeply incised drainage basins (American Fork and Provo Canyons) were useful for assessing the accuracy of simulated water levels in the mountain block. Other high-gradient streams likely interact with smaller zones of perched ground water and do not appear to be connected with the regional mountain-block aquifer.

Recharge from streams and canals within the primary recharge area of the valley also is simulated by using the Stream Package. Streams and irrigation canals traverse coarse-grained, permeable sediments near the mountain front in the primary recharge area where the water table is well below the bottom of the streambed. Seepage from streams that occurs in this area is one of the two largest sources of natural recharge to the basin-fill aquifers in northern Utah Valley (72,000 acre-ft

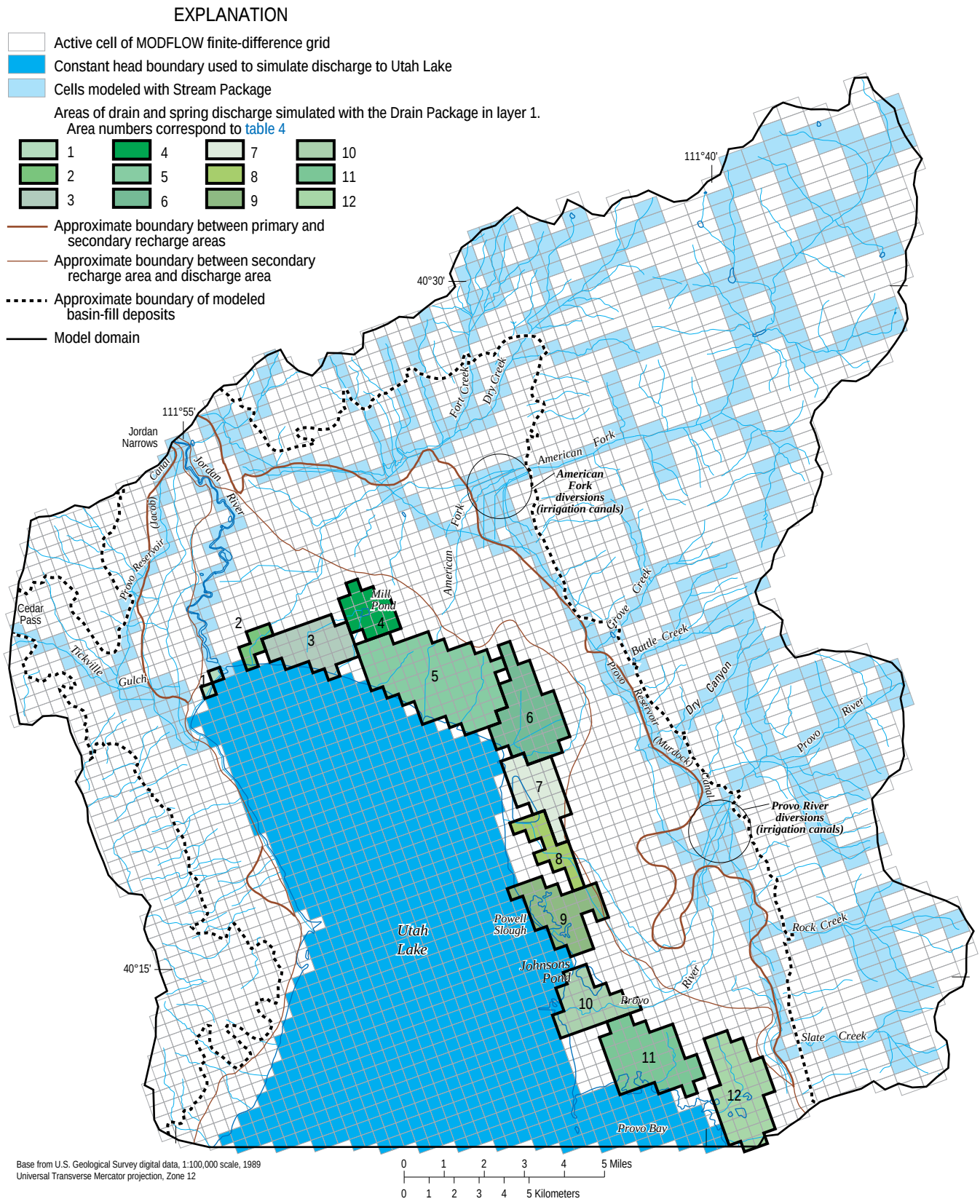

Figure 18. Model cells used to define (1) head-dependent flux boundaries that simulate aquifer interaction with selected streams, (2) head-dependent flux boundaries that simulate discharge to drains and springs near Utah Lake, and (3) the constant head boundary at Utah Lake in layer 1 of the ground-water flow model of northern Utah Valley, Utah.

and 63,000 acre-ft simulated in 1947 and 2004, respectively). Losing valley streams and their diversions (irrigation canals) that are simulated include the Provo Reservoir (Jacob) Canal, the Provo Reservoir (Murdock) Canal, Fort Creek, Dry Creek, and their major irrigation canals, American Fork and its major irrigation canals, Battle Creek, Grove Creek, the Provo River and its major irrigation canals, Rock Creek, and Slate Creek (fig. 18). Rather than routing the simulated base flow from the mountain streams into the downstream (valley) segments, gaged or estimated values of annual streamflow were specified at the head of the uppermost valley segment of each stream at the beginning of each stress period. This ensured that the proper flow was in each stream at the beginning of each stress period and allowed the model to simulate the routing of surface water into diversions and the seepage from these streams and canals that becomes recharge. The streambed hydraulic-conductivity parameters (STR_VAL, STR_PvoVal, STR_Jrdn, STR_Murdck, STR_EstCnl, and STR_WstCnl) as well as some of the conductance multipliers for particular stream segments were adjusted during calibration so that simulated stream losses approximated estimates of recharge by stream seepage in the primary recharge area reported by Cederberg and others (2009).

The Jordan River is estimated to gain 3,500–5,600 acre-ft/yr of ground water as upward leakage from the principal aquifer (Clark and Appel, 1985). This is the only gaining stream in the valley that was simulated with the stream package. Because ground-water levels in the discharge area were higher in 1947 than they have been in recent decades, the upper end of this estimated range (5,600 acre-ft/yr) was used as the calibration target for the steady-state simulation.

Drain Package

Ground-water discharge to flowing wells, drains, and springs in the discharge area of northern Utah Valley is simulated as head-dependent boundaries using the Drain Package (Harbaugh and others, 2000, p. 71). The Drain Package simulates a head-dependent flux boundary for each cell to which it is assigned, and discharge is a function of the simulated water level and drain conductance (McDonald and Harbaugh, 1988, fig. 41). Data required for the Drain Package are the altitude and conductance of the drain.

Drain and spring discharge occurs along ditches, at discrete points, and as diffuse seepage in large ponds or marshes. Measurements of drain and spring discharge were made where flow from these sources is channelized at the surface. Discharge measurements of drains and springs made at 35 locations (Cederberg and others, 2009, table 17) were grouped and modeled as 12 drain areas in model layer 1 (table 4). In some cases, multiple measurements apply to a common area of ground-water discharge. For instance, measurements from sites 25 and 26 in Cederberg and others (2009, table 17) represent different components of water discharging from Powell Slough and measurements from sites 27 and 28 in Cederberg and others (2009, table 17) represent separate components of water discharging from Johnsons Pond (fig. 18). Powell Slough and Johnsons Pond are both wetland areas fed by

Table 4. Drain areas and grouped measurements used as calibration targets for simulated discharge from drains and springs in layer 1 of the ground-water flow model of northern Utah Valley, Utah

Drain area number, see figure 17	Drain area name	Site ID of measurements from Cederberg and others (2009, table 17) that are included in each drain area	Minimum drain discharge[1], in acre-feet per year	Maximum drain discharge[1], in acre-feet per year
1	Saratoga Springs	1, 2, 3	1,500	1,500
2	Dry Creek	5	0	100
3	BYU Group 1	6, 7, 8, 9, 10	1,600	4,900
4	Mill Pond	11	3,900	21,900
5	BYU Group 2	12, 13, 14, 15, 16, 17	6,100	13,200
6	BYU Group 3	20	7,100	21,300
7	Geneva Group	21, 22	3,400	13,500
8	BYU Group 4	23, 24	500	1,500
9	Powell Slough	25, 26	1,000	18,100
10	Johnsons Pond	27, 28	400	1,700
11	Big Dry Creek	29, 30, 31	1,500	2,200
12	South Springs Group	32, 33, 34, 35	9,000	35,900
Total discharge from drains and springs			36,000	135,800

[1]Spring and drain discharge measurements were reported by Cordova and Subitzky (1965), Clark and Appel (1985), and Cederberg and others (2009).

The values listed for each group are the sum of the minimum and maximum of all point measurements that make up a group.

The minimum and maximum flows listed are the sum of all the largest or smallest measurements made, not necessarily from the same time.

ground-water discharge that is measured where it leaves ponds in ditches or small channels. In other cases, multiple measurements were grouped where they represent discharge from areas where hydrologic properties that control drain discharge are assumed to be similar (table 4).

Annual discharge from the basin-fill aquifers to drains, ditches, and springs in the discharge area surrounding Utah Lake has been reported to be as low as 54,000 acre-ft, based on measurements made in 2003–04 (Cederberg and others, 2009, table 17), and as high as 103,000 acre-ft, based on measurements made in 1980–82 (Clark and Appel, 1985, table 15). Discharge to these sources is a combination of two components: (1) deep ground water from the principal basin-fill aquifers and (2) ground water from the shallow, unconfined aquifer that was recharged locally as infiltrating runoff or irrigation water (Cederberg and others, 2009). One cause for the reduced drain and spring flows measured for 2003–04 is that water levels in confined aquifers are generally 10–20 ft lower in the discharge area than they were in 1980–82, resulting in reduced natural discharge from the primary basin-fill aquifers. However, less water was applied for irrigation in 2003–04 as a result of more-efficient irrigation practices and changes in land use from irrigated agricultural to commercial and residential, resulting in reduced recharge to the shallow unconfined aquifer. This indicates that the contribution to drain and spring discharge from local recharge to the shallow unconfined aquifer had likely decreased as well (Cederberg and others, 2009). The model is designed to simulate only the component of drain and spring discharge derived from the principal basin-fill aquifers in layer 1. Because of the range in measured drain and spring discharge and the uncertainty in the amount contributed by the deep ground-water component, the complete range of reported measurements for each drain area was considered to be a reasonable calibration target.

Twelve parameters (DRN_SARATOGA, DRN_DRYCRK, DRN_BYU_G1, DRN_MILPND, DRN_BYU_G2, DRN_BYU_G3, DRN_GENEVA, DRN_BYU_G4, DRN_POWELL, DRN_JOHNSON, DRN_BGDRCK, DRN_SSPRGS) were used to define drain hydraulic conductance and each parameter corresponds to a drain area simulated in model layer 1 (tables 2 and 4, fig. 18). The altitude of drains modeled in layer 1 was set to land surface, estimated from USGS 1:24,000-scale topographic maps and 10-m resolution Digital Elevation Models (National Center for Earth Resources Observation & Science, 1999). The drain hydraulic-conductance parameters were adjusted during calibration so that simulated steady-state discharge to modeled drain areas was within the range of grouped spring and drain measurements shown in table 4. Input to the drain package was not changed during the transient simulation. Simulated spring and drain discharge in model layer 1 varied from a maximum of about 85,700 acre-ft/yr in 1984 to a minimum of about 41,200 acre-ft/yr in 2003 as simulated water levels within the model domain vary during the transient simulation.

Hunt and others (1953) reported 27,000–32,000 acre-ft/yr in total withdrawal from wells in northern Utah Valley at a time (1938–40) when nearly all well withdrawal was from flowing wells in the discharge area. Clark and Appel (1985, p. 76) reported an average of 28,000 acre-ft/yr of withdrawal from flowing wells in northern Utah Valley from a field study done in 1981 and 1982. Flowing-well discharge is controlled by the hydraulic head in the confined aquifer penetrated by the well and by the length of time that the well is allowed to flow each year. Because the wells can be shut off, the annual discharge from flowing wells is not strictly a head-dependent process. However, hydraulic head exerts enough control on volumetric flow rates (Cederberg and others, 2009, fig. 21) that flowing well discharge was simulated as a head-dependent process by using the Drain Package.

MODFLOW-2000 allows the value of the drain conductance to be defined as the product of a parameter and a conductance multiplier (Harbaugh and others, 2000, p. 72) for each drain cell. Flowing-well discharge from the SP and DP confined aquifers was simulated from layers 2 and 3 for most of the discharge area in northern Utah Valley. The spatial distribution of drain conductance was based on the total flowing-well discharge per section (referring to the cadastral land-survey system of the U.S. Government) from the flowing-well survey done in the 1930s reported by Hunt and others (1953). In the model, areas with the largest actual flowing-well discharge were assigned the highest values of drain conductance (fig. 19). The same areal distribution is used in model layers 2 and 3 to represent flowing-well discharge from the SP and DP aquifers. One parameter (FloWel) was applied to all drain-conductance multipliers representing flowing wells in model layers 2 and 3. The parameter FloWel was varied during calibration until the simulated values of discharge from drains representing flowing wells approximated the range reported by Hunt (1953) for the steady-state simulation. The altitude of drains representing flowing wells modeled in layers 2 and 3 was specified as land surface, which was estimated from USGS 1:24,000-scale topographic maps and 10-m resolution Digital Elevation Models (National Center for Earth Resources Observation & Science, 1999). The rate of flowing-well discharge simulated by the model varied from a maximum of about 42,700 acre-ft/yr in 1984 to a minimum of about 16,500 acre-ft/yr in 2003 as simulated water levels vary during the transient simulation.

Constant Head Boundary Package

The Constant Head Boundary Package (Harbaugh and others, 2000, p. 78) was used in model layer 1 to simulate ground-water discharge to Utah Lake (fig. 18). This package allows head at the specified head boundary to vary with time between specified starting and ending heads for each stress period. Monthly lake levels were obtained from the Utah Department of Natural Resources, Division of Water Rights. At intermediate time steps during each stress period, the specified head is determined within MODFLOW by linear interpolation between the starting and ending head. MODFLOW parameters were not used with the Constant Head

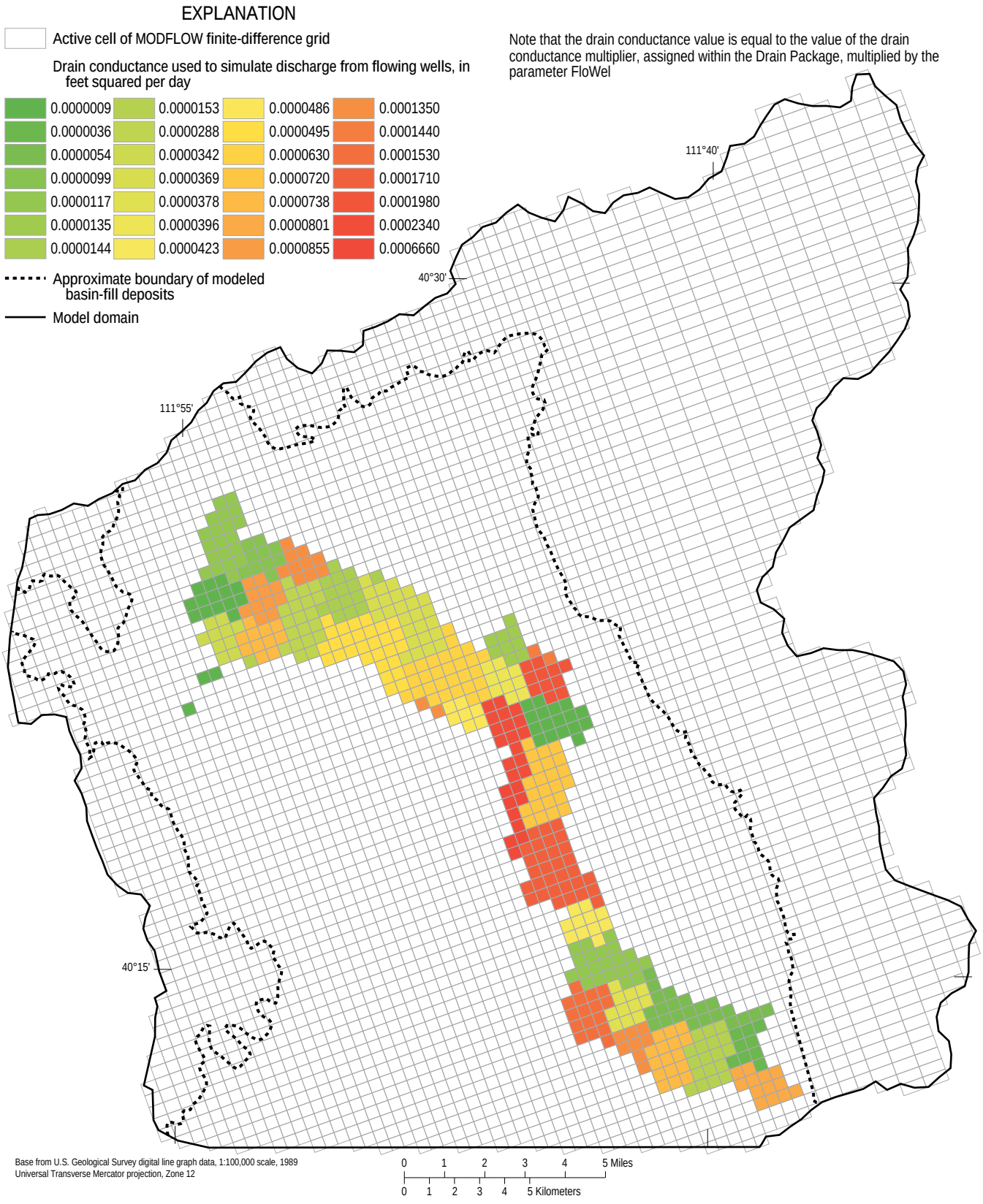

Figure 19. Distribution of drain conductance used to simulate flowing-well discharge from layers 2 and 3 with the Drain Package in the ground-water flow model of northern Utah Valley, Utah.

Boundary Package. Instead, the measured surface altitude of Utah Lake was entered at the beginning and end of each stress period. Average discharge to Utah Lake in northern Utah Valley occurs as diffuse seepage through the lake bottom and as discharge to springs in the lake near the shore. Because of the inability to make direct measurements, this is probably the most difficult component of the water budget to constrain. Total discharge to Utah Lake by these mechanisms has been estimated to be between 20,400 and 36,000 acre-ft/yr by various methods (and investigators) that are summarized by Cederberg and others (2009). Simulated annual discharge to the constant head boundary representing Utah Lake varied between about 33,500 acre-ft/yr in 1986 and 23,200 acre-ft/yr in 1992, which compares well the range of estimated values.

Model Calibration

The following section discusses the model calibration, or the process of adjusting model parameter values (such as hydraulic conductivity and specific storage) to minimize the difference between simulated and measured or estimated quantities (such as water levels, inflows, and outflows). The calibration is assessed by examining how closely the model simulates the ground-water system. The model has been developed to simulate general ground-water conditions throughout the principal aquifer in northern Utah Valley. Although the model should adequately represent long-term water-level fluctuations and basin-wide responses to changes in recharge and ground-water withdrawals, it has not been developed to simulate local effects of withdrawals or water budgets on a cell-by-cell basis.

Calibration Data

MODFLOW-2000 Observation and Sensitivity Processes were used to guide model calibration (Hill and others, 2000). These processes require that specific observations be defined in the model in order to calculate various metrics of model fit and sensitivity to individual parameters. The northern Utah Valley ground-water model was calibrated using both water-level and flow observations (drain discharge and stream seepage). Hill and Tiedeman (2007, p. 284) stress the importance of incorporating multiple kinds of observations based on field measurements rather than interpolation for the successful use of formal parameter estimation methods in non-linear ground-water models. Water-level observations used in the model are based on USGS measurements of known accuracy. Flow observations used in the model (such as spring discharge and stream seepage) are generally derived from measurements or estimates that are accompanied by significant uncertainty. Measurements of drain and spring discharge are complicated by the range of values reported by different investigators and the uncertainty in the fraction of these flows that are derived from the principal basin-fill aquifers versus the fraction that is from the shallow unconfined aquifer. Furthermore, estimates of stream seepage are based on few data.

Forty-six water-level observations were used to calibrate the steady-state simulation and an additional 915 water-level measurements from 498 wells were used as observations in the transient simulation. All water-level observations are from the USGS National Water Information System (NWIS) database. Steady-state water-level observations are specified as an altitude, meaning they possess the uncertainty in the land-surface altitude of the well itself. Although land-surface altitudes have been surveyed at a few wells, most are derived from 1:24,000-scale topographic maps with contour intervals of 10, 20, or 40 ft. As a result, most water-level observations have an associated error of one half of the value of the contour interval (5, 10, or 20 ft). In the transient simulation, water-level change is used rather than water-level altitude for the purposes of specifying the water-level observation and calculating model sensitivity statistics. This procedure greatly reduces the associated error because differencing the absolute water-level observations cancels the land-surface altitude error assuming the land-surface datum is stable and repeat depth-to-water-level measurements are accurate to within about 0.1 ft. In order to avoid excessively long model execution times, water-level observations were used for only nine of the 58 stress periods. The stress periods for which water-level observations are included (1947, 1963, 1970, 1978, 1981, 1984, 1991, 1999, and 2004) were chosen to represent periods of average and extreme (peak high and low) water levels.

Twenty-five flow observations were used to calibrate the steady-state simulation and an additional 12 flow observations were used in the transient simulation. Steady-state flow observations include 12 values of drain discharge (table 5) that correspond to the drain areas shown on figure 18 and 13 values of stream gain or loss (table 5) that correspond to model cells where selected streams and canals are simulated with the Stream Package (fig. 18). Flow observations of gaining streams (where ground-water discharge occurs) are included for the canyon sections of the American Fork and the Provo River as well as for the Jordan River between Utah Lake and Salt Lake Valley. Flow observations representing losing streams and canals (where ground-water recharge occurs) are included for portions of all major streams and canals that cross the primary recharge area in northern Utah Valley. All of the flow observations used during the steady-state simulation are based on estimates rather than measurement because no measurements of these types were available from the late 1940s. The values used for drain observations are the average of measurements made during 1962–63, 1981–82, and 2003–04, by Cordova and Subitzky (1965), Clark and Appel (1985), and Cederberg and others (2009), respectively. The values used for stream gains and losses are estimates based on the methods described by Cederberg and others (2009).

When using the MODFLOW-2000 Observation and Sensitivity Processes, it is best to use observations based on measurements with known accuracy in order to properly weight the observations (Hill and others, 2000). Even though

Table 5. Flow observations used with the MODFLOW-2000 Observation and Sensitivity Processes in the ground-water flow model of northern Utah Valley, Utah.

[PRA, Primary recharge area for the basin-fill aquifer system in northern Utah Valley]

Name of flow observation	Description of flow observation	Observation value, in acre-feet per year[1]	Simulated equivalent, in acre-feet per year[1]
Saratoga_1	Saratoga Springs, drain discharge 1947	-1,500	-110
Saratoga_2	Saratoga Springs, drain discharge 2004	-1,600	-50
DryCrk_1	Dry Creek, drain discharge 1947	-100	0
DryCrk_2	Dry Creek, drain discharge 2004	0	0
BYU_grp1_1	BYU Group 1, drain discharge 1947	-3,100	-1,000
BYU_grp1_2	BYU Group 1, drain discharge 2004	-1,600	-600
MillPond_1	Mill Pond, drain discharge 1947	-15,900	-8,400
MillPond_2	Mill Pond, drain discharge 2004	-3,900	-3,300
BYU_grp2_1	BYU Group 2, drain discharge 1947	-10,100	-9,600
BYU_grp2_2	BYU Group 2, drain discharge 2004	-6,200	-5,700
BYU_grp3_1	BYU Group 3, drain discharge 1947	-14,200	-16,000
BYU_grp3_2	BYU Group 3, drain discharge 2004	-7,100	-9,800
GENEVA_1	Geneva Group, drain discharge 1947	-6,800	-7,100
GENEVA_2	Geneva Group, drain discharge 2004	-6,800	-3,500
BYU_grp4_1	BYU Group 4, drain discharge 1947	-1,000	-1,200
BYU_grp4_2	BYU Group 4, drain discharge 2004	-1,500	-500
Powell_1	Powell Slough, drain discharge 1947	-8,300	-7,600
Powell_2	Powell Slough, drain discharge 2004	-5,900	-4,900
Johnson_1	Johnsons Pond, drain discharge 1947	-900	-1,500
Johnson_2	Johnsons Pond, drain discharge 2004	-600	-900
BigDryCk_1	Big Dry Creek, drain discharge 1947	-1,900	-2,100
BigDryCk_2	Big Dry Creek, drain discharge 2004	-1,500	-1,200
S.Sprngs_1	South Springs Group, drain discharge 1947	-21,000	-19,000
S.Sprngs_2	South Springs Group, drain discharge 2004	-18,200	-11,500
JacobCanal	Loss from the Provo Reservoir (Jacob) canal in the PRA	500	400
JordanRiver	Jordan River gain in the valley	-5,600	-5,500
Fort&Dry_Val	Combined loss from Fort and Dry Creeks where they cross the PRA	7,600	10,300
AF_Cyn1947	American Fork gain in the mountains	-12,900	-13,000
AF_Mouth	Loss from the American Fork and associated irrigation canals in the PRA	13,900	14,300
Grove_Val	Loss from Grove Creek where it crosses the PRA	500	700
Battle_Val	Loss from Battle Creek where it crosses the PRA	500	700
Provo_Canyon	Provo River gain in the mountains	-3,000	-2,900
ProvVal_Loss	Loss from the Provo River in the PRA	30,000	27,000
Provo_Canals	Loss from selected Provo River irrigation canals in the PRA	7,000	7,000
Murdock	Loss from the Provo Reservoir (Murdock) Canal	9,500	9,400
Rock_Val	Loss from Rock Creek where it crosses the PRA	1,800	1,200
Slate_Val	Loss from Slate Creek where it crosses the PRA	800	700

[1]A negative value indicates flow out of the ground-water system (discharge) and a positive value indicates flow into the ground-water system (recharge).

these observations were not based on measurements with known accuracy, they were included (with much lower weighting than water-level measurements) to help constrain the steady-state model calibration prior to making transient model runs. Twelve additional flow observations were included for the final stress period of the transient model (table 5) that were based on measurements of spring and drain discharge made during 2003–04 by Cederberg and others (2009).

Parameter Adjustment and Sensitivity

During model calibration, parameters were adjusted to achieve a model that reasonably represents the ground-water system by minimizing the sum of squared errors between simulated and measured water levels, while still approximating known or estimated water-budget components. Parameter adjustments were made manually with the aid of sensitivity analyses from the MODFLOW-2000 Sensitivity Process. Horizontal and vertical hydraulic conductivity, specific yield and specific storage, and recharge from precipitation over the mountain block were adjusted both by modifying the distribution of values within multiplier arrays and by changing the parameter values. The conductance of head-dependent boundaries simulated with the Drain, Stream, and General Head Boundary Packages was adjusted by modifying the parameter values. Parameters defining recharge from precipitation and irrigation in the valley, withdrawal from wells, and maximum ET rate were not modified.

The sensitivity of model-simulated heads and flows to parameters was used to aid model calibration. Composite-scaled sensitivities (CSS) reflect the total amount of information provided by the observations for the estimation of each parameter (Hill and Tiedeman, 2007, p. 50). In other words, they provided an overall view of model sensitivity to each parameter within the context of the set of observations used. Generally, model observations provide enough information to estimate parameters that have CSS greater than 1 (fig. 20). The high CSS values of the parameters PumpWel, STR_VAL, and STR_PvoVal indicate that simulated heads and flows at observation locations are more sensitive to pumping and recharge by seepage from the major mountain streams than to other model parameters. Seepage from Fort Creek, Dry Creek, American Fork, and the Provo River are controlled by the streambed conductance parameters STR_VAL and STR_PvoVal. When examining CSS, the distribution of observations must be considered. The parameters STR_VAL and STR_PvoVal are associated with high CSS partly because they control a large overall fraction of ground-water recharge and partly because of the high concentration of water-level observations in the vicinity of this recharge. The MODFLOW-2000 Sensitivity Process can not adequately evaluate model-parameter sensitivity to a stress if there are few observations in the vicinity of that stress. Composite-scaled sensitivities indicate that simulated heads and flows also are sensitive to: (1) parameters that control hydrologic properties in many HUF units that represent alluvium and bedrock (hk_CF1, vani_CF1, SS_QT, hk_SP, SS_Valley, hk_rock5, hk_QT, hk_DP, hk_PLB, SS_Mtn, hk_rock2, hk_CF2, vani_CF2, hk_WBR, hk_CF3, and vani_CF3); (2) parameters that control other sources of recharge from stream seepage, irrigation, and precipitation over the mountains (STR_Murdck and STR_EstCnl , irr_rch, and rock1_rch and rock2_rch, respectively); and (3) discharge to flowing wells, ET, some drains, and the Jordan River (FloWel, base_et, DRN_BYU_G2 and DRN_GENEVA, and STR_Jrdn, respectively) (fig. 20). Though parameters controlling hydrologic properties of the shallow, confining unit on the east side of the valley (hk_CF1 and vani_CF1) have some of the highest CSS, parameters controlling the hydrologic properties for the deeper confining units (hk_CF2, vani_CF2, hk_CF3, and vani_CF3) have notably lower CSS. This likely is because the upper confining unit has direct control on major sources of ground-water discharge simulated with the Drain Package (flowing wells, drains, and springs) and, thereby, heads throughout the discharge area near Utah Lake.

Of the 55 parameters used in the model, 29 have CSS values greater than 1 (fig. 20), indicating that the observation data provided sufficient information to estimate more than half of the parameters used. Nearly all parameters that control recharge or horizontal hydraulic conductivity have CSS values greater than 1. Twenty-six of the 55 parameters (not shown in fig. 20) have CSS values less than 1 and 7 of those parameters have CSS values less than 0.1. Although the model is relatively insensitive to modifications in many of these parameters, they were included to make the model flexible and to allow adjustments to be easily made to specific components of the simulated ground-water system. For example, parameters controlling drain conductance for Mill Pond, Powell Slough, and Johnsons Pond (DRN_MILPND, DRN_POWELL, and DRN_JOHNSON) have CSS values less than 0.25. Despite the lack of sufficient information to reliably estimate these parameters, the ability to individually modify the conductance of these drains improved the match of simulated heads and drain discharge to measured heads and estimated discharge in each of these localized areas.

Hydraulic-Conductivity Parameters

Because of the complicated geology involving various types of bedrock and a lacustrine/alluvial depositional environment, 15 HK parameters and 7 VANI parameters were used to define horizontal hydraulic conductivity and vertical anisotropy. A separate HK parameter was assigned to each hydrogeologic unit representing basin-fill deposits by using multiplier arrays within hk_zone 1 (table 2, figs. 11a –11i and 11k). Bedrock HK was assigned using five HK parameters to five zones in hydrogeologic unit HUF10_BR (table 2, figs. 10 and 11j). The seven VANI parameters were constant over the entire hydrogeologic unit to which each is assigned (table 2) and, therefore vertical hydraulic conductivities in these units were spatially consistent with HK.

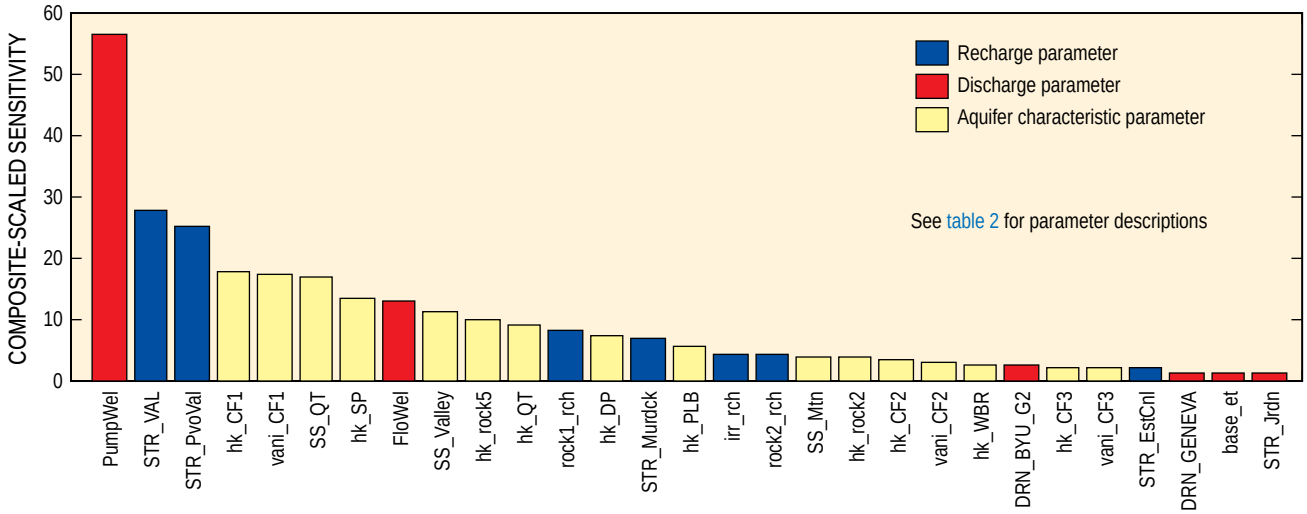

Figure 20. Composite-scaled sensitivity of selected model parameters (those with composite-scaled sensitivity values greater than 1) to observations for the steady-state simulation of northern Utah Valley, Utah.

The initial distribution of HK in basin-fill deposits was based on the previous calibrated model of northern Utah Valley (Clark, 1984). In that model, an early version of MODFLOW was used with a different numerical solver (McDonald and Harbaugh, 1984) that required values for transmissivity (T), rather than HK, to represent horizontal ground-water flow through cells in a confined model layer. In areas where the current and previous ground-water models spatially overlap, initial estimates for the HK parameters in the current model were calculated by dividing T from the previous model by the thickness of the corresponding hydrogeologic unit in the new model. In areas where the new model domain extends beyond the domain of the previous flow model, initial HK values were assumed to be similar to areas with analogous aquifer material, as discussed in the "Model Construction" section of this report. The confining unit (HUF8_CF4) and underlying aquifer (HUF9_WU) west of the Jordan River were assumed to have HK values within the same range as the shallow confining unit (HUF2_CF1) and underlying aquifer (HUF3_SP) east of the Jordan River and HK values of bedrock aquifers were assumed to fall within the range of values published by Domenico and Schwartz (1998, table 3.2, p. 39) for similar rock types (fig. 9).

Final simulated HK values (the product of the parameter and the value of the multiplier array at each model cell) in hydrogeologic units representing unconsolidated basin-fill aquifers (HUF1_surf, HUF3_SP, HUF5_DP, HUF7_QT, HUF9_WU, HUF11_PLB) range from about 1 to 1,000 ft/d (figs. 11a, 11c, 11e, 11g, 11i, and 11k). The range of HK values in basin-fill deposits is similar to that used in the previous model of 25 to more than 500 ft/d (Clark, 1984, p. 14) with the exception of smaller values used in the current model for the shallow unconfined aquifer. Simulated values in HUF units representing confining units range from 0.03 to 5 ft/d (figs. 11b, 11d, 11f, and 11h). The largest HK values in the confining hydrogeologic units likely represent localized lenses of coarse-grained material where fine-grained material is absent and are located near points of spring discharge in HUF2_CF1 and HUF4_CF2 and near where the Provo River enters the valley in HUF4_CF2 (figs. 11b and 11d).

Horizontal hydraulic conductivity in bedrock within the mountain block was adjusted during calibration mainly to simulate base flow to major mountain streams. The value of HK in the bedrock aquifer underlying basin-fill deposits on the west side of the valley was adjusted to improve the match between simulated and measured water levels in that area. Simulated values of HK in bedrock in the mountain block range from 0.02 to 0.55 ft/d (fig. 10). The largest value of HK in bedrock, 50 ft/d, occurs where fractured limestone underlies basin-fill deposits west of the Jordan River (fig. 11j) and short-term pumping tests show almost no drawdown.

Hydrogeologic units used to simulate confining layers have final VANI values ranging from 46 to 322 yielding vertical hydraulic-conductivity values of 5.0×10^{-4}–0.12 ft/d. The distribution and values of these parameters were adjusted during model calibration. The effective range of vertical hydraulic conductivity in hydrogeologic units representing confining units compares well with the average value of 1.0×10^{-3} ft/d reported for similar material in northern Utah Valley by Clark and Appel (1985, p. 47) and the range of values from 5.7×10^{-5} to 5.8×10^{-2} ft/d for similar material from nearby Salt Lake Valley reported by Thiros (1992, table 12). The smallest simulated values of vertical hydraulic conductivity in the confining units occur near or beneath Utah Lake and the largest values occur where ground water is discharged from springs in the overlying hydrogeologic units. It is likely that the areas of highest vertical conductivity coincide with localized lenses of coarse-grained material where fine-grained material is absent.

Storage Parameters

Two parameters were used to define specific yield for unconfined ground-water flow and three to define specific storage for confined ground-water flow simulated in the model. One specific-yield parameter (SY_Valley) is used for all hydrogeologic units representing basin-fill deposits and another (SY_Mtn) for HUF10_BR, which represents all areas of bedrock (table 2). Two specific-storage parameters (SS_Valley and SS_QT) were used for hydrogeologic units representing basin fill and another (SS_Mtn) for HUF10_BR (table 2). Sixteen individual specific-storage parameters originally were assigned; one to each of the 11 HUF units and one to each HK_zone in the mountain block. Simulated values of hydraulic head and flow generally were insensitive to each of the 16 originally defined specific-storage parameters. Thus, specific-storage parameters were combined into two parameters (SS_Valley and SS_Mtn) in order to reduce the total number of MODFLOW parameters and execution times of the Sensitivity Process. Further sensitivity analysis indicated that a larger specific storage was required for HUF7_QT than for the other basin-fill units, resulting in the addition of the SS_QT parameter.

The storage parameter values were adjusted during model calibration and sensitivity analysis. Generally, storage was reduced during model calibration. No multiplier arrays were used to define storage; thus the simulated values are equal to the parameter values listed in table 2. Final specific-yield values for the basin-fill and bedrock aquifers are 0.01 and 0.005, respectively. Final specific-storage values for basin fill (exclusive of the QT aquifer), bedrock, and deep QT aquifers are 4.0×10^{-5} ft^{-1}, 7.0×10^{-7} ft^{-1}, and 1.35×10^{-5} ft^{-1}, respectively. When converted from values of specific storage to storage coefficients (specific storage multiplied by the aquifer thickness), the simulated values range from 3.5×10^{-5} to 1.2×10^{-2} and compare well to the range of storage coefficients derived from aquifer tests (Clark and Appel, 1985, table 9) and used in the previous model (Clark, 1984, p. 18), which range from 6.0×10^{-6} to 1.0×10^{-3}.

Recharge Parameters

Recharge from precipitation over the mountain block was adjusted during calibration by varying recharge parameters in two zones where this component of recharge is applied (table 2). This is estimated to be the largest component of recharge to the principal aquifer as well as the one with the most uncertainty. The initial distribution of recharge from precipitation over the mountain block was assigned by using a multiplier array derived directly from the results of the BCM. Cederberg and others (2009) explain that recharge estimates from the BCM are likely too low, specifically in the American Fork drainage basin. Therefore, the multiplier array was divided into two zones: one that encompasses the American Fork drainage basin and another that includes the remainder of the mountain block (fig. 11) so that recharge could be increased in the American Fork drainage basin. Changes were made to these recharge parameters to better match water levels in wells around the Highland and Provo benches and base flow in the mountain stretches of the American Fork and Provo Rivers. In the primary recharge area, estimates of recharge from the infiltration of precipitation and by seepage from irrigated fields were calibration targets rather than calibration variables and thus, were not varied during calibration.

Other Parameters

Twenty-two conductance parameters at head-dependent boundaries simulated with the Drain, Stream, and General Head Boundary Packages also were adjusted during calibration. Measurements of these conductance values are not available; therefore, they were considered calibration variables. Changes were made to these conductance parameters to better match discharge observations at springs, estimated base flow to streams in the mountains, estimated recharge by stream seepage near the mountain front, and estimated subsurface ground-water flow between northern Utah and neighboring valleys. Four streambed conductance parameters that control recharge near the mountain front (STR_Val, STR_PvoVal, STR_Murdck, and STR EstCnl), one streambed conductance parameter that controls discharge from the Jordan River (STR_Jrdn), and three drain conductance parameters (FloWel, DRN_BYU_G2, and DRN_GENEVA) have CSS values greater than 1 (fig. 20). The remaining 14 conductance parameters associated with the Drain, Stream, and General Head Boundary Packages (not shown in fig. 20) have CSS values ranging from 0.7 to as low as 1×10^{-3}.

Assessment of Steady-State Calibration

Ground-water levels measured in March 1947 and the conceptual ground-water budget for 1947 were compared to simulated values to determine if the model adequately simulates the ground-water system as it was at that time. MODFLOW-2000 calculates simulated values of water levels at the location of observations, the difference between observation values and simulated values (residuals), and other statistical measures of model fit. The model calibration was assessed according to the model fit to observations and to the ability of the model to simulate estimated components of basin-wide ground-water budgets. Forty-seven water levels measured by the USGS were used as hydraulic-head observations in model layers 1–4 and 25 flow estimates, including 13 of stream seepage and 12 of spring and drain discharge, were used as observations that represent recharge or discharge in model layer 1.

The steady-state ground-water flow model adequately simulates water levels measured in March 1947 in most areas. Evaluation of the steady-state water-level residuals at the 47 sites in model layers 1–4 shows that 19 simulated levels are within 5 ft of measured water levels, 17 are within 5 to 10 ft of measured levels, and 11 are more than 10 ft different (fig. 21).

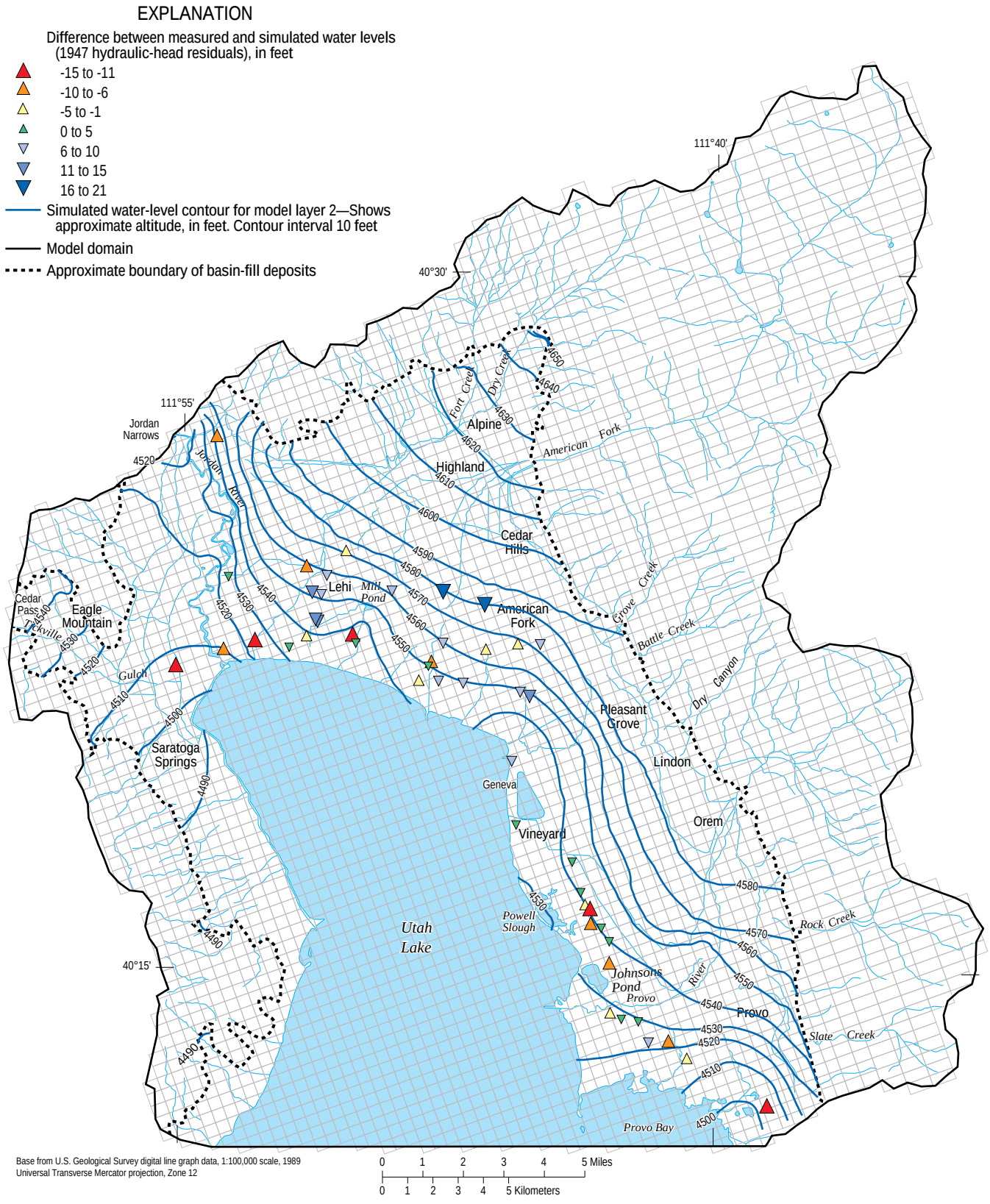

Figure 21. Hydraulic-head residuals (measured minus simulated water levels) in model layers 1–4 for the steady-state simulation (1947) and simulated water-level contours in model layer 2 of the ground-water flow model of northern Utah Valley, Utah.

Hydraulic head residuals in all model layers are distributed evenly throughout the area indicating no significant model bias. Simulated water-level contours from model layer 2 illustrate the general direction of horizontal ground-water movement in the basin-fill aquifers (fig. 21).

Conceptual and simulated ground-water budgets are presented in table 6. The conceptual budget is composed of estimates derived from several investigations that represent hydrologic conditions in 1947. Recharge by seepage from streams and canals generally is estimated as a percentage of annual streamflow as reported by Clark and Appel (1985) and Cederberg and others (2009). Subsurface inflow from Cedar Valley is the average value reported by Feltis (1967). Methods used to estimate recharge by irrigation and precipitation are explained by Cederberg and others (2009). Estimates for discharge by ET, to flowing wells, to the Jordan River, and to Utah Lake were reported by Clark and Appel (1985). Discharge by pumping wells is derived from records archived by the USGS and the Utah Division of Water Rights. Discharge to the mountain segments of the American Fork and Provo River represent base flow to these streams and are estimated according to the methods described by Cederberg and others (2009). Estimates of subsurface outflow to Salt Lake Valley and of discharge to drains and springs around Utah Lake were made by multiple investigators and are discussed in Cederberg and others (2009).

Conceptual ground-water water budgets for the principal basin-fill aquifer system in northern Utah Valley presented by Clark and Appel (1985, table 5) and Cederberg and others (2009, table 5) comprise a large component of recharge referred to as "subsurface inflow from bedrock" or "subsurface inflow from the mountain-block." This refers to ground water that originates as seepage from precipitation over the mountain block. The current model domain includes large areas of the mountain block that surround the basin fill, and recharge that originates as seepage from precipitation in these areas is

Table 6. Conceptual ground-water budget for 1947 and ground-water budget simulated in the steady-state ground-water flow model of northern Utah Valley, Utah.

Budget component	Conceptual flow, in acre-feet per year	Method of simulation	Simulated flow, in acre-feet per year
Recharge			
Seepage from the Provo Reservoir (Jacob) Canal	500	STR package	400
Seepage from Fort Creek and Dry Creek and associated irrigation canals	7,600	STR package	10,300
Seepage from American Fork and associated irrigation canals	13,900	STR package	14,300
Seepage from Grove Creek	500	STR package	700
Seepage from Battle Creek	500	STR package	700
Seepage from Provo River and associated irrigation canals	37,000	STR package	35,000
Seepage from Rock Creek	1,800	STR package	1,200
Seepage from Slate Creek	800	STR package	700
Seepage from the Provo Reservoir (Murdock) Canal	9,500	STR package	9,400
Subsurface inflow from Cedar Valley	7,500	GHB package	8,800
Seepage from irrigated fields, lawns, and gardens in the primary recharge area	7,000	RCH package	7,000
Infiltration from precipitation on primary recharge area in the valley	3,200	RCH package	3,100
Infiltration from precipitation over the mountain block	68,500	RCH package	78,400
Total Recharge (rounded)	**158,000**		**170,000**
Discharge			
Evapotranspiration	8,000	ET package	8,800
Pumping wells	1,300	WEL package	1,300
Flowing wells (includes stock wells)	27,000 to 32,000	DRN package	32,900
Drains and springs around Utah Lake	54,000 to 103,000	DRN package	73,500
Subsurface outflow to Salt Lake Valley	2,500	GHB package	2,500
Discharge to the Jordan River	3,500 to 5,600	STR package	5,500
Discharge to the American Fork in the mountains	12,900	STR package	13,000
Discharge to the Provo River in the mountains	3,000	STR package	2,900
Discharge to Utah Lake	25,000 to 37,000	CHD package	31,200
Total Discharge (rounded)	**137,000 to 205,000**		**172,000**

simulated as a specified flux with the Recharge Package. The recharge that originates as seepage from precipitation over the mountain block moves downward, through fractured bedrock, and toward the valley. A fraction of this recharge emerges, still within the mountain block, as discharge in the form of base flow in perennial streams or springs. The remaining fraction enters the unconsolidated basin fill as "subsurface inflow from the mountain-block." The model equivalent to "subsurface inflow from the mountain block" is the difference between the recharge as infiltration of precipitation over the mountain block and the base flow in perennial mountain streams, simulated as discharge to the mountain segments of the American Fork and Provo River (table 6).

Simulated budget components generally compare well with conceptual budget components. The largest absolute differences are associated with recharge as seepage from Fort and Dry Creeks and associated canals, as seepage from the Provo River and associated canals, and as infiltration from precipitation over the mountain block (table 6). More than 40 percent (72,700 acre-ft/yr) of the total recharge (170,000 acre-ft/yr) occurs as seepage from streams and canals that are simulated as head-dependent boundaries. Simulated recharge from Fort Creek, Dry Creek, and their associated canals exceed recharge estimated for the conceptual model by 2,700 acre-ft (about 35 percent of the conceptual model estimate) during the steady-state simulation. Seepage estimates from Fort and Dry Creeks were based on correlations with measurements made on the American Fork. Because Fort and Dry Creeks have only a few years of gaged data, flow in those streams also is an estimate for most years. Many values of stream seepage in the conceptual budget are based on similar estimates and likely possess considerable uncertainty. Considering the uncertainty in these estimates and the generalizations pertaining to streambed hydrologic characteristics used in the Stream Package, this is not an unreasonable error in the model. Simulated recharge from the Provo River and associated canals is 2,000 acre-ft less than the estimated conceptual-model recharge during the steady-state simulation, or about 5 percent less than the estimated recharge of 37,000 acre-ft. Simulated recharge from the infiltration of precipitation over the mountain block, a calibration variable and one of the most uncertain components of the ground-water budget (Cederberg and others, 2009), exceeds the estimated amount by almost 9,900 acre-ft. Recharge from irrigated fields, lawns and gardens, and from precipitation on the valley is specified in the model and was not adjusted during calibration. Simulated recharge from these sources matches conceptual recharge within the error imparted by discretizing the recharge rates and rounding the results.

Some of the conceptual discharge components in table 6 (flowing wells, drains and springs around Utah Lake, discharge to the Jordan River, and discharge to Utah Lake) are reported as a range of measurements or as estimates made by different investigators. None of these values is based on actual measurements made in 1947. Therefore, simulated discharge for these components was compared to the range of conceptual discharge. Discharge to flowing wells, the Jordan River, and Utah Lake were all considered calibration targets during calibration. The simulated values for these ground-water budget components are either within or, in the case of flowing-well discharge, near the upper end of the estimated range. The conceptual ground-water budget component with the largest estimated range is discharge to drains and springs around Utah Lake. As previously discussed, the fraction of measured discharge to these drains and springs that comes from the underlying confined basin-fill aquifers is unknown. Therefore, drains and springs were grouped by area as discussed in the "Model Construction" section of this report and simulated discharge during the steady-state simulation was compared with the estimated range of discharge to each area (fig. 22, table 4).

Simulated discharge is within the range of estimated discharge for all of the areas except BYU-Group 1 and Saratoga Springs (areas 1 and 3 in table 4 and fig. 18). During calibration, the model was not capable of simulating sufficient discharge to BYU-Group 1 without affecting the nearby drain and spring areas, Mill Pond and BYU-Group 2. When the model was adjusted to allow more discharge to BYU-Group 1, discharge to Mill Pond and BYU-Group 2 was reduced. Mill Pond is a large natural spring area near the northern part of Utah Lake with substantial ground-water discharge from the principal aquifer indicated by water-level contours from 1947 (Clark, 1984, fig. 11), 1981 (Clark and Appel, 1985, fig. 23), and 2004 (Cederberg and others, 2009). In order to simulate sufficient discharge to Mill Pond, discharge to BYU-Group 1 had to be reduced. It is possible that discharge from BYU-Group 1 chiefly is return flow of shallow ground water that originated as nearby runoff or unconsumed irrigation water, which is not simulated.

It was not possible to increase the discharge from Saratoga Springs without causing water levels to be too high in the Saratoga Springs area. Discharge to Saratoga Springs is warmer than most ground water in northern Utah Valley (Dustin and Merritt, 1980) and likely incorporates fault-related discharge from a deeper, regional flow system that is not simulated by this model. Saratoga Springs is located on the northwestern end of Utah Lake and west of the Jordan River. Because few water-level or flow data are available west of the Jordan River, especially during the early stress periods, model calibration is considered to be less accurate in that area. Similarities between simulated and measured water levels and comparison of the simulated and conceptual ground-water budgets indicate that most recharge and discharge is adequately simulated and that the distribution of aquifer characteristics in the model adequately represents the ground-water system.

The remaining head-dependent components of discharge (discharge by ET, to the mountain segments of the American Fork and Provo River, and as subsurface outflow to Salt Lake Valley through the Jordan Narrows) were considered calibration targets, and simulated values compare well with estimated values for all of these components during the steady-state simulation. Withdrawal from pumping wells was specified and not varied during calibration of the steady-state simulation.

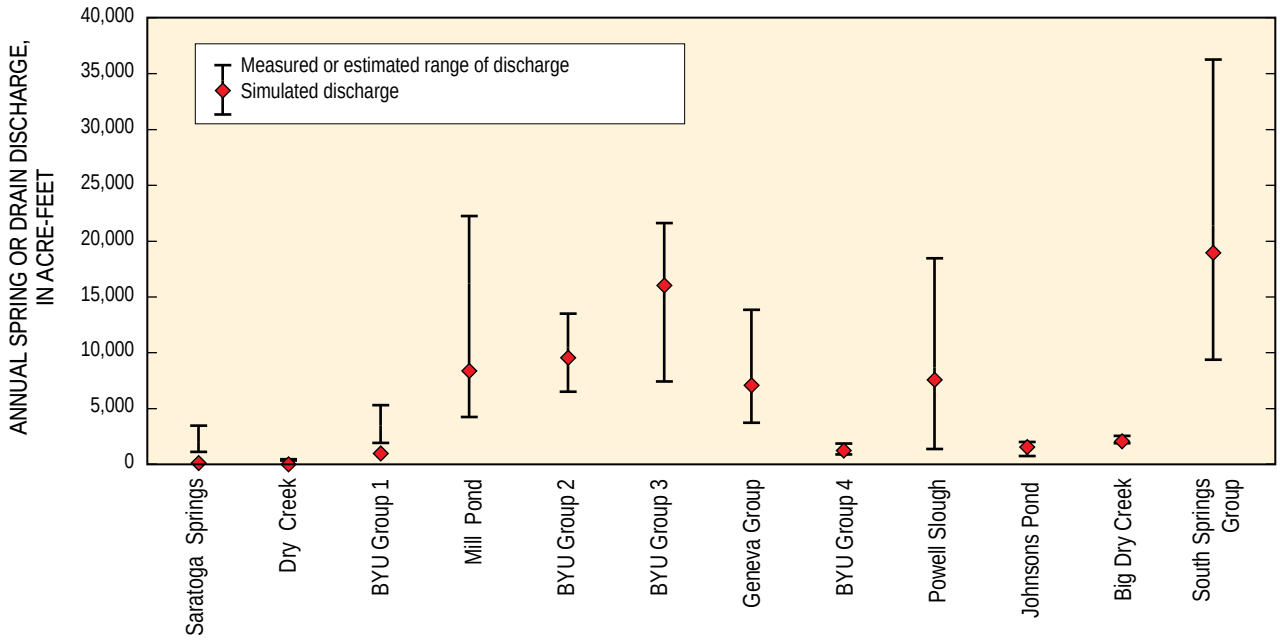

Figure 22. Simulated and measured or estimated range of discharge from drains and springs in model layer 1 in the steady-state simulation of northern Utah Valley, Utah.

Assessment of Transient-State Calibration

Water-level measurements made in March or April for the years 1947, 1963, 1970, 1978, 1981, 1984, 1991, 1999, and 2004 were used as observations in the transient simulation. At wells with more than one water-level measurement, the change in water level between measurements was used as an observation instead of the water level. In the transient simulation, 915 water-level measurements from 498 wells were used as hydraulic-head observations in model layers 1–4 and an additional 12 estimates of spring and drain flows were used as observations that represent discharge from model layer 1.

The emphasis of the transient calibration was to adjust the model to more-accurately simulate measured water-level fluctuations and individual components of the hydrologic budget through time while keeping the aquifer properties in an acceptable range. Water levels measured in 42 wells throughout the valley (figs. 23 and 24) were compared to simulated water levels. These wells were selected on the basis of their period of record (generally more that 20 years of consecutive annual water-level measurements) and their representation of the range of hydrologic conditions at different locations and depths. Wells 1 through 39 are the same as those used to evaluate the performance of the previous ground-water model (Clark, 1984) in a post-audit simulation for the 20-year period following its calibration (Thiros, 2006, figs. 8 and 9). Wells 40, 41, and 42 were added to evaluate the performance of the current model in areas along or outside of the previous model boundary.

Measured water levels generally fluctuate in response to annual and long-term changes in precipitation and to well withdrawals (fig. 24). Simulated water levels also fluctuate in response to these changes and, in most cases, the magnitude and timing of these fluctuations reasonably match the changes in measured water levels. For example, the highest measured and simulated water levels in many wells occur in 1984 in response to the wetter-than-normal conditions during 1982–84. In some areas, simulated water levels do not match the magnitude of short-term measured water-level fluctuations. The best example of this is in well 4 during the 1990s when measured year-to-year water-level changes are from 10 to 30 ft (fig. 24). Both measured and simulated water-level fluctuations at individual wells probably are influenced by local ground-water withdrawals. Incorrect estimates of annual withdrawals at individual wells or water-level measurements made when nearby production wells are active may contribute to some of the difference between the measured and simulated values in these areas.

Many of the largest measured water-level variations occur in wells 3, 4, 8, 29, 31, and 33 which are located close to the mountain front on the east side of the valley where the basin-fill aquifer is unconfined (fig. 23). Overall, simulated water-level trends closely approximate measured water-level trends in these wells (fig. 24), which indicates that the updated methods of simulating recharge over the mountain block with the Recharge Package and as seepage from streams and canals in the primary recharge area with the Stream Package are appropriate.

Less water-level variation is seen in wells located closer to the discharge area, near Utah Lake. Wells 5, 7, 30, 32, and 34 are examples of wells located between the recharge and discharge areas, where aquifers are confined but water levels generally are not above land surface. Measured water levels in most of these wells show an overall long-term decline and

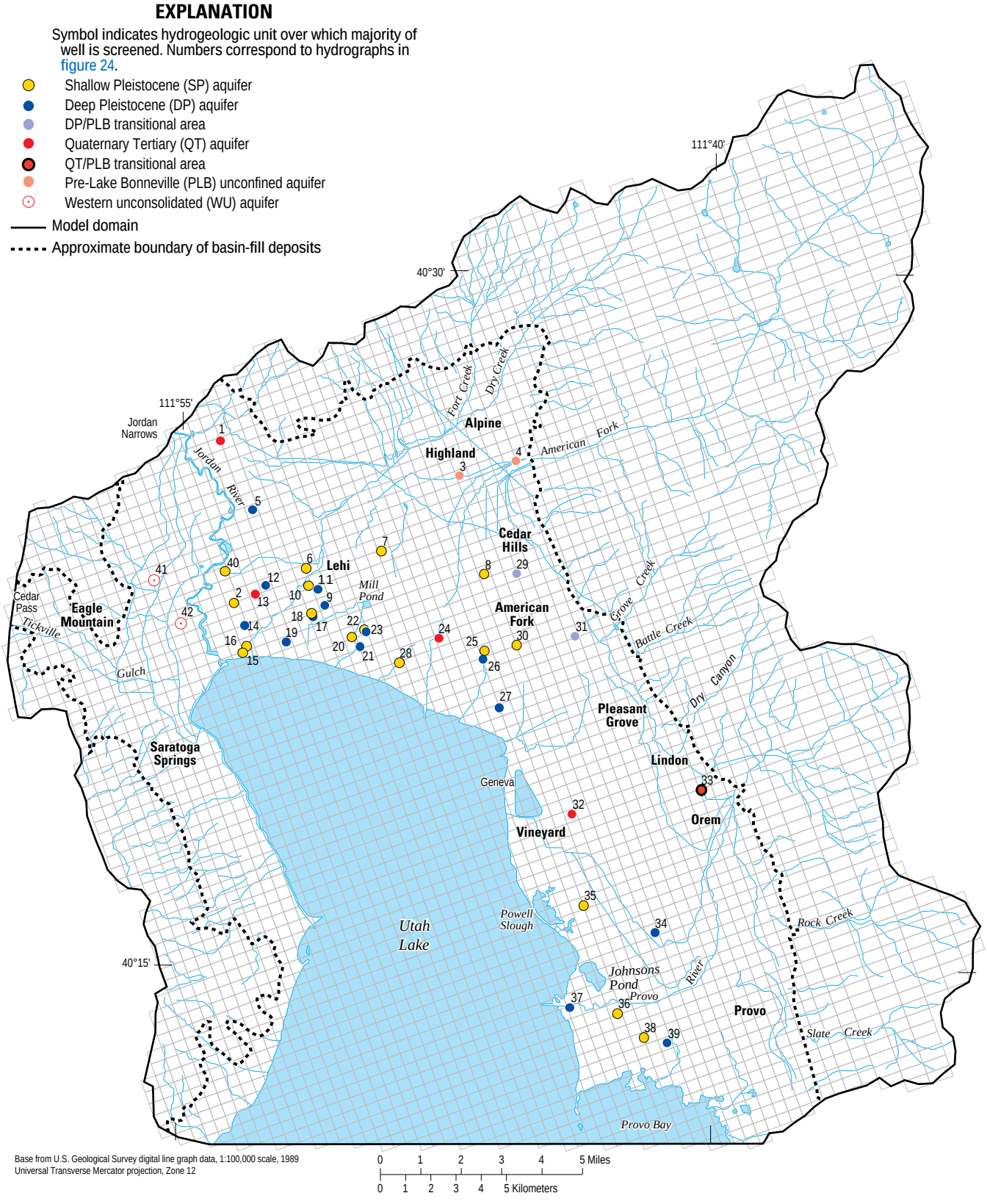

Figure 23. Location of selected wells used for the comparison of measured and simulated water levels in the transient ground-water flow model of northern Utah Valley, Utah.

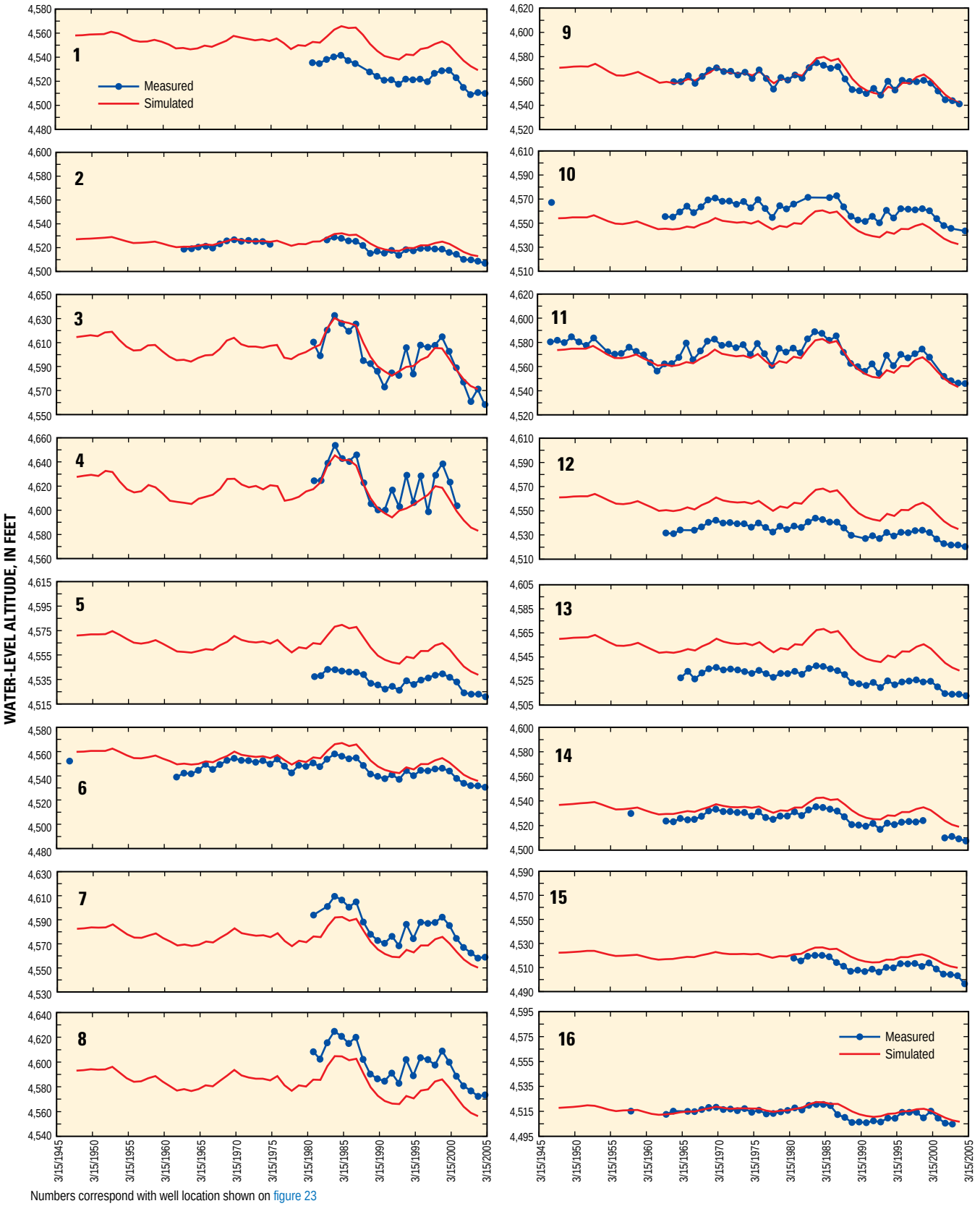

Figure 24. Water-level altitudes simulated at the end of each stress period in the transient ground-water flow model and measured water-level altitudes at selected wells during 1947–2004, northern Utah Valley, Utah.

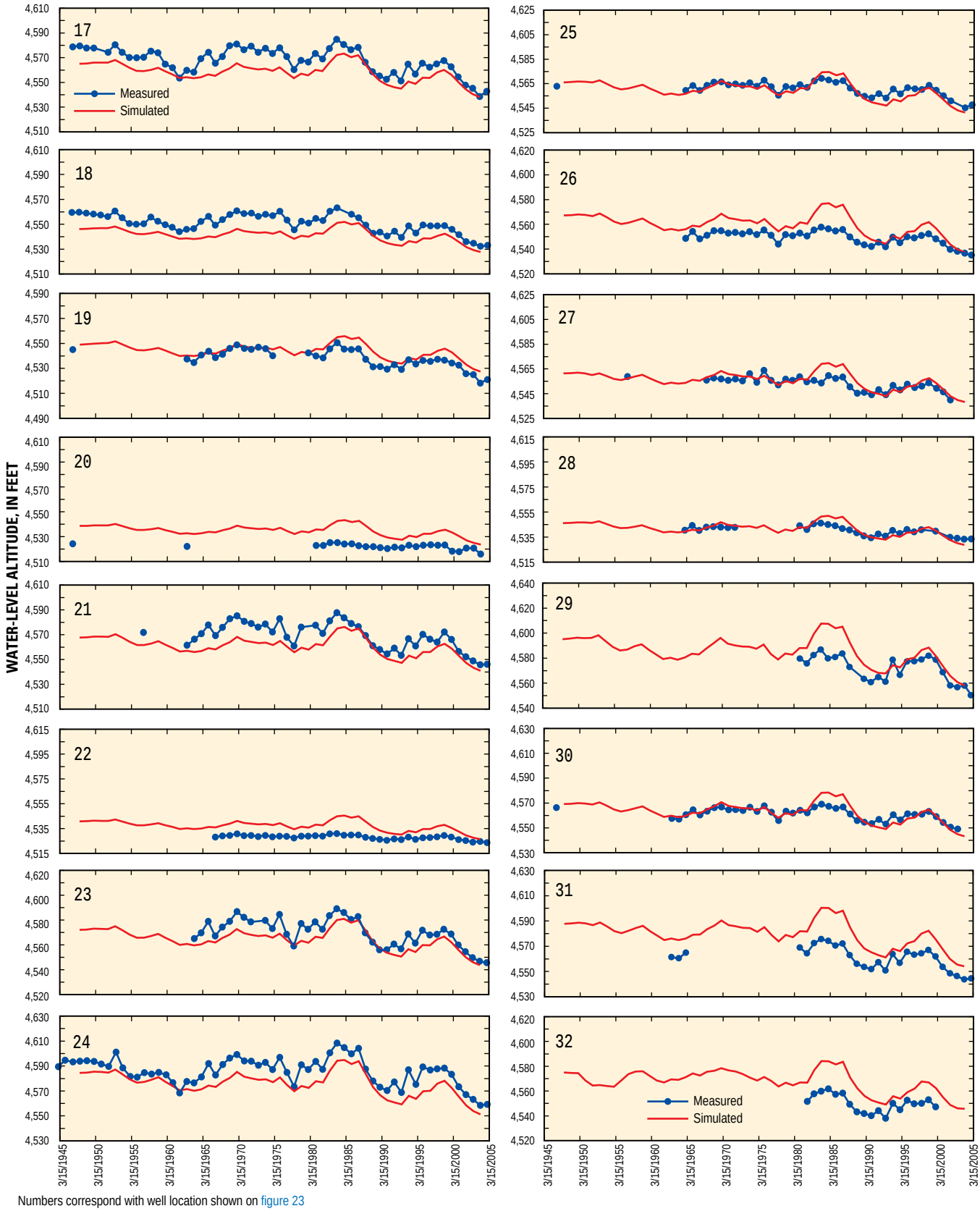

Figure 24. Water-level altitudes simulated at the end of each stress period in the transient ground-water flow model and measured water-level altitudes at selected wells during 1947–2004, northern Utah Valley, Utah—Continued.

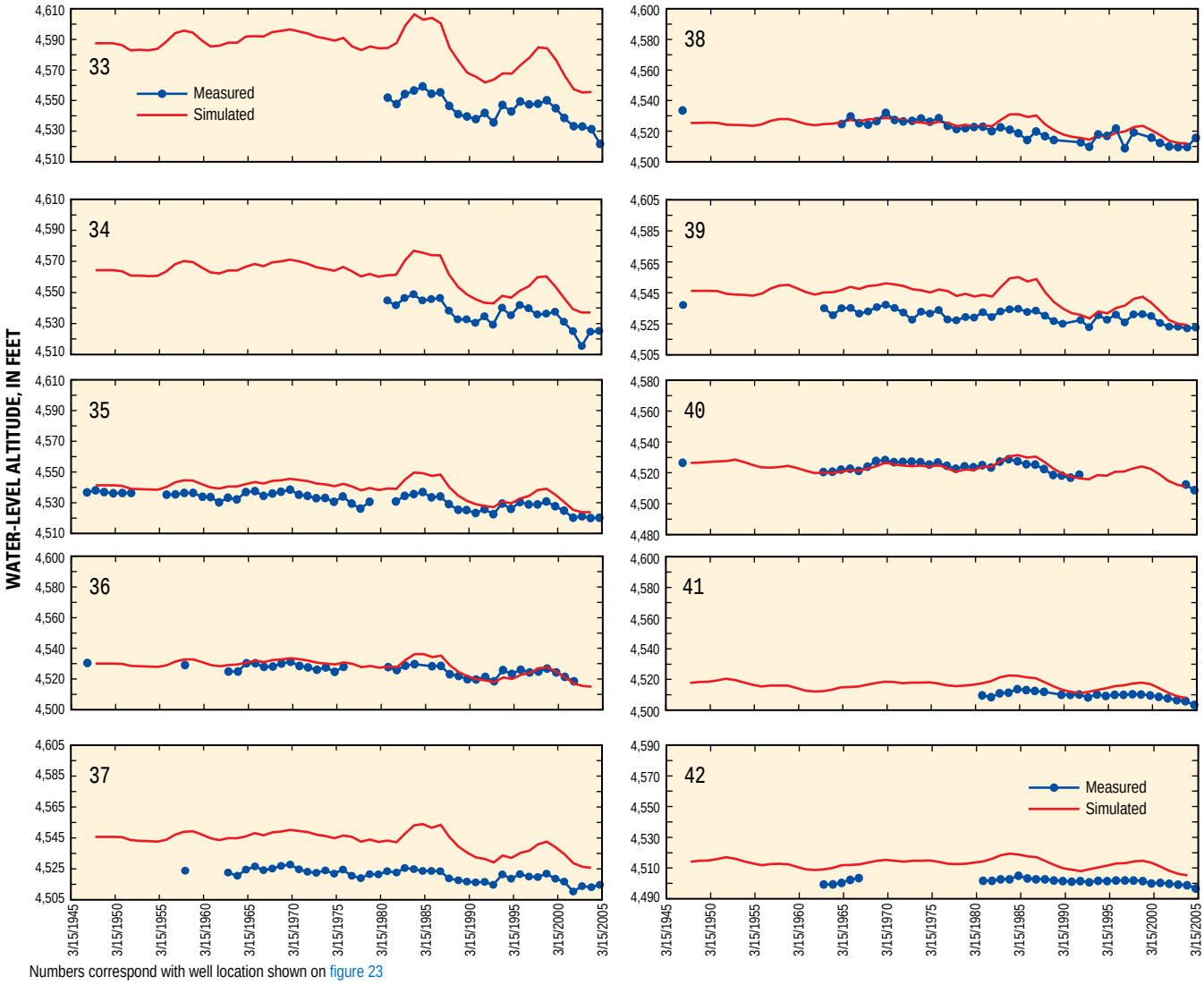

Figure 24. Water-level altitudes simulated at the end of each stress period in the transient ground-water flow model and measured water-level altitudes at selected wells during 1947–2004, northern Utah Valley, Utah—Continued.

annual fluctuations of about 5–15 ft (fig. 24). Most wells modeled in the SP aquifer near Utah Lake from Lehi south to Provo Bay also show long-term water-level declines but vary much less in their amplitude, probably because natural ground-water discharge to springs, drains, and Utah Lake controls water levels in this area (figs. 23 and 24, wells 15, 16, 20, 22, 28, 35, 36, and 38). Hydrographs from wells in the deeper DP aquifer in the same general areas show water-level fluctuations of greater amplitude than those in the SP aquifer but still show some long-term decline (figs. 23 and 24, wells 14, 19, 21, 23, 26, 27, 37, and 39). This may be related to discharge that occurs from the DP aquifer to flowing wells or to areas where the overlying confining unit is leaky, allowing ground water to move into the SP aquifer and out to drains and springs or to discharge into Utah Lake. In general, simulated water-level altitude and fluctuations match measured water-levels better in the SP aquifer than in the lower DP and QT aquifers where simulated water-level fluctuations are sometimes greater than or less than measured values (figs. 23 and 24, wells 12, 13, 21, 23, 24, 26, 32, and 39). This indicates that the spring and drain discharge measurements used as flow observations provided important information which allowed for better calibration in the SP aquifer.

Simulated water-level altitudes are generally about 10–30 ft too high in wells 1, 5, 8, 12, 13, 33, 34, 37, and 42; particularly in the wetter-than-normal mid-1980s. Some error is expected because the altitude of these wells is only known to an accuracy of plus or minus 10 ft. However the systematic error among these wells indicates that the problem may be related to low effective hydraulic conductivity. Even though the hydrogeologic units representing the aquifers in these areas have relatively high conductivity values, model cells may include thick sections of low-permeability deposits that effectively lower the overall model cell horizontal and vertical

conductance calculated by the HUF Package. Thick hydrogeologic units representing confining units are derived from simplifying assumptions in the hydrogeologic framework model (Cederberg and others, 2009). This error also could be caused by the use of VANI parameters to define vertical hydraulic conductivity as a ratio of horizontal to vertical hydraulic conductivity.

Limited long-term water-level data are available from the western part of the valley. Available data indicate a relatively flat hydraulic gradient (Cederberg and others, 2009, fig. 28) and annual water-level fluctuations of less than about 2–3 ft (wells 41 and 42, fig. 24). Long-term water-level decline in these wells was only about 5–6 ft from 1981 to 2004. Simulated water-levels generally reproduce these characteristics but are somewhat greater than the measured values. Few hydrologic property data are available for this area and, as a result, the model parameters controlling these properties in hydrogeologic units west of Utah Lake do not vary much in their distribution. Some observation wells in this area are completed in fractured limestone that underlies basin fill. Bedrock underlying basin fill is simulated as a porous medium rather than as a fractured medium with significant secondary porosity. As previously mentioned, this model does not accurately simulate the heterogeneity of bedrock.

In addition to long-term hydrographs, the ability of the transient model to match March 2004 measured water levels also was evaluated by inspection of hydraulic head residuals in model layers 1–4 in the final stress period of the transient simulation (fig. 25). Simulated water levels are within 10 ft of most measured water levels and vary more than 20 ft for only 28 of the 247 measured water levels (fig. 25). The mean of the residuals for water levels in the final stress period was 0.5 ft, the standard error (mean of the absolute values of residuals) was 12.7 ft, and the standard deviation was 24.5 ft. Large and small differences between measured and simulated water levels are distributed throughout the model. Many of the largest hydraulic head residuals, both positive and negative, occur near the boundary of the mountain front and basin fill and in the Lehi area (fig. 25). Some simulated water levels in these areas vary more than 50 ft from measured water levels. The hydraulic conductivity of bedrock is extremely heterogeneous and this model does not accurately simulate fracture flow that may control where ground-water flow from the mountain block to the basin fill is focused. Measured water levels in the Lehi area may be influenced (temporarily lowered) when nearby wells are actively pumping. Because the model simulates pumping over annual stress periods, it is not expected to reproduce these localized, short-term effects.

The relation of all observations to simulated values is shown in figure 26. Residuals for hydraulic head, change in hydraulic head, and flow observations are distributed fairly evenly about a 1:1 line, which indicates that the calibrated model is unbiased. In general, the model accurately simulates water levels and water-level fluctuations and can be considered an adequate tool to help determine the valley-wide effects on water levels of additional ground-water withdrawal and changes in water use.

The conceptual ground-water budget for 2004 was compared with the ground-water budget simulated for the final stress period in the transient ground-water flow model to determine if the transient simulation adequately represented changes in the ground-water system through time (table 7). Simulated total recharge is about 7 percent greater than the total recharge from the conceptual model. Most of this difference occurs where simulated stream seepage in the valley and infiltration from precipitation over the mountain block are higher than that estimated in the conceptual model. Simulated total discharge is about 3 percent greater than total discharge from the conceptual model with ground water released from storage supplying about 8 percent (12,700 acre-ft) of the total simulated discharge. Discharge simulated to drains and springs around Utah Lake is about 23 percent less than measured or estimated discharge. Model-simulated discharge to grouped drains and springs in the final stress period was compared with the conceptual discharge derived from the average of measurements made during 2003–04 (Cederberg and others, 2009). Simulated and conceptual discharge compare reasonably well for all of the groups except Saratoga Springs, BYU-Group 3, the Geneva Group and the South Springs Group (fig. 27). The simulated discharge was less than measured for nearly all groups, but this is expected because the measurements likely include some unknown amount of shallow ground water that originated as infiltrating runoff or irrigation water rather than upward flow from the principal aquifer system.

Estimates of average subsurface inflow from the mountain block to the basin-fill aquifer system in northern Utah Valley range from 43,200 to 112,000 acre-ft/yr (Cederberg and others, 2009, table 12). The corresponding simulated value for 2004 is equal to the difference between the recharge as infiltration of precipitation over the mountain block and the base flow in perennial mountain streams, simulated as discharge to the mountain segments of the American Fork and Provo River in the final stress period of the transient simulation (table 7). Simulated recharge from precipitation over the mountain block in the final stress period of the transient simulation is 74,600 acre-ft/yr and discharge to mountain streams (calculated as the sum of discharge to the mountain segments of the American Fork and Provo River) is 6,900 acre-ft/yr, indicating that the net simulated subsurface inflow from the mountain block is 67,700 acre-ft/yr. This is about equal to the average subsurface inflow from the mountain block (66,000 acre-ft/yr) estimated by Cederberg and others (2009, table 5). It is possible that the inaccuracies in the way the model simulates flow in the mountain block result in inaccurate transient discharge to mountain streams and that those values are too low for the final stress period. However, 2004 was the fifth consecutive year of drought in Utah and low base flow was observed in many streams. Thus it seems likely that the model is simulating accurate fluxes of subsurface inflow from the mountain block to the basin-fill aquifer system.

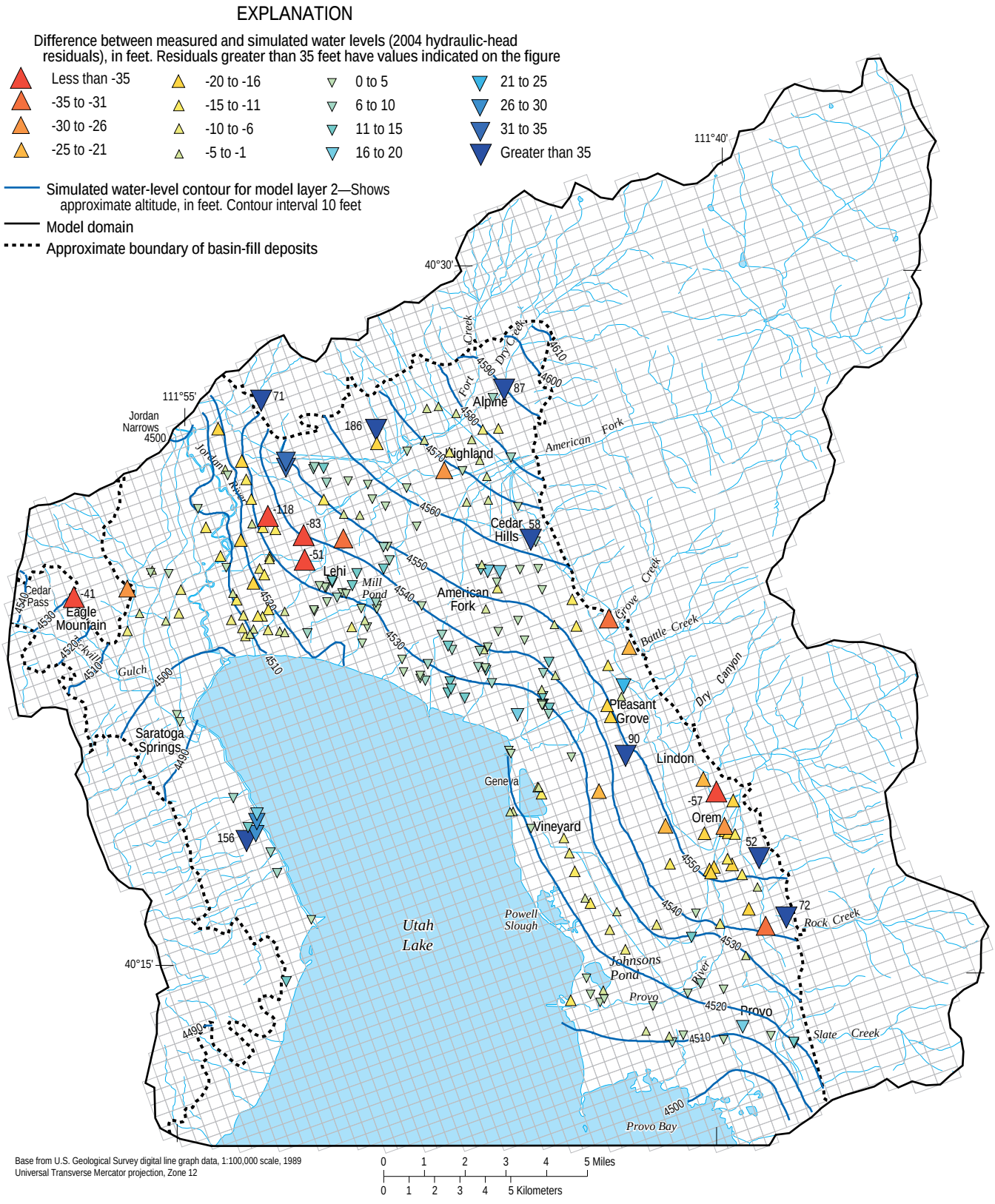

Figure 25. Hydraulic-head residuals (measured minus simulated water levels) in model layers 1–4 for the final stress period of the transient simulation (2004) and simulated water-level contours in model layer 2 of the ground-water flow model of northern Utah Valley, Utah.

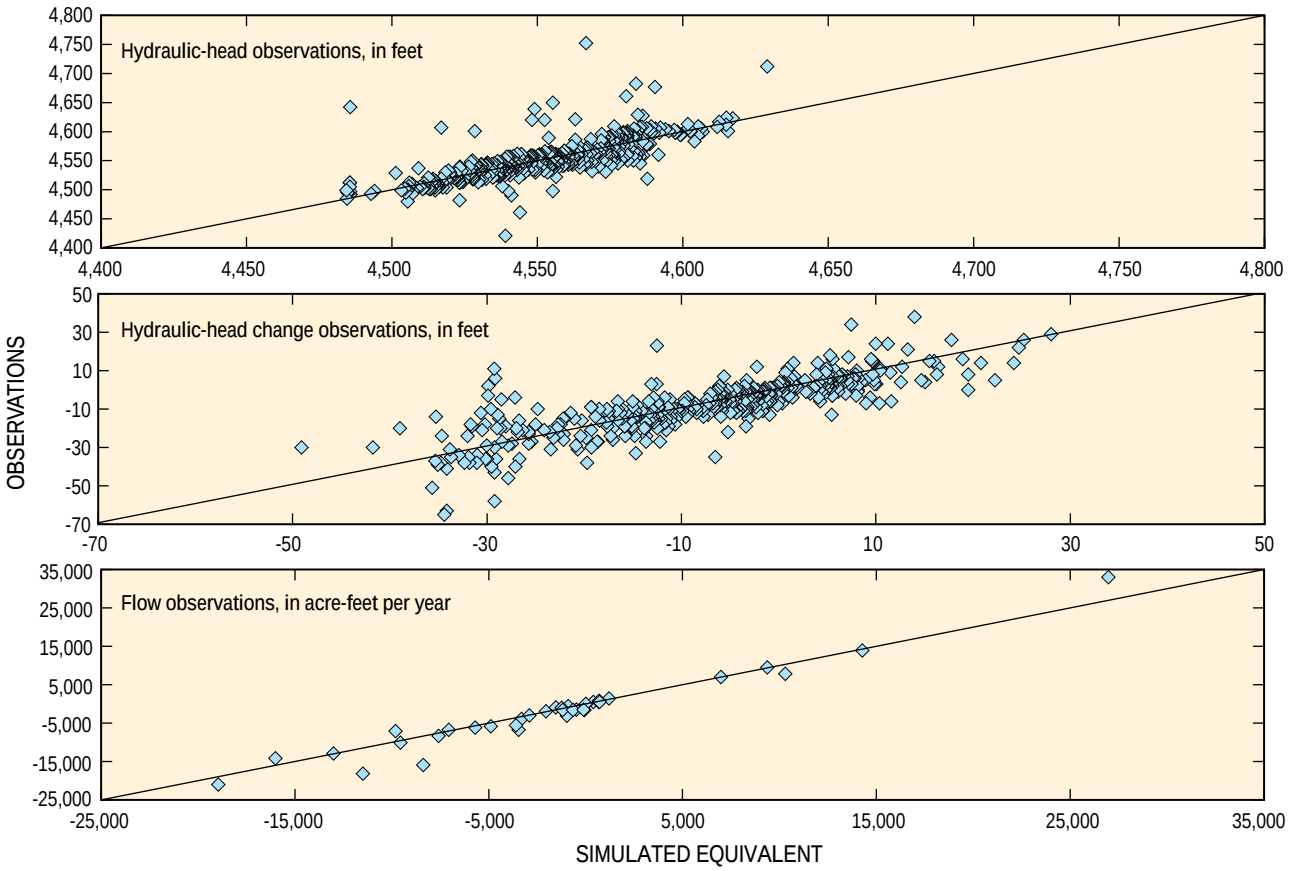

Figure 26. Relation of model observations to simulated equivalents for hydraulic head, change in hydraulic head, and flow observations used to calibrate the ground-water flow model of northern Utah Valley, Utah.

Sensitivity Analysis, Parameter Correlation, and Suggestions for Future Data Collection

Hydrologic properties simulated in this model are reasonable approximations of the hydrologic properties estimated on the basis of available data. Most model parameters are considered to be independent of one another meaning, for instance, that it is not likely that increasing both recharge and hydraulic conductivity at the same time would produce similar results. The model parameters that do possess significant correlation are shown in table 8. For example, the HK and VANI parameters for a particular confining unit are perfectly correlated, indicating that it is not possible to estimate them separately as they are defined in this model. The remaining correlated parameters control streambed hydraulic conductivity and hydraulic conductivity of aquifer material in the eastern part of the valley. It is not surprising that increasing recharge through stream seepage or lowering aquifer hydraulic conductivity will result in similar water-level increases. Correlation between these parameters could likely be lowered with the inclusion of more-accurate flow observations in streams and canals in the eastern part of the valley.

Sensitivity analysis involves evaluating the effects of changes in individual model parameters on model results and provides an indication of the uncertainty within which the model parameters have been estimated. The sensitivity of the model results to various parameter values was assessed by using statistics generated by the MODFLOW Sensitivity Process. Composite-scaled sensitivities (a dimensionless statistic) were used to assess the relative sensitivity of model parameters given the set of observations used in the model. One-percent scaled sensitivities (1SS) have the same units as the observation and indicate the change in simulated water level or flow that would result from a 1-percent increase in the parameter value (Hill and Tiedeman, 2007, p. 54). One-percent scaled sensitivities were used in two ways: (1) 1SS maps for select parameters and stress periods were examined for water-level changes at every node of the model grid, and (2) 1SS values for each combination of parameter and observation were calculated individually.

Numerical instability, caused by model layer 1 becoming dry and streams becoming disconnected from the underlying aquifer, prevented the calculation of sensitivity statistics and parameter correlations during the transient, unconfined simulation. All statistics derived from the MODFLOW Sensitivity Process are calculated on the basis of a version of the transient model that approximates the ground-water system as confined everywhere with the top of model layer 1 equal to the water-table surface determined at the end of the steady-state simulation. Although the top layer in the simulated flow system is

Table 7. Conceptual ground-water budget for 2004, and ground-water budget simulated in the final stress period (2004) of the ground-water flow model of northern Utah Valley, Utah.

Budget component	Conceptual flow, in acre-feet per year	Method of simulation	Simulated flow, in acre-feet per year
Recharge			
Seepage from the Provo Reservoir (Jacob) Canal	500	STR package	400
Seepage from Fort Creek and Dry Creek and associated irrigation canals	7,500	STR package	8,900
Seepage from American Fork and associated irrigation canals	13,400	STR package	8,100
Seepage from Grove Creek	300	STR package	700
Seepage from Battle Creek	400	STR package	700
Seepage from Provo River and associated irrigation canals	33,600	STR package	38,700
Seepage from Rock Creek	1,200	STR package	1,100
Seepage from Slate Creek	900	STR package	700
Seepage from the Provo Reservoir (Murdock) Canal	5,900	STR package	3,900
Subsurface inflow from Cedar Valley	7,500	GHB package	9,800
Seepage from irrigated fields, lawns, and gardens in the primary recharge area	5,600	RCH package	5,500
Infiltration from precipitation on primary recharge area in the valley	3,200	RCH package	3,100
Infiltration from precipitation over the mountain block	68,500	RCH package	74,600
Contribution from storage	not estimated		1,400
Total Recharge (rounded)	**148,000**		**158,000**
Discharge			
Evapotranspiration	4,400	ET package	7,200
Pumping wells	46,900	WEL package	44,500
Flowing wells (includes stock wells)	11,900	DRN package	16,600
Drains and springs around Utah Lake	54,700	DRN package	42,200
Subsurface outflow to Salt Lake Valley	2,600	GHB package	1,800
Discharge to the Jordan River	2,500	STR package	3,500
Discharge to American Fork in the mountains	9,700	STR package	6,000
Discharge to the Provo River in the mountains	1,800	STR package	900
Discharge to Utah Lake	20,400	CHD package	24,000
Release from storage	not estimated		12,700
Total Discharge (rounded)	**155,000**		**159,000**

clearly unconfined, comparisons show that defining its thickness from an estimated potentiometric-surface map and representing it as confined closely approximates water levels and budget components and is much more efficient numerically.

Composite-scaled sensitivity values for parameters with CSS values greater than 1 are shown in figure 28 along with the maximum, minimum, and mean 1SS value from the set of 247 water-level observations used in the final stress period of the simulation. Positive values of 1SS indicate that an increase in the parameter would cause an increase in head or flow at the observation location and negative values of 1SS indicate that the same parameter change would cause a decrease in head or flow. Some model parameters (for example, SS_QT) have comparatively high CSS but relatively low mean 1SS values indicating that changes in those parameters will have an affect on water levels of small magnitude, but that these affects will be seen at many observation locations. Other model parameters (for example hk_WBR) have much lower CSS that is dominated by fewer observations with larger absolute values of 1SS indicating that few observation locations are highly sensitive to changes in the parameter value, but that those locations are quite sensitive. This may indicate that the model is sensitive to the parameter only in a small area or that few observations exist where the sensitivity is high.

Analysis of 1SS maps indicate that most of the observation wells used during calibration are located in the areas most sensitive to important model parameters. Table 9 lists water-level observations with the highest 1SS values to selected model parameters in the final stress period of the transient model. The large number of observations makes it impractical to list all 1SS values, even for a single parameter. Therefore, only observations with 1SS values greater than 0.1 ft that illustrate where the model is most sensitive to a particular parameter are shown. The locations of water-level observations with the highest 1SS values are shown in figure 29.

Water levels in all model layers are sensitive to a number of parameters that define recharge, discharge, and hydrologic properties. Recharge by seepage from streams and canals

Table 8. Highly correlated parameters in the ground-water flow model of northern Utah Valley, Utah.

PARAMETER	PARAMETER	CORRELATION
hk_CF1	vani_CF1	1
hk_CF2	vani_CF2	1
hk_CF3	vani_CF3	1
hk_CF4	vani_CF4	1
STR_VAL	STR_PvoVal	0.98
STR_PvoVal	hk_QT	0.97
STR_PvoVal	hk_SP	0.95
STR_VAL	hk_QT	0.95
STR_VAL	hk_PLB	0.94
STR_PvoVal	hk_PLB	0.94
STR_VAL	hk_SP	0.93
STR_PvoVal	hk_DP	0.91
hk_SP	hk_QT	0.91

constitutes a major fraction of the ground-water budget (tables 6 and 7) and the importance of this source of recharge is reflected in the relatively large values of CSS and 1SS for streambed conductance parameters at many locations. The parameters STR_VAL, STR_PvoVal, and STR_Murdck all have CSS values greater than 1 (fig. 28) and several observations on the east side of the valley have 1SS values greater than 0.1 ft for STR_VAL and STR_PvoVal (table 9 and fig. 29). Although adjustments in these parameters have the greatest effect on water levels near the stream segments they are associated with, the effects of adjusting these parameters can be seen in all model layers. Areal recharge over the mountain block is controlled by the parameters rock1_rch and rock2_rch. Water levels are similarly sensitive to these parameters in all model layers on the east side of the valley with 1SS values as high as 0.14 ft for rock1_rch and 0.12 ft for rock2_rch (fig. 28).

Model sensitivity to hydrologic-property parameters on the east side of the valley tend to be fairly evenly distributed in the area to which the parameter applies. For example, a 1-percent increase in hk_CF1 would uniformly lower water levels by about 0.1 ft across much of the eastern half of the valley with somewhat more decline occurring near the eastern shore of Utah Lake (e.g (D-6-2)28acb-4, (D-5-1)14cdc-1, and (D-5-2)31dba-1 in table 9). Similar patterns follow for other hydrologic-property parameters in the basin fill that are shown in figure 28 (vani_CF1, SS_QT, hk_SP, SS_Valley, hk_QT, hk_DP, hk_PLB, SS_Mtn, hk_CF2, vani_CF2, hk_WBR, hk_CF3, and vani_CF3).

Simulated water levels on the west side of the valley are sensitive to hk_WBR, with 1SS as low as -0.16 ft for observations in that area (fig. 28, table 9). This indicates that more long-term water-level data would be particularly useful for improving the estimate of hydraulic conductivity in the bedrock that underlies basin fill west of Utah Lake and the Jordan River. Valley water levels have significant sensitivity to the hydraulic conductivity of bedrock in the mountains controlled by parameters hk_rock2 and hk_rock5. Observations have 1SS values as high as 0.39 ft for hk_rock5 and 0.07 ft for hk_rock2 (fig. 28).

Although the 1SS values for the parameter FloWel in the final stress period indicate that a 1-percent increase in the parameter value would result in water-level declines of less than about 0.1 ft at individual observation locations, the high CSS value for the same parameter indicates significant overall model sensitivity to flowing well discharge (fig. 28). Flowing

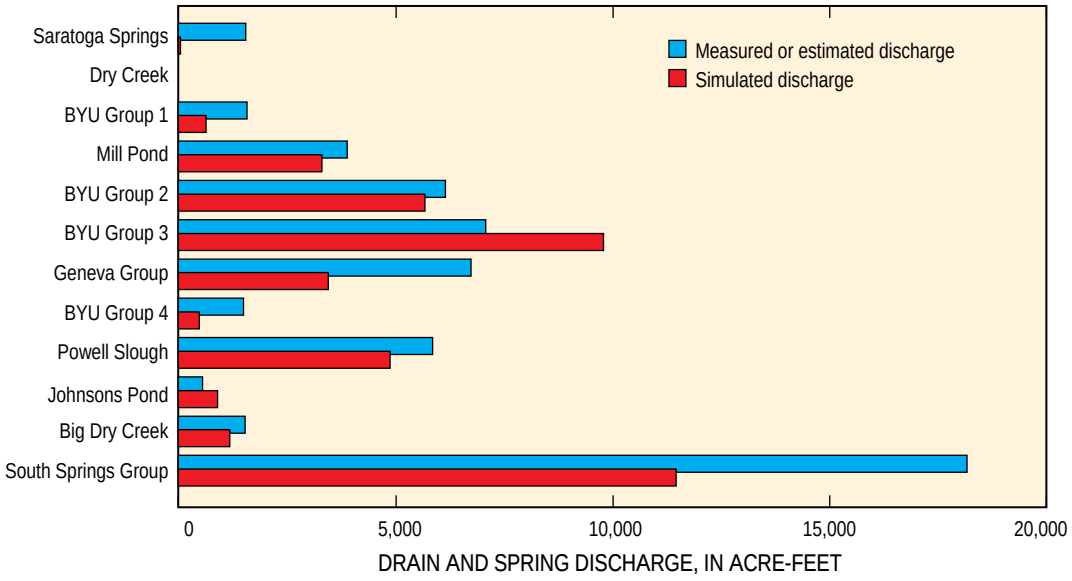

Figure 27. Simulated and measured or estimated discharge from drains and springs in the final stress period (2004) of the ground-water flow model of northern Utah Valley, Utah.

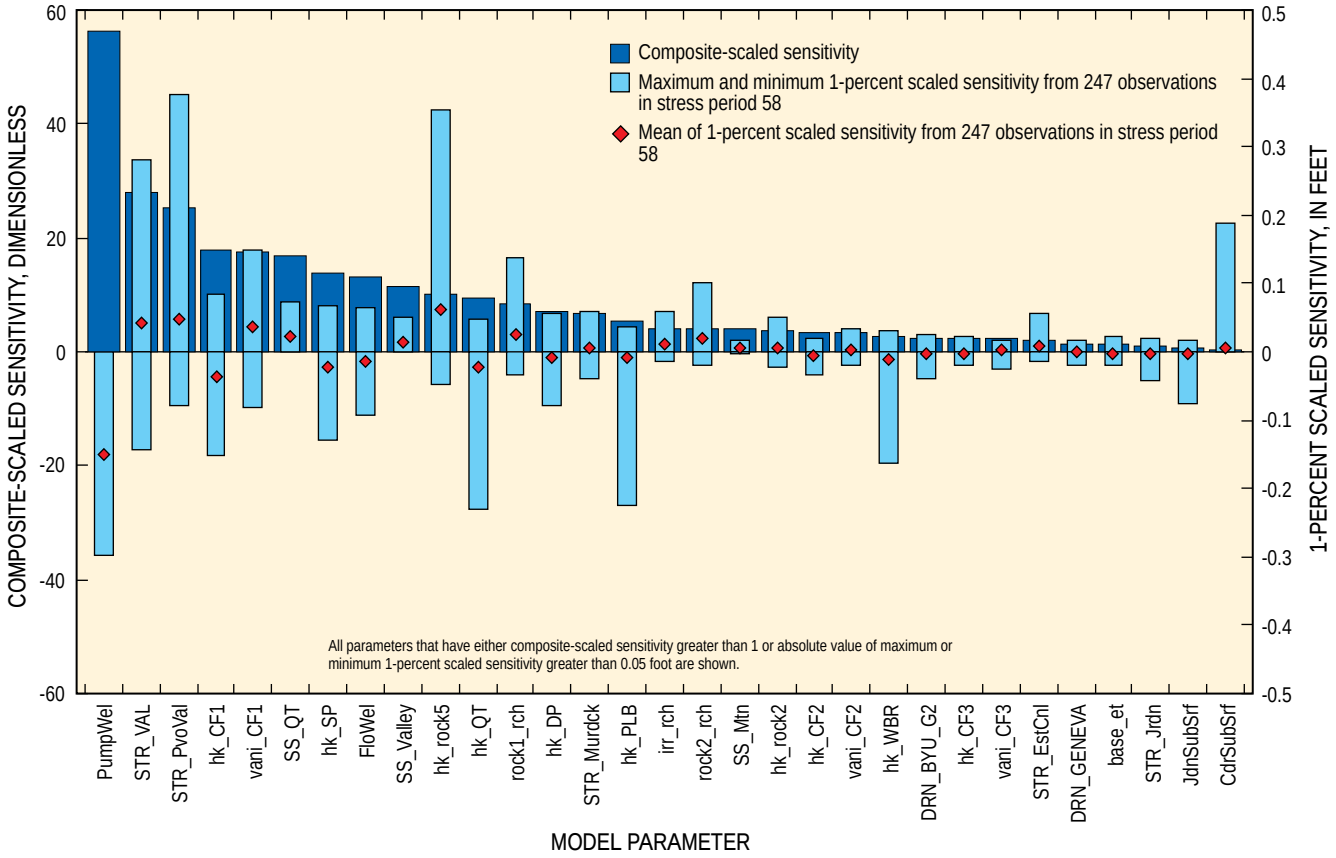

Figure 28. Composite-scaled sensitivity for selected model parameters and statistics related to 1-percent scaled sensitivity for observations in the final stress period of the ground-water flow model of northern Utah Valley, Utah.

wells are simulated as a head-dependent drain boundary and discharge estimates used for calibration have been updated from those used by Clark (1984) in the previous ground-water model. However, updated estimates of flowing-well discharge are based on an outdated survey of wells and few actual measurements of flowing-well discharge. Future simulations of ground-water flow in northern Utah Valley might be substantially improved if the estimates and spatial distribution of annual flowing-well discharge were improved. This improvement would require performing a new survey of flowing wells and estimating flows from annual measurements of discharge made for a set of representative wells.

The large CSS associated with the parameter PumpWel indicates that the model is more sensitive to pumping than to any other parameter (fig. 28). The parameter PumpWel is applied for the purposes of sensitivity analysis only. Although the parameter could be used as a factor to uniformly scale all specified pumping up or down, it was not used in this way. Rather, the rate and distribution of ground-water withdrawal from pumping wells was specified as determined by well and pumping records as previously described in this report.

The set of water-level observations used in the transient model is distributed fairly evenly throughout much of the valley with the exception of areas west of the Jordan River and Utah Lake. Water-level data collected at sites where data were not available during the calibration period may help refine the model and the conceptual understanding of the ground-water system west of the Jordan River and Utah Lake. Furthermore, long-term water-level fluctuations measured at new sites or multiple-well aquifer tests would help to refine estimates of specific yield, specific storage, and horizontal-to-vertical anisotropy in these areas.

Table 9. Water-level observations with the highest 1-percent scaled sensitivity to selected model parameters simulated in the final stress period of the transient ground-water flow model of northern Utah Valley, Utah.

[An explanation of the numbering system used for hydrologic data sites in Utah is provided in the text at the beginning of the report]

Model parameter	Observation well	Top layer - bottom layer of observation well[1]	Approximate change in simulated water level, in feet, for a 1-percent increase in the parameter
STR_VAL	(D-4-2)19cab-1	1 - 3	0.28
	(D-4-2)30cdc-1	4 - 4	.27
	(D-4-1)25bca-1	4 - 4	.26
	(D-4-1)25dcc-1	1 - 3	.26
	(D-4-1)26abc-1	2 - 4	.26
STR_PvoVal	(D-6-2)13dab-2	1 - 1	.38
	(D-6-3)18cbb-1	2 - 4	.37
	(D-6-2)12dbc-1	3 - 4	.37
	(D-6-2)24aac-1	1 - 1	.36
hk_CF1	(D-5-2)31dba-1	2 - 3	- .15
	(D-6-2)28acb-4	2 - 2	- .13
	(D-5-1)14cdc-1	1 - 2	- .13
	(D-5-2)16ccc-1	2 - 2	- .12
	(D-4-1)36adc-1	1 - 3	- .12
	(D-4-1)34bac-1	4 - 4	- .11
	(D-7-2)12acd-1	2 - 2	- .11
	(D-6-3)19dcc-1	4 - 4	- .11
	(D-5-1)20dbb-2	2 - 2	- .11
	(D-5-1) 7bab-1	2 - 2	- .10
hk_SP	(D-5-2)17bdc-1	1 - 3	- .13
	(D-5-2)16ccc-1	2 - 2	- .13
	(D-6-3)30ddc-1	2 - 4	- .13
	(D-4-1)33ccc-2	2 - 2	- .13
	(D-5-2)21add-1	1 - 2	- .13
	(D-5-2)16ccc-1	2 - 2	- .13
	(D-4-1)36adc-1	1 - 3	- .12
	(D-4-1)34bac-1	4 - 4	- .12
	(D-6-3)19dcc-1	4 - 4	- .12
hk_rock5	(D-4-2)19cab-1	1 - 3	.35
	(D-4-2)30cdc-1	4 - 4	.31
	(D-4-1)25bca-1	4 - 4	.30
	(D-4-1)25dcc-1	1 - 3	.29
	(D-4-1)26abc-1	2 - 4	.29
hk_QT	(D-4-2)19cab-1	1 - 3	- .23
	(D-4-2)30cdc-1	4 - 4	- .21
	(D-4-1)25bca-1	4 - 4	- .20
	(D-4-1)25dcc-1	1 - 3	- .19
	(D-4-1)26abc-1	2 - 4	- .19
	(D-4-1)36adc-1	1 - 3	- .18
	(D-4-1)34bac-1	4 - 4	- .16
rock1_rch	(D-6-3)29bcd-1	2 - 3	.14
	(D-6-3)19dcc-1	4 - 4	.10
hk_PLB	(D-4-2)19cab-1	1 - 3	- .22
	(D-4-2)30cdc-1	4 - 4	- .17
	(D-4-1)25bca-1	4 - 4	- .14
	(D-4-1)25dcc-1	1 - 3	- .13
	(D-4-1)26abc-1	2 - 4	- .12
	(D-4-1)36adc-1	1 - 3	- .12
rock2_rch	(D-4-2)19cab-1	1 - 3	.10
hk_WBR	(C-5-1)20aaa-1	2 - 4	- .16
	(C-5-1)15aba-1	1 - 2	- .11
	(C-5-1)14bbd-1	1 - 2	- .10
	(C-5-1)15cdb-1	3 - 4	- .10
	(C-5-1)14dbc-2	3 - 3	- .10
CdrSubSrf	(C-5-1)20aaa-1	2 - 4	.19

[1] Well screen information is used to determine to which model layer or layers the water-level observation applies.

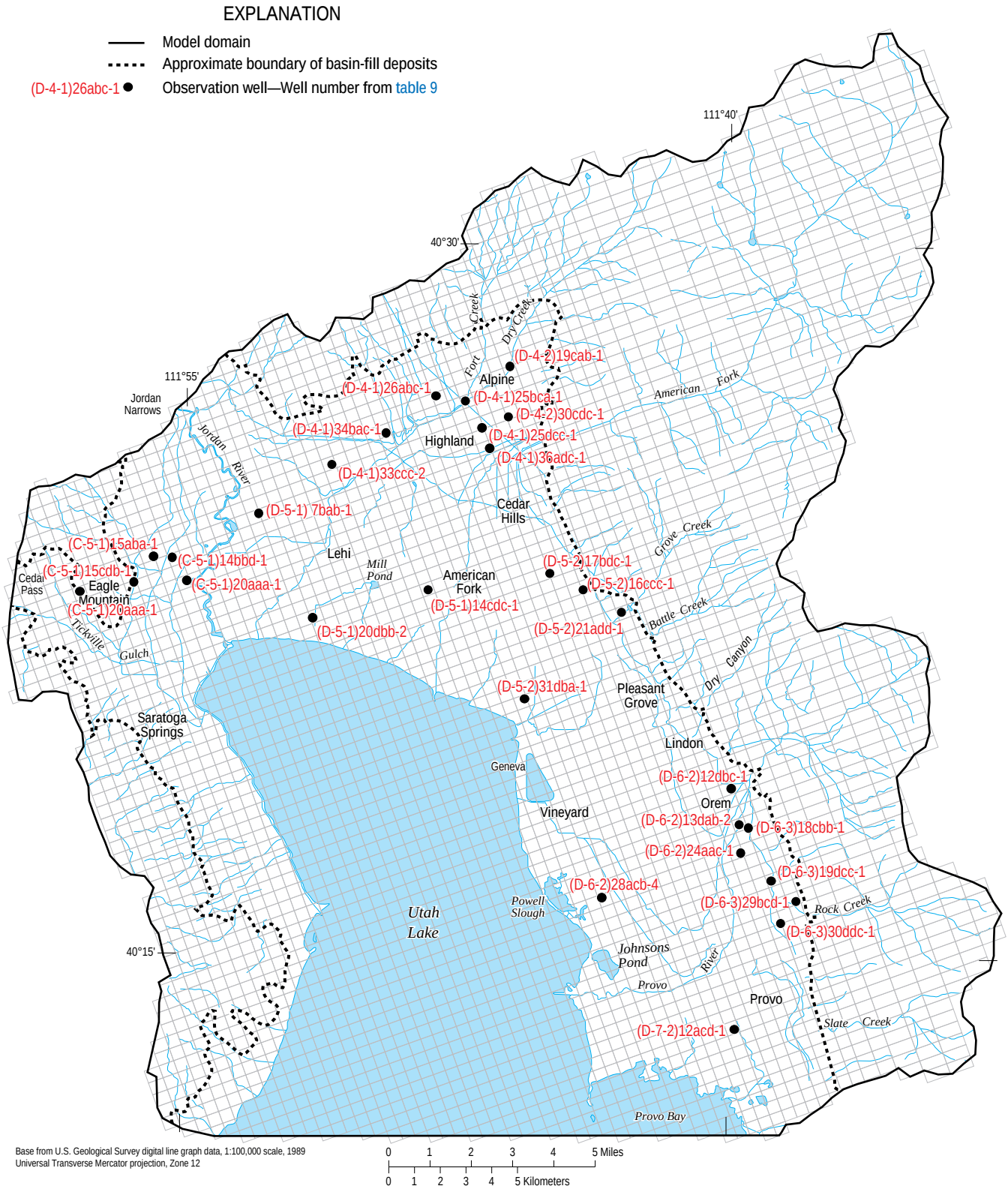

Figure 29. Location of simulated water-level observations with the highest 1-percent scaled sensitivity to selected model parameters in the final stress period of the transient ground-water flow model of northern Utah Valley, Utah.

Model Limitations

The model presented in this report is a mathematical representation of ground-water flow based on simplifying assumptions about the complex hydrologic system in northern Utah Valley. In general, owing to model scale and level of detail, the model is most applicable to analysis of valley-wide ground-water supplies. Although the model provides a relatively good fit between simulated and measured or estimated quantities, indicating that the overall simulated ground-water flow is a reasonable representation of ground-water flow in northern Utah Valley, it is subject to limitations. Local-scale heterogeneity in hydrologic properties, recharge, and discharge are not accurately represented. The objective of the modeling analysis and the range of stresses over which the model is calibrated influence the approach to simulating the ground-water system. Boundary conditions and the representation of various components of the flow system that were appropriate for the calibrated range of stresses may be inappropriate when the ground-water system is stressed beyond the range used during calibration.

The boundaries of the model domain simulate no-flow boundaries. This assumes, in general, that the surface-water divide coincides with the ground-water divide throughout the northern Utah Valley model domain. It is likely that ground water does cross this boundary in places, but much of the boundary occurs in mountainous areas where wells do not exist and ground-water withdrawal does not occur. Exceptions are at Cedar Pass and the Jordan Narrows where subsurface flow across the model domain is simulated by using the General Head Boundary Package. The properties that control flow at the general head boundaries are based on calibration to estimates of flow into or out of the system at these locations. If these estimates are incorrect, simulated water levels near these boundaries may be inaccurate. The no-flow boundary in the southeastern part of the valley, between the mountain front and Provo Bay, generally coincides with the boundary used in the previous models of northern and southern Utah Valleys. Water-level contours, both simulated and measured, indicate that ground water flows toward this boundary from the north to discharge at springs and drains near Utah Lake or in Provo Bay. It is possible that increased withdrawals in this area could induce flow from the south across the boundary that is not represented in the model.

The model simulates large areas of bedrock in the mountains and beneath basin fill in the western parts of the valley as a porous medium rather than as a fractured flow system. The actual hydraulic conductivity of bedrock is extremely heterogeneous and the simplifications in this model prevent accurate simulation of the flow through fractures that likely focuses where ground-water is entering the valley aquifer system. This may cause inaccuracies in the simulation of water levels and water-level changes near the boundary between the basin fill and the mountain front.

Measured water levels, water-level changes, and estimated flows between the aquifer and streams or canals were not accurately reproduced everywhere in all stress periods during the simulation period. In some cases, this is related to the discretization of time and space in the model. Model cells are about 0.3 mi on a side throughout much of the domain, and annual stress periods are used from 1947 to 2004. Pumping from large-volume production wells might induce temporary drawdown in neighboring wells and runoff-related recharge events may cause water levels to rise rapidly in areas close to the source. The local effects that result from these types of stresses may occur on a spatial or temporal scale that is not represented by and cannot be reproduced by the model.

Ground-water flow models are generally considered to be more accurate representations of flow systems in areas where they more closely match available data. This model is calibrated by using estimates of recharge and discharge at various locations and an extensive set of water-level data that covers much of the area within the valley. However, hydrologic properties in the western part of the valley are currently calibrated to few water-level data. Because of the lack of hydrologic data available for the western part of the valley, especially south of Saratoga Springs, the model likely is less accurate in those areas. Much of the area west of the Jordan River and south along the western shore of Utah Lake is undergoing rapid residential development. Additional ground-water withdrawals in this area may induce hydraulic gradients that were not present during the calibration and reveal aquifer characteristics not included in the model. As more data become available, the model may need to be revised in this area.

Hypothetical Simulations

The ground-water flow model was used to simulate possible effects on water levels and discharge components of the water budget caused by increased withdrawal from wells, artificial recharge, and changing water use from irrigation to municipal supply. These model simulations were made to show how the model might be used to investigate the impacts of future water-resource scenarios on the ground-water system. All simulations are designed to investigate hypothetical anthropogenic effects on the ground-water system and are compared to a “base simulation” that represents a hypothetical steady-state condition that would be reached if 2004 withdrawal rates remained constant under average meteorological conditions. The base simulation begins with water levels from the end of the 1947–2004 transient simulation and simulates 30 annual stress periods of average (1971–2000) streamflow and recharge from precipitation in the valley and average (1970–2004) recharge from precipitation over the mountain block. The distribution and rates of recharge specified on agricultural and urban/residential lands in the primary recharge area are constant for all stress periods and unchanged from the final stress period of the 1947–2004 transient simulation. The

constant head boundary specified at Utah Lake remains equal to 4,489 ft in altitude. Under these conditions, the ground-water system approaches a steady-state condition after the first 15 stress periods, at which time the volume of ground water coming out of storage is only about 0.2 percent of the total ground-water budget, and by stress period 30 the base simulation is essentially at steady state. Water levels and budget components from the following three simulations (scenario 1, scenario 2, and scenario 3) at stress periods 15 and 30 are compared to the water levels and budget components from stress period 30 of the base simulation to indicate how they are affected by the change in stresses represented through time for each of the three scenarios. Water-level changes are referred to as drawdowns to show the effects of various changes in stresses, relative to the base simulation. For the purpose of this discussion, drawdown is the simulated change in water level between the base simulation at the end of 30 years and the scenario of interest. A negative drawdown indicates a water-level rise. The following simulations assume the same spatial distribution of ground-water withdrawal as for the final stress period (year 2004) of the transient simulation.

Scenario 1 simulates a 100-percent increase in well withdrawal from 2004 rates over 30 annual stress periods (30 years). The simulation begins with water levels from the end of the 1947–2004 transient simulation and uses the same constant values for average streamflow, recharge from precipitation in the valley, and recharge from precipitation over the mountain block as are used in the base simulation. The distribution and rates of recharge from irrigation and the constant head boundary at Utah Lake also are simulated as in the base simulation. Ground-water pumping rates for all wells are increased linearly from the 2004 rates to twice the initial rates by the end of the 30th stress period in this simulation. This simulation demonstrates the possible effects of increased withdrawals in the upcoming decades as the population and economy of northern Utah Valley continue to grow.

Scenario 2 simulates the effects of artificial recharge near the mouth of American Fork Canyon. The simulation is identical to that of scenario 1 with the addition of 20,000 acre-ft/yr of recharge specified across an area of about 650 acres. The addition of artificial recharge to the ground-water system near the mountain front is considered by water managers in northern Utah Valley to be one option for increasing the storage capacity for water supply in the future. This simulation is included to show the general effects of one artificial recharge scenario during a period of increased well withdrawals.

Scenario 3 simulates the effects of reduced recharge from land-use change. Recent trends in changing land use suggest that most lands presently irrigated for agricultural purposes in the primary recharge area of northern Utah Valley could be converted for residential and commercial uses in the upcoming decades. The transient model specifies an approximate recharge rate of 8.4 to 12.3 in/yr to simulate the seepage from irrigated fields in nearly all agricultural areas. There are a few fields near the northwestern corner of Utah Lake that are irrigated by more efficient center-pivot sprinklers where the specified recharge rate from irrigated fields is only about 2.8 in/yr. Recharge rates in areas classified as urban or residential are about 3.5 in/yr. All aspects of this simulation are identical to the base simulation except that recharge rates related to agricultural irrigation in the primary recharge area were changed to recharge rates specified for urban and residential areas. This represents a conversion of about 2,000 acres previously irrigated for agriculture. The total area for which recharge from irrigation (including agricultural and urban/residential) is applied is about 16,500 acres. Simulated ground-water withdrawal remains constant at 2004 rates for all 30 stress periods. Constant withdrawal rates were specified for this simulation so that water-level changes caused by reduced recharge resulting from this change in land use could be assessed without the interference of increased pumping.

Simulation Results

In all three scenarios, declines are seen in ground-water levels and head-dependent discharges (table 10, figs. 30, 31, and 32). The greatest declines are attributed to increased ground-water withdrawal from wells in scenario 1. Water levels and discharges continue to decline throughout the simulation as ground-water withdrawal from wells continues to increase. The magnitude and distribution of drawdown for layer 3 at stress periods 15 and 30 of scenario 1 are shown in figure 30. Because the magnitude and distribution of drawdown are similar for all model layers within the basin-fill boundary, layer 3 is shown to illustrate the results of all three hypothetical simulations. The water levels most affected by increased pumping are beneath the Highland and Provo benches where drawdowns are on the order of 10–12 ft by stress period 15 and 20–26 ft by stress period 30 (fig. 30). Drawdowns of about 10–17 ft are simulated in all layers along the north and east shores of Utah Lake by stress period 30, indicating that this level of increased pumping would likely result in substantial lowering of heads in the discharge area. Selected components of the ground-water budget for each hypothetical simulation are compared in table 10. The 100-percent increase in pumping by stress period 30 in scenario 1 causes substantial decreases in all head-dependent components of ground-water discharge. Simulated values indicate a 22-percent decrease in subsurface discharge to Utah Lake, a 25-percent decrease in discharge to the Jordan River, a 15-percent decrease in ET, and a 37-percent decrease in discharge to drains, springs, and flowing wells. Discharge from drains, springs, and flowing wells are simulated with the Drain Package and are grouped for the purpose of discussing the results of the hypothetical simulations. These values are based on the assumption that flowing wells remain open for the same amount of time each year and that the decrease in flowing-well discharge only is dependent upon the change in hydraulic head. Because the constant recharge rates used in these simulations (long-term average) are substantially higher that those in the final stress periods of the transient model, ground-water storage is being replenished for approximately the first eight

Table 10. Selected components of the ground-water budget for hypothetical scenarios 1, 2, and 3 compared to the steady-state condition (the base simulation) that includes average recharge from precipitation and stream seepage and constant pumpage using 2004 rates of well withdrawal in northern Utah Valley, Utah.

[—, not calculated]

Budget component	Base simulation, stress period 30	Scenario 1, stress period 15	Change, in percent	Scenario 1, stress period 30	Change, in percent	Scenario 2, stress period 15	Change, in percent	Scenario 2, stress period 30	Change, in percent	Scenario 3, stress period 15	Change, in percent	Scenario 3, stress period 30	Change, in percent
Specified recharge, in acre-feet	87,028	87,028	0	87,028	0	107,025	23	107,025	23	86,273	-1	86,273	-1
Annual well withdrawal, in acre-feet	44,478	65,950	48	88,956	100	65,950	48	88,956	100	44,478	0	44,478	0
Subsurface discharge to Utah Lake, in acre-feet	25,440	22,845	-10	19,782	-22	26,123	3	23,155	-9	25,244	-1	25,315	0
Discharge to the Jordan River, in acre-feet	4,551	4,031	-11	3,403	-25	4,860	7	4,249	-7	4,514	-1	4,521	-1
Sum of discharge to springs, drains, and flowing wells, in acre-feet	86,154	71,324	-17	54,059	-37	85,859	0	68,532	-20	85,437	-1	85,606	-1
Discharge to evapotranspiration, in acre-feet	8,247	7,721	-6	7,008	-15	8,197	-1	7,559	-8	8,225	0	8,230	0
Ground water coming from storage, in acre-feet	0	1,779	—	2,257	—	1,806	—	1,955	—	0	—	0	—

stress periods of the simulation. For the remainder of the simulation, the amount of water released from storage exceeds the amount taken into storage. Although the ground-water system has not yet reached steady state, the amount of ground water released from storage (2,257 acre-ft/yr) is only about 1-percent of the total budget (191,252 acre-ft/yr) in stress period 30, indicating that the water levels and budget components are not likely to change significantly if the simulation is extended for a longer period.

The addition of artificial recharge in scenario 2 results in a general water-level rise throughout much of the northern part of the valley. This water-level rise is as high as 22 ft on the Highland Bench in stress period 15 and reduces to a maximum of about 11 ft in stress period 30 as the ground-water withdrawal continues to increase when compared to the base simulation (fig. 31). The southeastern part of the valley displays similar patterns of drawdown as in scenario 1, although the magnitude of drawdown is somewhat dampened by the effects of the artificial recharge. Most of the area along the Provo Bench only experiences 20 ft of drawdown by stress period 30 compared to 25 ft of drawdown in scenario 1. Head-dependent components of ground-water discharge remain relatively constant with slight increases in discharge to Utah Lake and the Jordan River through stress period 15, indicating that the artificial recharge counteracts the effects of increased withdrawal for as many as 15 years into the simulation (table 10). However, the continued increases in ground-water withdrawal cause decreases of 7 to 9 percent in discharge to the Jordan River, Utah Lake, and ET; and 20 percent in discharge to springs, drains, and flowing wells by stress period 30.

Minimal effects were caused by the reduction in recharge from land use change in scenario 3. Maximum declines in ground-water levels were only about 1 ft anywhere in the valley (fig. 32) and head-dependent discharges are reduced only by about 1-percent (table 10). This result is not surprising given that the conversion of agricultural to urban or residential land use in the entire primary recharge area reduces diffuse recharge from irrigation by only 1 percent when compared to the final stress period (2004) in the transient model. This simulation indicates that any significant impacts on the ground-water system caused by recharge of unconsumed irrigation water have already occurred. It is possible, however, that more significant effects could occur if more efficient irrigation methods are implemented in urban and residential areas in the future.

The results of these hypothetical simulations should not be used to predict actual water levels at some future date, but can provide some general insights into the possible water-level and discharge responses to the stresses simulated in each scenario. The drawdown and changes in discharge in these simulations are based on simplifying assumptions that prevent accurate predictions. For example, recharge from precipitation and stream seepage is not likely to approximate the long-term average for years at a time. Furthermore, the constant head boundary at Utah Lake is artificially fixed and would likely fluctuate in response to surface-water management and climatic conditions in the future. Different hydraulic gradients between the aquifer and lake would result in somewhat different discharge values than those reported in table 10.

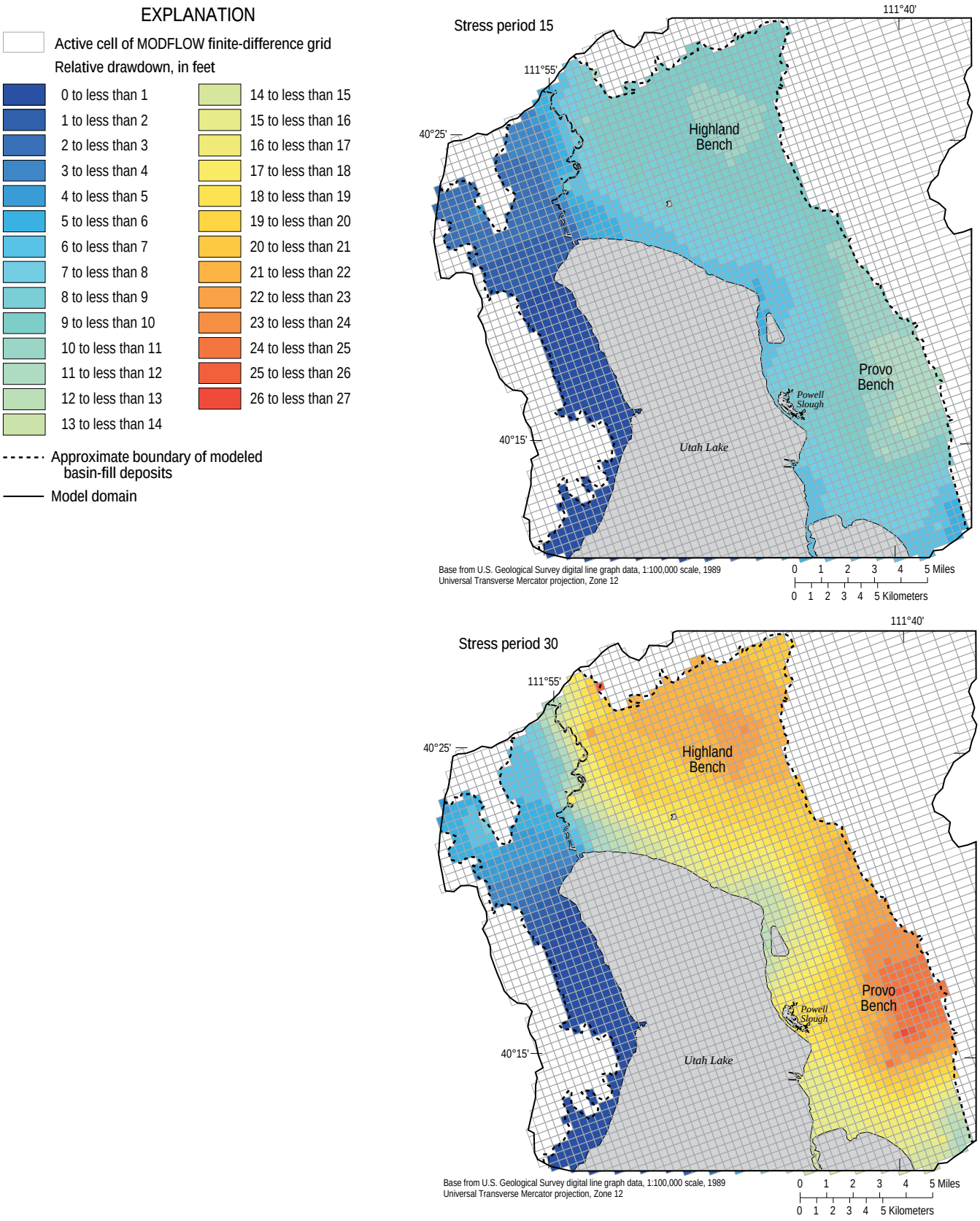

Figure 30. Simulated relative drawdown between the steady-state condition (the base simulation) and hypothetical scenario 1 at stress periods 15 and 30 in layer 3 of the ground-water flow model of northern Utah Valley, Utah.

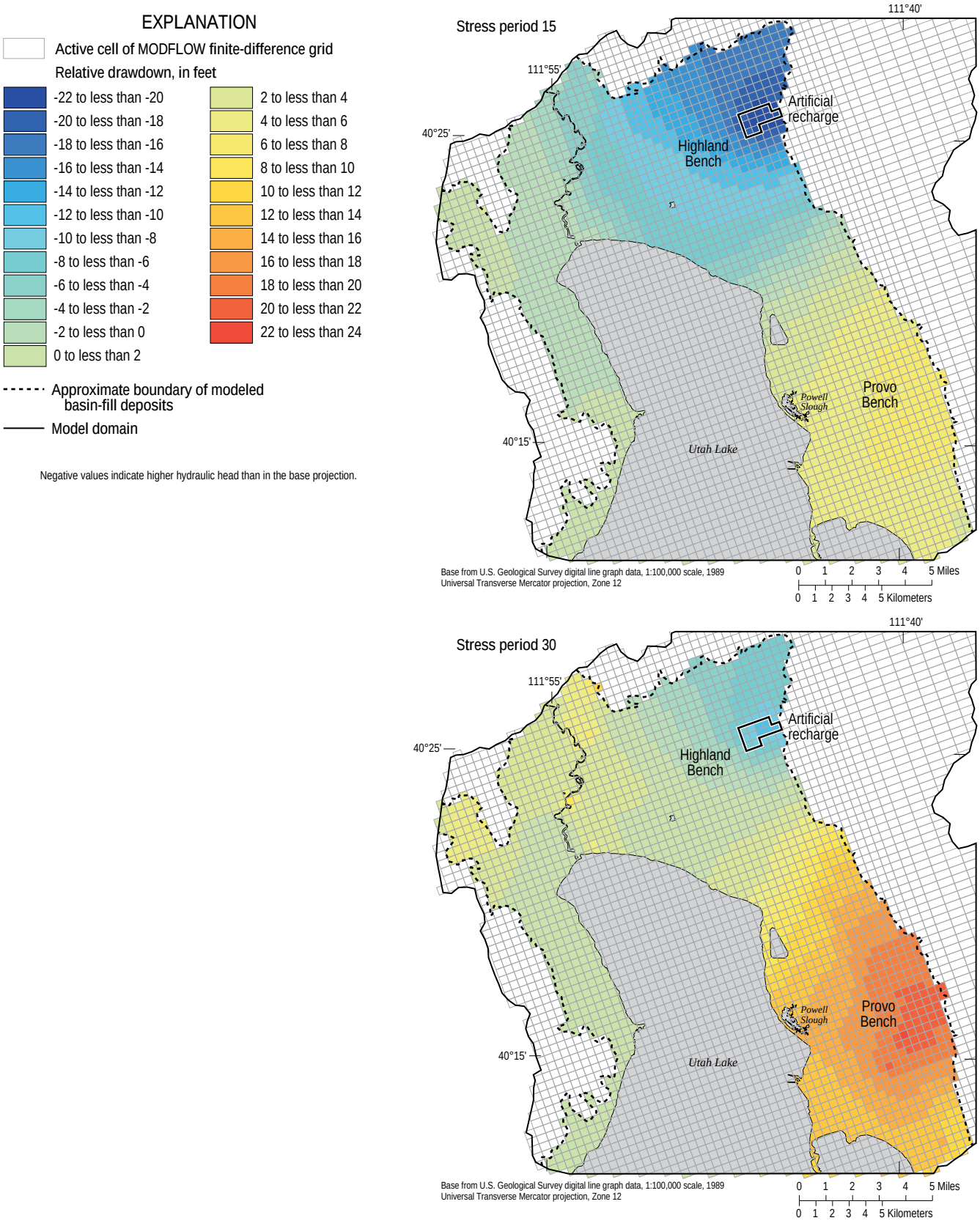

Figure 31. Simulated relative drawdown between the steady-state condition (the base simulation) and hypothetical scenario 2 at stress periods 15 and 30 in layer 3 of the ground-water flow model of northern Utah Valley, Utah.

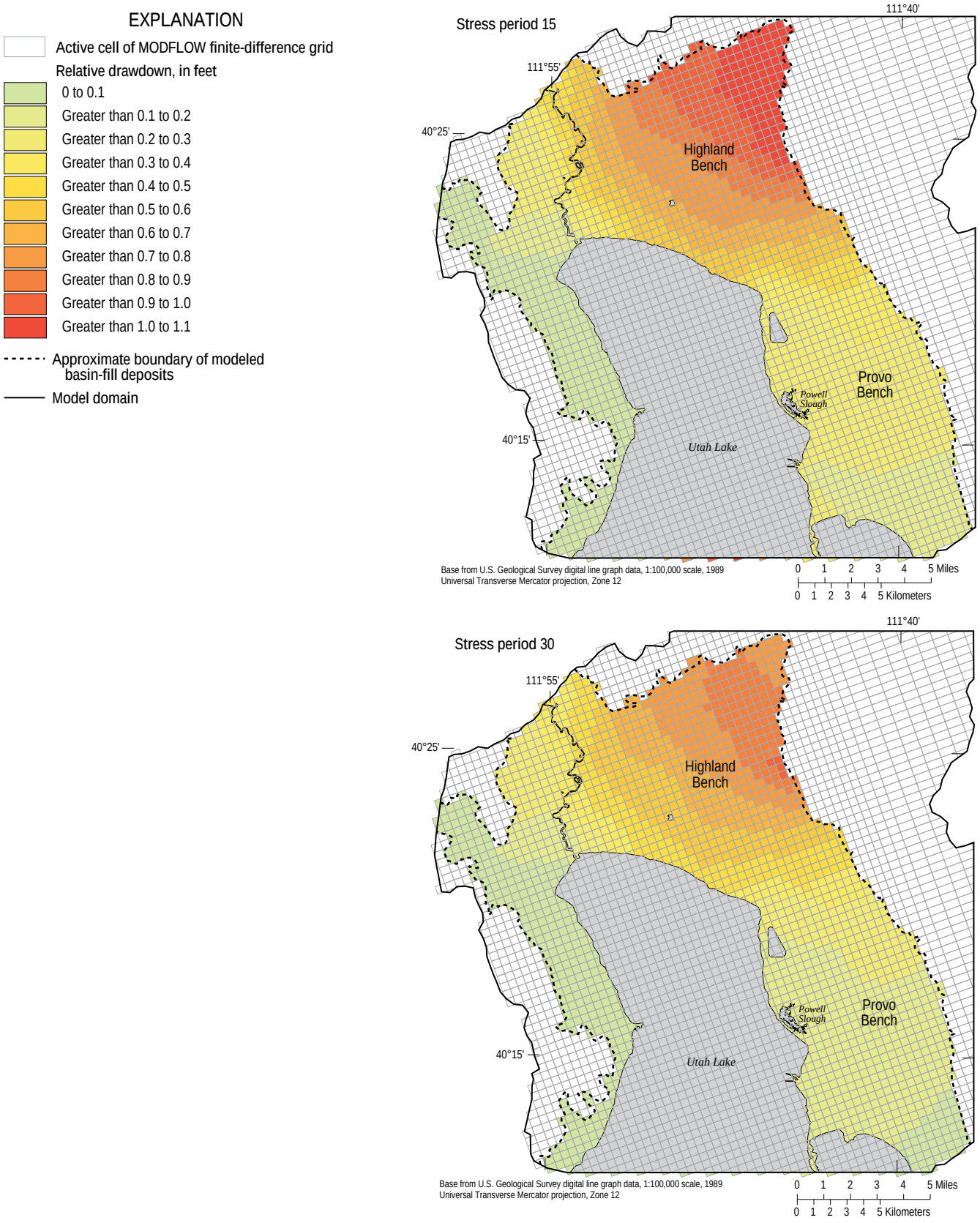

Figure 32. Simulated relative drawdown between the steady-state condition (the base simulation) and hypothetical scenario 3 at stress periods 15 and 30 in layer 3 of the ground-water flow model of northern Utah Valley, Utah.

Summary

In 2003, the U.S. Geological Survey, in cooperation with the Central Utah Water Conservancy District; Jordan Valley Water Conservancy District representing Draper City; Highland Water Company; Utah Department of Natural Resources, Division of Water Rights; and the municipalities of Alpine, American Fork, Cedar Hills, Eagle Mountain, Highland, Lehi, Lindon, Orem, Pleasant Grove, Provo, Saratoga Springs, and Vineyard began a study of hydrologic conditions in northern Utah Valley, Utah. The study included the development of a three-dimensional, finite-difference, numerical model of the ground-water flow system. The ground-water flow model described in this report can be used to evaluate the movement of ground water, the effects of water use on ground-water levels, and changes to the ground-water budget.

The ground-water flow model used to simulate ground-water flow in northern Utah Valley was developed using MODFLOW-2000. The model was calibrated to steady-state and transient-state conditions. The steady-state simulation was developed and calibrated to data defining hydrologic conditions for 1947. The transient-state simulation was developed and calibrated using hydrologic data for 1947 to 2004 and the results of the steady-state simulation as the initial condition. Areally, the model grid is 79 rows by 70 columns, with variable cell size. Cells throughout most of the model domain are 0.3 mile on a side. Vertically, the aquifer system is divided into 4 layers which incorporate 11 hydrogeologic units. The transient-state simulation was divided into 58 annual stress periods that represent conditions from 1947 to 2004.

Boundary conditions that define inflow and outflow components are implemented using packages in MODFLOW-2000. The Recharge Package is used to simulate recharge by (1) infiltration of precipitation over the mountain block, (2) infiltration of precipitation on the valley floor, and (3) seepage of unconsumed irrigation water from fields, lawns, and gardens. The Well Package is used to simulate withdrawal from pumping wells. The Stream Package is used to simulate recharge by seepage from streams and canals and discharge to mountain streams and the Jordan River. Discharge to streams in the mountains was modeled to provide some method of analyzing the accuracy of the model in bedrock. Subsurface inflow from Cedar Valley through Cedar Pass and outflow to Salt Lake Valley through the Jordan Narrows was simulated with the General Head Boundary Package. The Evapotranspiration Package was used to simulate ground water discharged by evapotranspiration from the principal aquifer system. The Drain Package was used to simulate head-dependent discharge to flowing wells and to drains and springs near Utah Lake. Finally, the Constant Head Boundary Package was used to assign annual head values for all of Utah Lake.

Available data were assembled and evaluated to construct and calibrate the model. Results of a lithologic framework model constructed from analysis of drillers' logs from more than 900 wells in northern Utah Valley were used to define the configuration of the aquifer system and confining units within the study area. The Hydrogeologic Unit Flow Package of MODFLOW-2000 was used to delineate 11 hydrogeologic units within the model that are spatially independent of the 4 model layers. Ground-water flow was simulated in basin-fill deposits and in bedrock in the western part of the valley and all surrounding mountains. Initial estimates and probable ranges of values for hydrologic properties used during model calibration were defined from data collected during this and previous studies for areas where they were available. Probable ranges of hydrologic properties for bedrock were based on published values.

In the transient-state simulation, specified recharge simulating infiltration from precipitation over the mountain block, precipitation over the valley, and unconsumed irrigation water was varied with time. The areal distribution of recharge over the mountain block was simulated by using the results of a GIS-based basin characterization model of net infiltration and varied as a function of the ratio of annual recharge to average recharge from 1970 to 2004. Results from the basin characterization model were not available prior to 1970, and recharge over the mountain block from 1947 to 1969 was varied in a similar way by using discharge in the American Fork River as a proxy for annual recharge. Annual variation in recharge from precipitation over the valley was simulated as a function of the ratio of annual precipitation to average precipitation at Pleasant Grove. Streamflow also was varied by specifying gaged or estimated values of annual streamflow at the head of the uppermost valley segment of each stream at the beginning of each stress period. Specified discharge from public-supply, industrial, and irrigation wells was varied based on values reported by water users and on unpublished records of the U.S. Geological Survey.

The MODFLOW-2000 Observation and Sensitivity Processes were used to guide model calibration. Forty-six water-level observations were used together with 25 flow observations to calibrate the steady-state simulation. An additional 12 flow observations and 915 water-level measurements from 498 wells were used as observations during the transient simulation. The model calibration focused on matching historical water levels, annual water-level changes, and estimated components of the ground-water budget for the steady-state (1947) and final (2004) stress periods of the simulation. During calibration, model parameters were adjusted within probable ranges until a reasonable match between model-simulated and measured or estimated conditions was achieved. Parameter adjustment was based largely on statistics generated by the MODFLOW-2000 Sensitivity Process. In general, the simulated water levels and flows (gains and losses in streams, canals, drains, and springs) are in good agreement with measured or estimated water levels and flows throughout most of the valley. The calibration also resulted in a reasonable match between simulated and measured annual water-level changes in most of the modeled area. The greatest discrepancies are generally near the boundary between the bedrock in the mountain block and the basin fill in the valley. Simulated discharge

compares well with conceptual discharge for most components of the ground-water budget. Simulated discharge was less than measured discharge for nearly all springs and drains during the final stress period but was within the range of expected uncertainty because the measurements likely include an unknown amount of shallow ground water that originated as infiltrating runoff or irrigation water rather than upward discharge from the principal aquifer system.

The model described in this report was calibrated with significantly more data than was used in the previous model of northern Utah Valley. The relatively good fit between simulated and measured or estimated quantities indicates that the overall simulated ground-water flow is a reasonable representation of ground-water flow in northern Utah Valley that can adequately approximate trends in water levels caused by fluctuations in recharge and ground-water withdrawal. Nonetheless, measured water levels, water-level changes, and estimated flows were not accurately reproduced everywhere in all stress periods during the simulation. In particular, the match to measured water-level change in the deeper confined aquifers in the eastern part of the valley could likely be improved by improving the estimates of flowing-well discharge that the model is calibrated to. Updated estimates of flowing-well discharge are still based on outdated information and few actual flow measurements. Hydrologic properties in the western part of the valley are currently based on few water-level data and the model is presently considered less accurate in that area. As ground-water development continues, more data will become available that demonstrate how the ground-water system responds to that development. This will likely provide valuable information that can be incorporated to improve the model in the future.

Acknowledgments

The author thanks the following individuals who provided data, valuable discussion and assistance that were essential to the construction and calibration of the ground-water flow model presented in this report. Jay Cederberg and Susan Thiros of the USGS compiled historical data and collected hundreds of water-level measurements used in construction of the model. Lynette Brooks of the USGS provided important suggestions and technical direction. Victor Heilweil and Linda Woolfenden of the USGS and David Pitcher, K.C. Shaw, and Michael Whimpey of the Central Utah Water Conservancy District provided technical reviews of this report. Also, the Utah Department of Natural Resources, Division of Water Rights; the Central Utah Water Conservancy District; and all local water managers and representatives from municipalities in northern Utah Valley who participated in biannual meetings and offered direction and cooperator input during the development of the ground-water model are gratefully acknowledged.

References Cited

Anderman, E.R., and Hill, M.C., 2000, MODFLOW-2000, The U.S. Geological Survey modular ground-water model—Documentation of the Hydrogeologic-Unit Flow (HUF) Package: U.S. Geological Survey Open-File Report 00-342, 89 p., *http://pubs.er.usgs.gov/usgspubs/ofr/ofr00342*, accessed March 26, 2008.

Anderson, P.B., Susong, D.D., Wold, S.R., Heilweil, V.M., and Baskin, R.L., 1994, Hydrogeology of recharge areas and water quality of the principal aquifers along the Wasatch front and adjacent areas, Utah: U.S. Geological Survey Water-Resources Investigations Report 93-4221, 74 p., *http://pubs.er.usgs.gov/usgspubs/wri/wri934221*, accessed March 9, 2008.

Appel, C.L., Clark, D.W., and Fairbanks, P.E., 1982, Selected hydrologic data for northern Utah Valley, Utah, 1935-82: U.S. Geological Survey Open-File Report 82-1023, 97 p.

Biek, R.F., 2005, Geologic map of the Jordan Narrows quadrangle, Salt Lake and Utah Counties, Utah: Utah Geological Survey Map 208, 2 plates, scale 1:24,000.

Brooks, L.E. and Stolp, B.J., 1995, Hydrology and simulation of ground-water flow in southern Utah and Goshen Valleys, Utah: Utah Department of Natural Resources Technical Publication No. 111, 96 p.

Burden, C.B., and others, 2004, Ground-water conditions in Utah, spring of 2004: Utah Department of Natural Resources Cooperative Investigations Report No. 45, 120 p., *http://ut.water.usgs.gov/publications/GW2004.pdf*, accessed March 9, 2008.

Cederberg, J.R., Gardner, P.M., and Thiros, S.A., 2009, Ground-water hydrology of northern Utah Valley, Utah County, Utah, 2003-05: U.S. Geological Survey Scientific Investigations Report 08-5197, 98 p.

Chow, V.T., 1959, Open-channel hydraulics: New York, McGraw-Hill Book Co., 680 p.

Clark, D.W., 1984, The ground-water system and simulated effects of ground-water withdrawals in northern Utah Valley, Utah: U.S. Geological Survey Water-Resources Investigations Report 85-4007, 56 p., *http://pubs.er.usgs.gov/usgspubs/wri/wri854007*, accessed March 9, 2008.

Clark, D.W., and Appel, C.L., 1985, Ground-water resources of northern Utah Valley, Utah: Utah Department of Natural Resources Technical Publication No. 80, 115 p.

Cordova, R.M., and Subitzky, Seymour, 1965, Ground water in northern Utah Valley, Utah: A progress report for the period 1948-63: Utah Department of Natural Resources Technical Publication No. 11, 41 p.

Domenico, P.A., and Schwartz, F.W., 1998, Physical and chemical hydrogeology: New York, John Wiley and Sons, 506 p.

Dustin, J.D., and Merritt, L.B., 1980, Hydrogeology of Utah Lake with emphasis on Goshen Bay: Utah Geological and Mineral Survey Water Resources Bulletin 23, 50 p.

Feltis, R.D., 1967, Ground-water conditions in Cedar Valley, Utah County, Utah: Utah State Engineer Technical Publication No. 16, 34 p.

Flint, A.L., Flint, L.E., Hevesi, J.A., and Blainey, J.B., 2004, Fundamental concepts of recharge in the desert Southwest: A regional modeling perspective, *in* Hogan, J.F., Phillips, F.M., and Scanlon, B.R., eds., Groundwater recharge in a desert environment: The Southwestern United States: Washington D.C., American Geophysical Union, p. 159-184.

Harbaugh, A.W., Banta, E.R., Hill, M.C., and McDonald, M.G., 2000, MODFLOW-2000, The U.S. Geological Survey modular ground-water model—User guide to modularization concepts and the ground-water flow process: U.S. Geological Survey Open-File Report 00-92, 121 p., *http://pubs.er.usgs.gov/usgspubs/ofr/ofr200092*, accessed March 9, 2008.

Harrill, J.R., and Prudic, D.E., 1998, Aquifer systems in the Great Basin region of Nevada, Utah, and adjacent states, Summary report: U.S. Geological Survey Professional Paper 1409A, 61 p., *http://pubs.er.usgs.gov/usgspubs/pp/pp1409A*, accessed March 26, 2008.

Hecker, Suzanne, 1993, Quaternary tectonics of Utah with emphasis on earthquake-hazard characterization: Utah Geological Survey Bulletin 127, 157 p., 2 pls.

Hevesi, J.A., Flint, A.L., and Flint, L.E., 2003, Simulation of net infiltration and potential recharge using a distributed-parameter watershed model of the Death Valley Region, Nevada and Califonia: U.S. Geological Survey Water-Resources Investigations Report 03-4090, 161 p., *http://pubs.er.usgs.gov/usgspubs/wri/wri034090*, accessed March 26, 2008.

Hill, M.C., Banta, E.R., Harbaugh, A.W., and Anderman, E.R., 2000, MODFLOW-2000, The U.S. Geological Survey modular ground-water model—User guide to the observation, sensitivity, and parameter-estimation processes and three post-processing programs: U.S. Geological Survey Open-File Report 00-184, 209 p., *http://pubs.er.usgs.gov/usgspubs/ofr/ofr00184*, accessed March 9, 2008.

Hill, M.C., and Tiedeman, C.R., 2007, Effective groundwater model calibration: New York, John Wiley and Sons, 455 p.

Hintze, L.F., Willis G.C., Laes, D.Y.M., Sprinkel, D.A., and Brown, K.D., 2000, Digital geologic map of Utah: Utah Geological Survey Map 179DM.

Hunt, C.B., Varnes, H.D., and Thomas, H.E., 1953, Lake Bonneville: Geology of northern Utah Valley, Utah: U.S. Geological Survey Professional Paper 257-A, 99 p., *http://pubs.er.usgs.gov/usgspubs/pp/pp257A*, accessed March 9, 2008.

Lambert, P.M., 1995, Numerical simulation of ground-water flow in basin-fill sediments in Salt Lake Valley, Utah: Utah Department of Natural Resources Technical Publication No. 110-B, 58 p.

Maxey, G.B., and Eakin, T.E., 1949, Ground water in White River Valley, White Pine, Nye, and Lincoln Counties, Nevada: Nevada State Engineer, Water Resources Bulletin 8, 59 p.

McDonald, M.G., and Harbaugh, A.W., 1984, A modular three-dimensional finite-difference ground-water flow model: U.S. Geological Survey Open-File Report 83-875, 528 p., *http://pubs.er.usgs.gov/usgspubs/ofr/ofr83875*, accessed March 26, 2008.

McDonald, M.G., and Harbaugh, A.W., 1988, A modular three-dimensional finite-difference ground-water flow model: U.S. Geological Survey Techniques of Water-Resources Investigations, book 6, chap. A1, [variously paged]., *http://pubs.er.usgs.gov/usgspubs/twri/twri06A1*, accessed March 26, 2008.

National Center for Earth Resources Observation & Science, 1999, National Elevation Dataset: U.S. Geological Survey data available on the World Wide Web, accessed April 2005, at *http://ned.usgs.gov/*

Spatial Climate Analysis Service, 2004, Parameter-elevation Regressions on Independent Slopes Model (PRISM): Oregon State University data available on the World Wide Web, accessed April 2005, at *http://www.prism.oregonstate.edu/*

Prudic, D.E., 1989, Documentation of a computer program to simulate stream-aquifer relations using a modular, finite-difference, ground-water flow model: U.S. Geological Survey Open-File Report 88-729, 113 p., *http://pubs.er.usgs.gov/usgspubs/ofr/ofr88729*, accessed March 26, 2008.

Richardson, G.B., 1906, Underground water in the valleys of Utah Lake and Jordan River, Utah: U.S. Geological Survey Water-Supply and Irrigation Paper 157, 81 p., *http://pubs.er.usgs.gov/usgspubs/wsp/wsp157*, accessed March 9, 2008.

Theis, C.V., Brown, R.H., and Meyer, R.R., 1964, Estimating the transmissibility of aquifers from the specific capacity of wells, *in* Bentall, Ray, compiler, Methods of determining permeability, transmissibility, and drawdown: U.S. Geological Survey Water-Supply Paper 1536-I, p. 331-340., *http://pubs.er.usgs.gov/usgspubs/wsp/wsp1536I*, accessed March 26, 2008.

Thiros, S.A., 1992, Selected hydrologic data for Salt Lake Valley, Utah, 1990-92, with emphasis on data from the shallow unconfined aquifer and confining layers: U.S. Geological Survey Open-File Report 92-640, 44 p., *http://pubs.er.usgs.gov/usgspubs/ofr/ofr92640*, accessed March 26, 2008.

Thiros, S.A., 2006, Evaluation of the ground-water flow model for northern Utah Valley, Utah, updated to conditions through 2002: U.S. Geological Survey Scientific Investigations Report 2006-5064, 20 p., *http://pubs.er.usgs.gov/usgspubs/sir/sir20065064*, accessed March 26, 2008.

Utah Department of Natural Resources, 2004, Downloadable GIS land use data, accessed April 2006, at *http://www.water.utah.gov/planning/landuse/gisdata.htm*

Appendix

This appendix includes the individual figures that comprise the interactive maps of figures 6, 11, and 15.

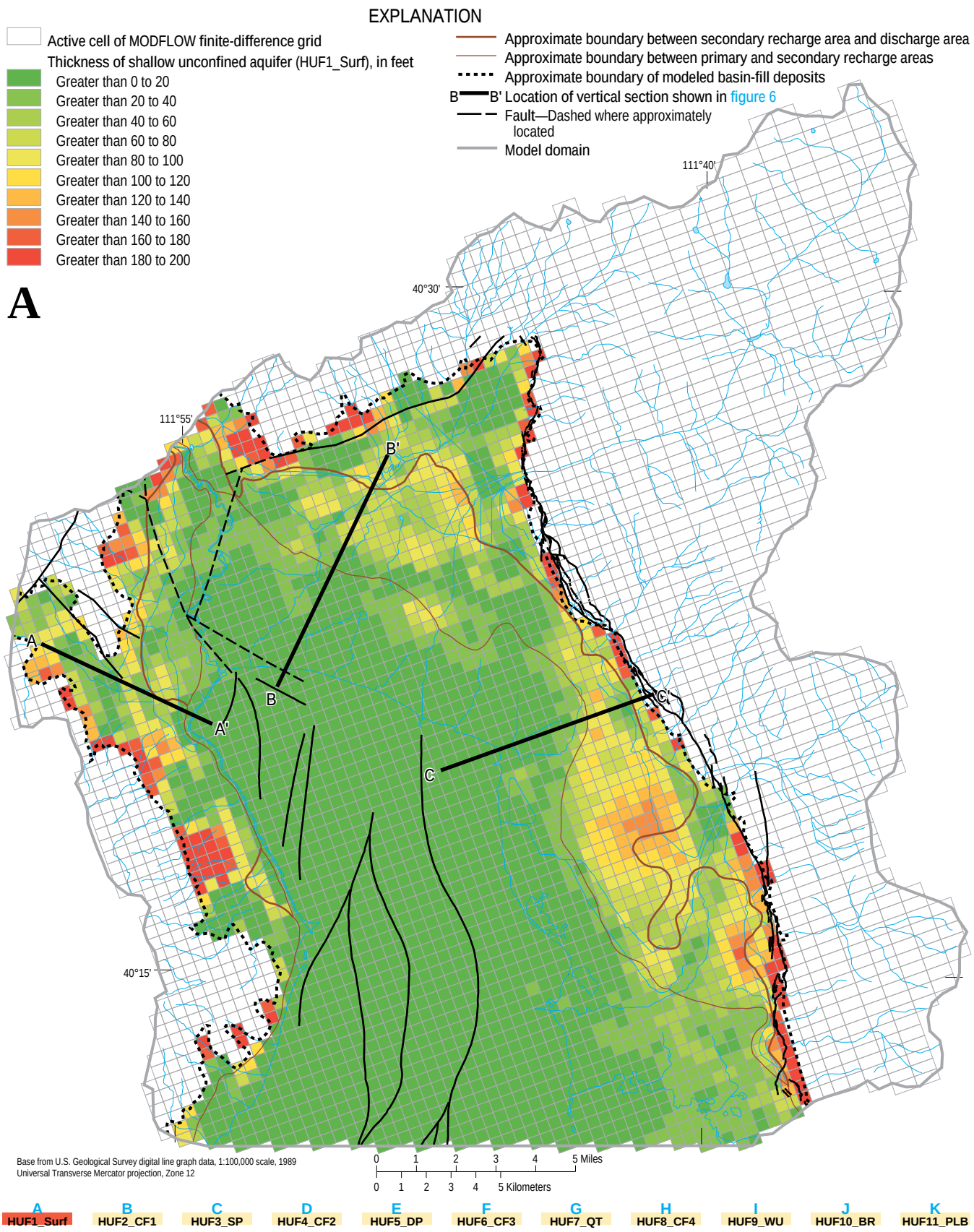

Figure 5a. Thickness and areal extent of the hydrogeologic unit HUF1_Surf simulated with the Hydrogeologic Unit Flow Package in the ground-water flow model of northern Utah Valley, Utah.

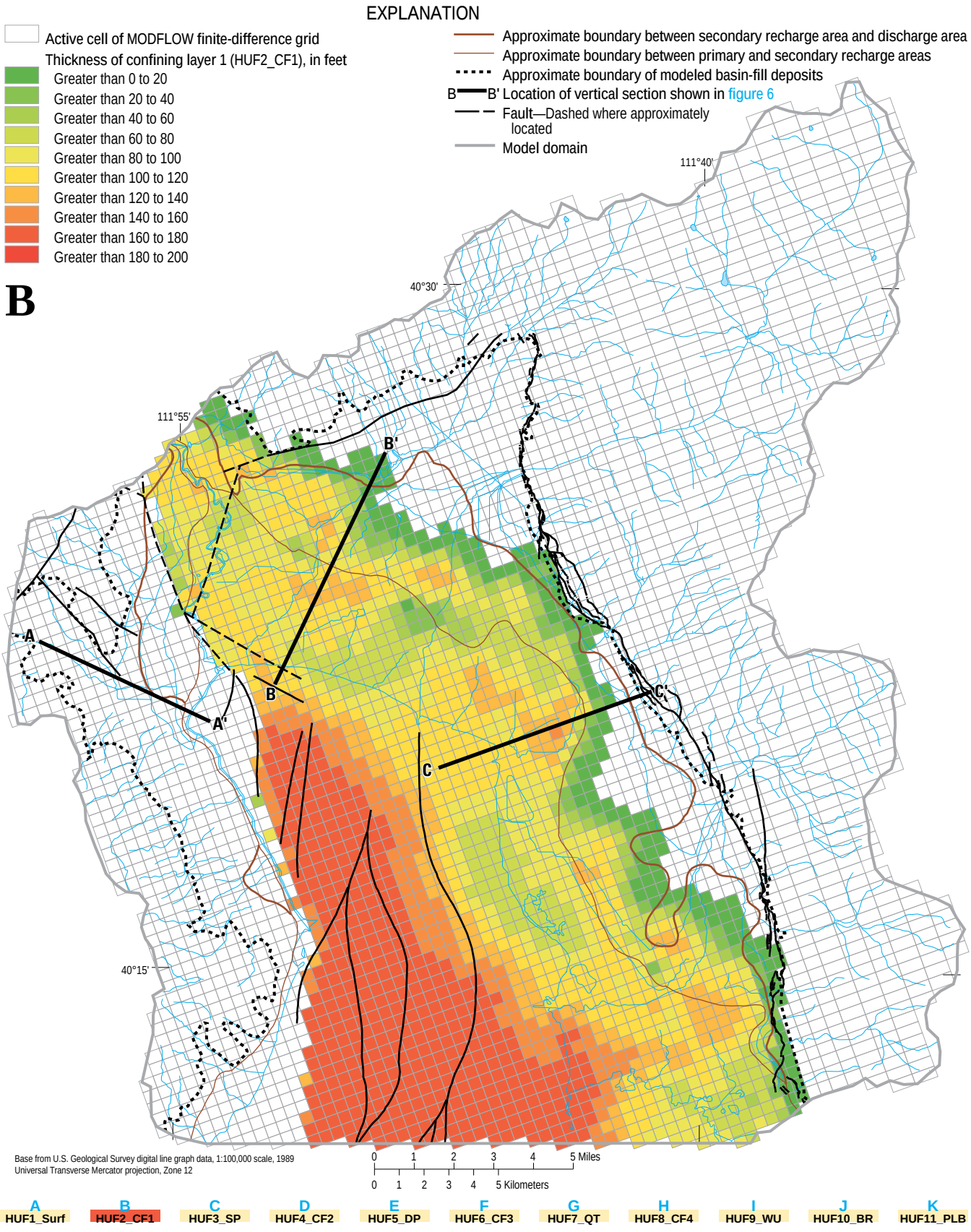

Figure 5b. Thickness and areal extent of the hydrogeologic unit HUF2_CF1 simulated with the Hydrogeologic Unit Flow Package in the ground-water flow model of northern Utah Valley, Utah.

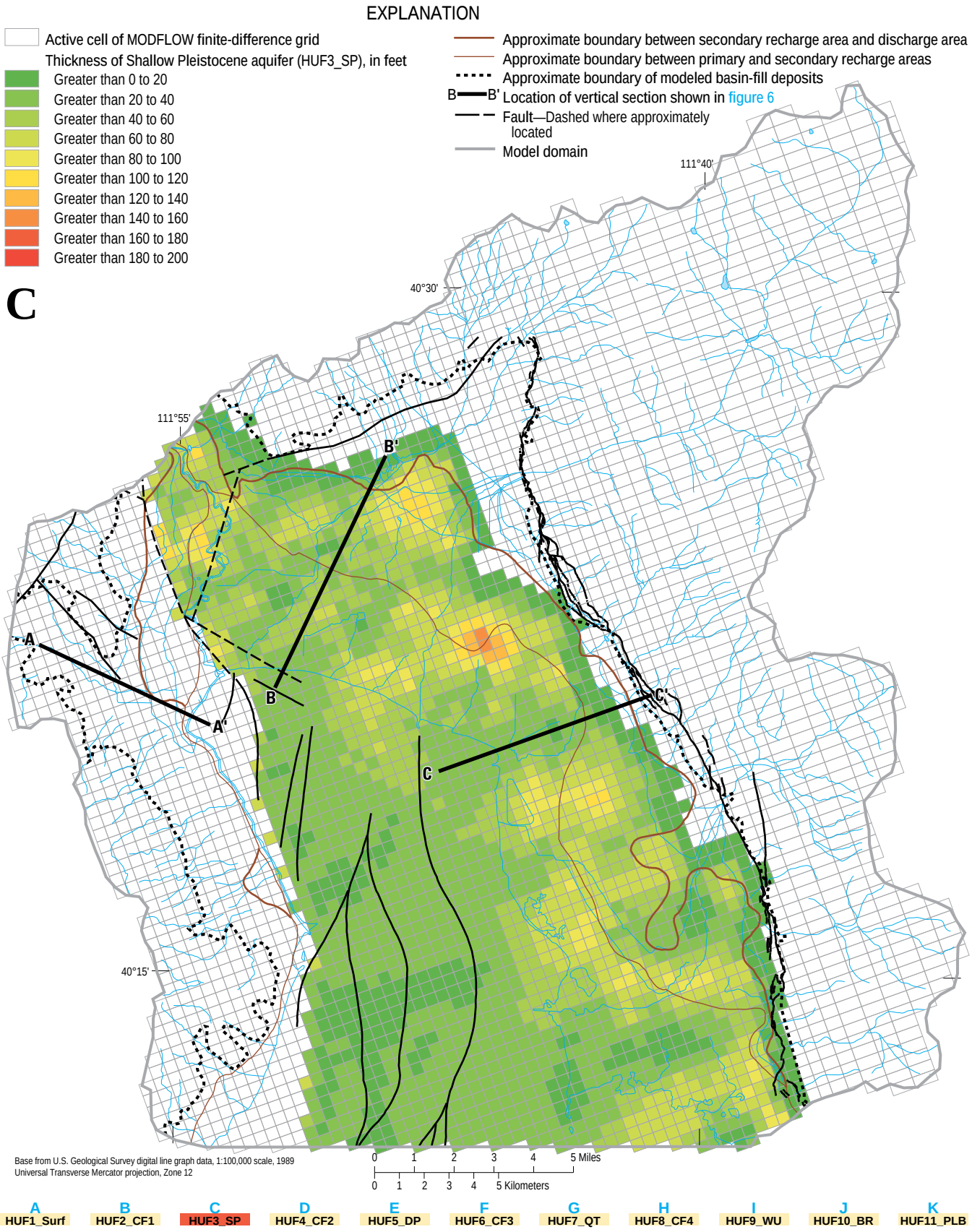

Figure 5c. Thickness and areal extent of the hydrogeologic unit HUF3_SP simulated with the Hydrogeologic Unit Flow Package in the ground-water flow model of northern Utah Valley, Utah.

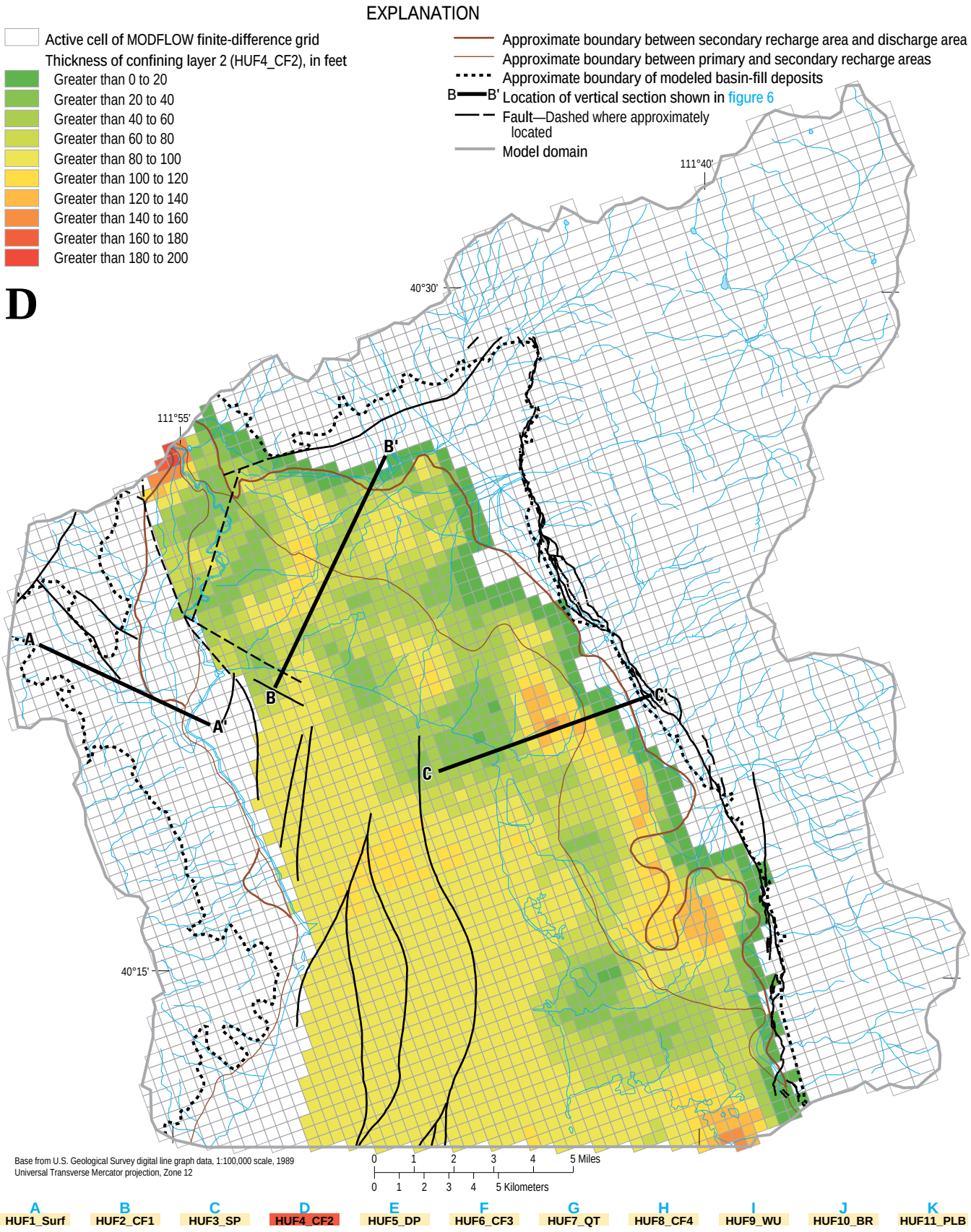

Figure 5d. Thickness and areal extent of the hydrogeologic unit HUF4_CF2 simulated with the Hydrogeologic Unit Flow Package in the ground-water flow model of northern Utah Valley, Utah.

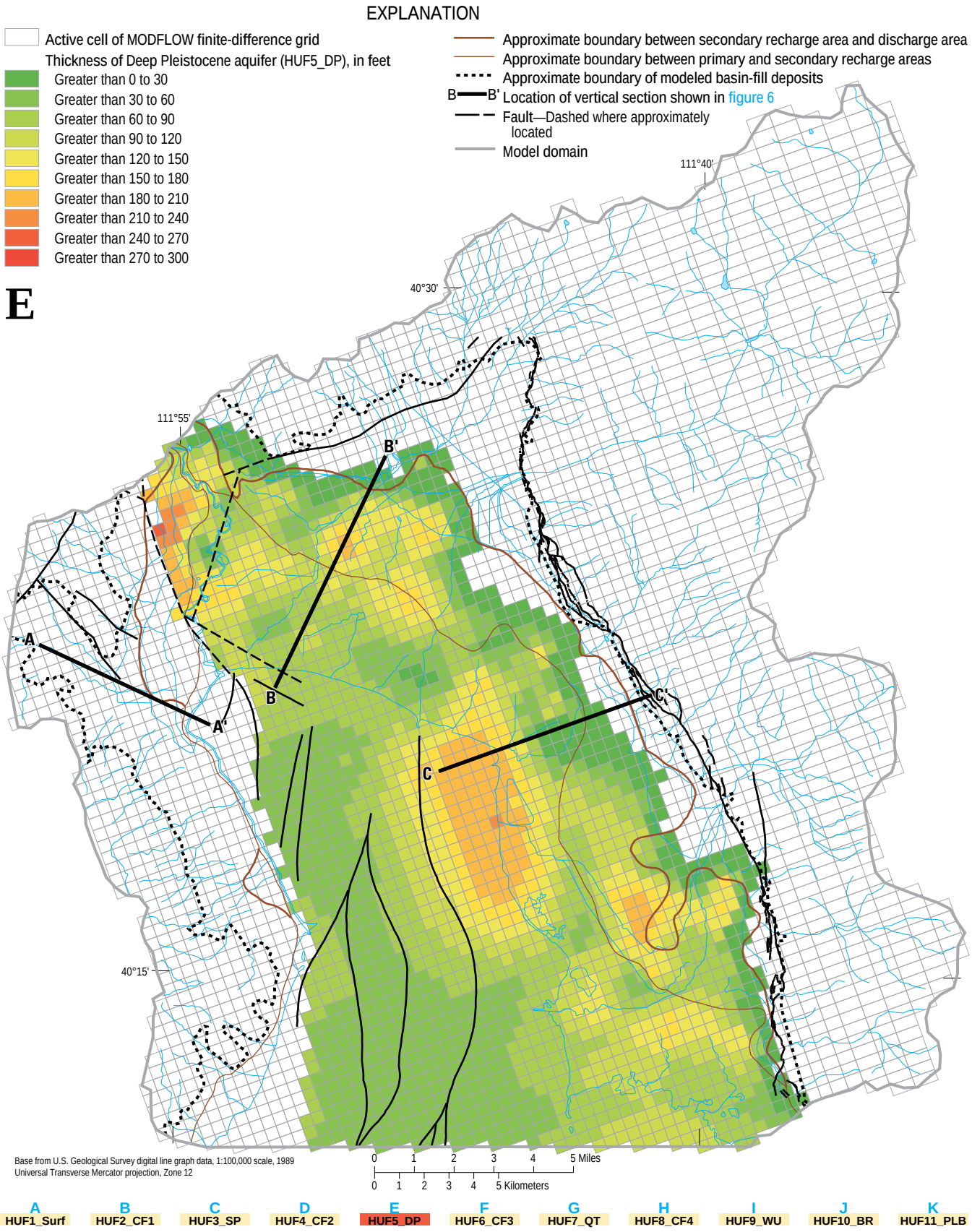

Figure 5e. Thickness and areal extent of the hydrogeologic unit HUF5_DP simulated with the Hydrogeologic Unit Flow Package in the ground-water flow model of northern Utah Valley, Utah.

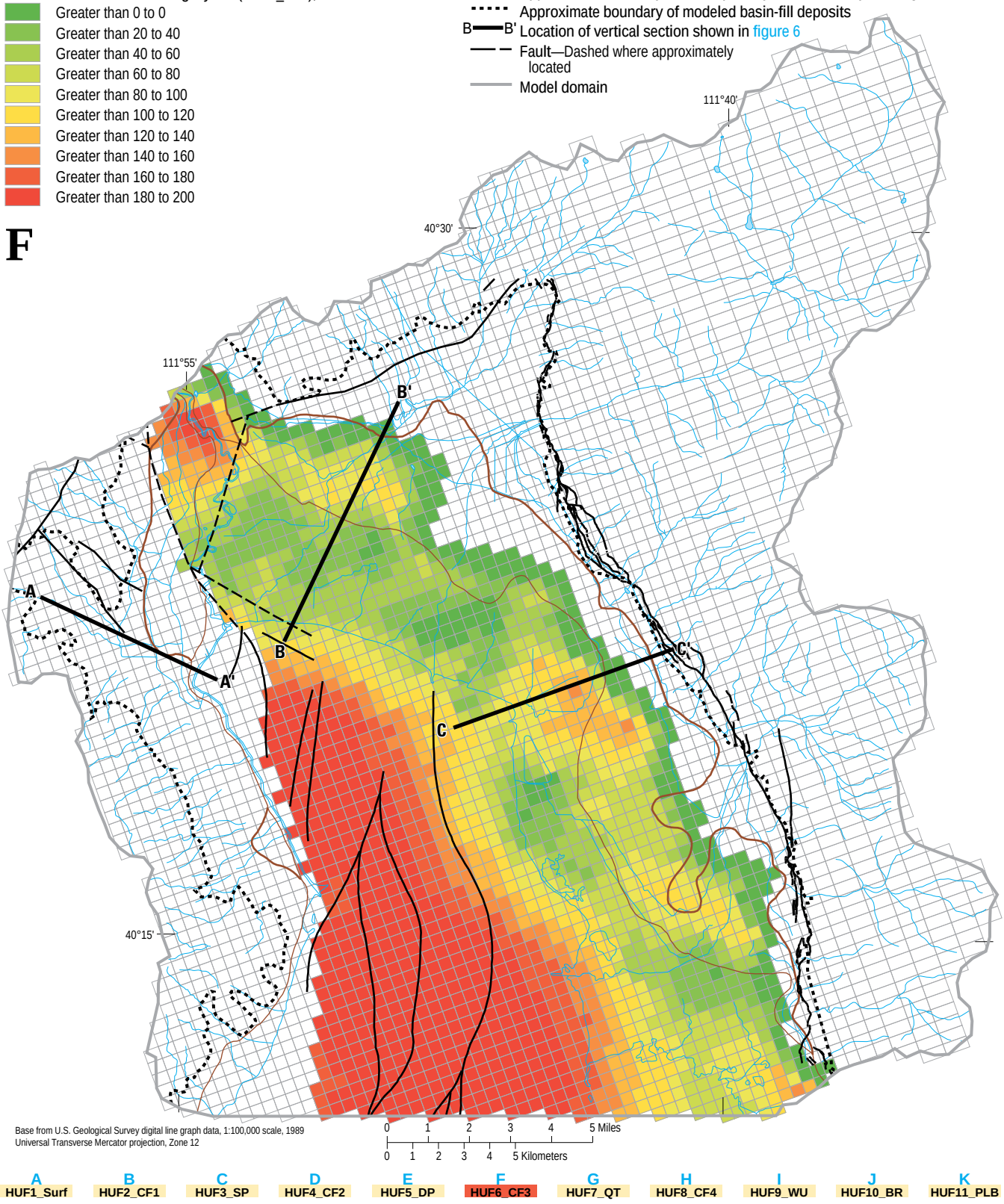

Figure 5f. Thickness and areal extent of the hydrogeologic unit HUF6_CF3 simulated with the Hydrogeologic Unit Flow Package in the ground-water flow model of northern Utah Valley, Utah.

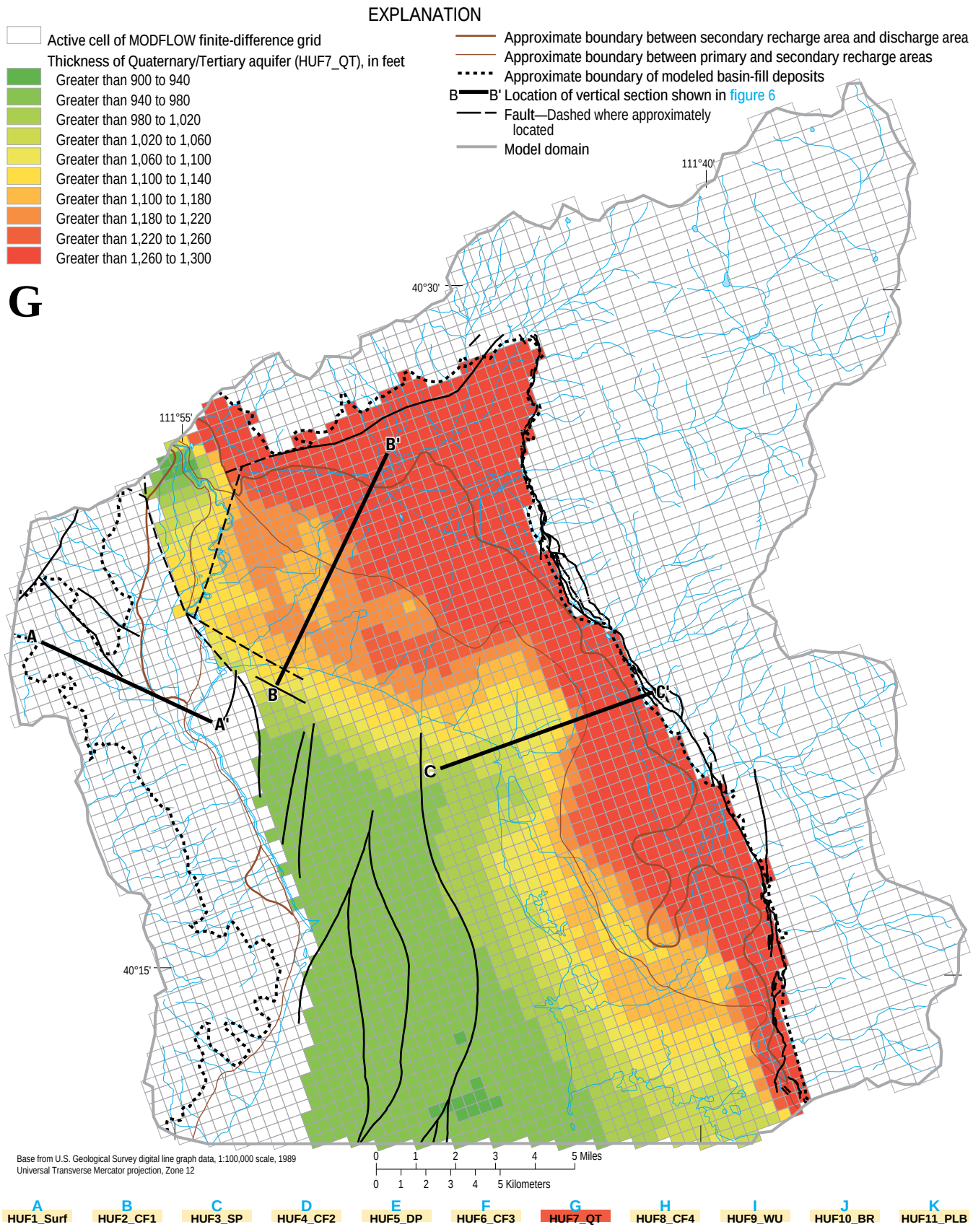

Figure 5g. Thickness and areal extent of the hydrogeologic unit HUF7_QT simulated with the Hydrogeologic Unit Flow Package in the ground-water flow model of northern Utah Valley, Utah.

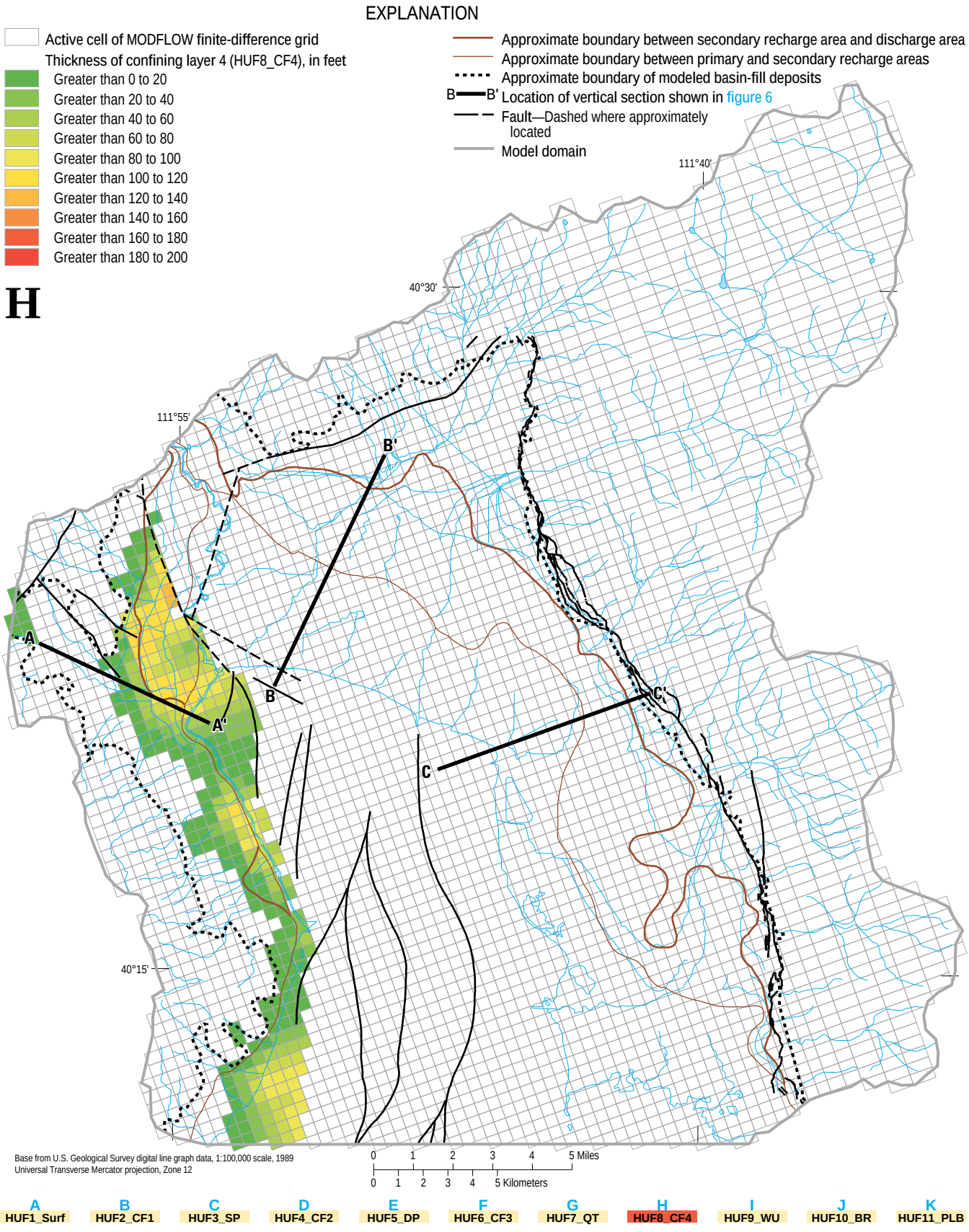

Figure 5h. Thickness and areal extent of the hydrogeologic unit HUF8_CF4 simulated with the Hydrogeologic Unit Flow Package in the ground-water flow model of northern Utah Valley, Utah.

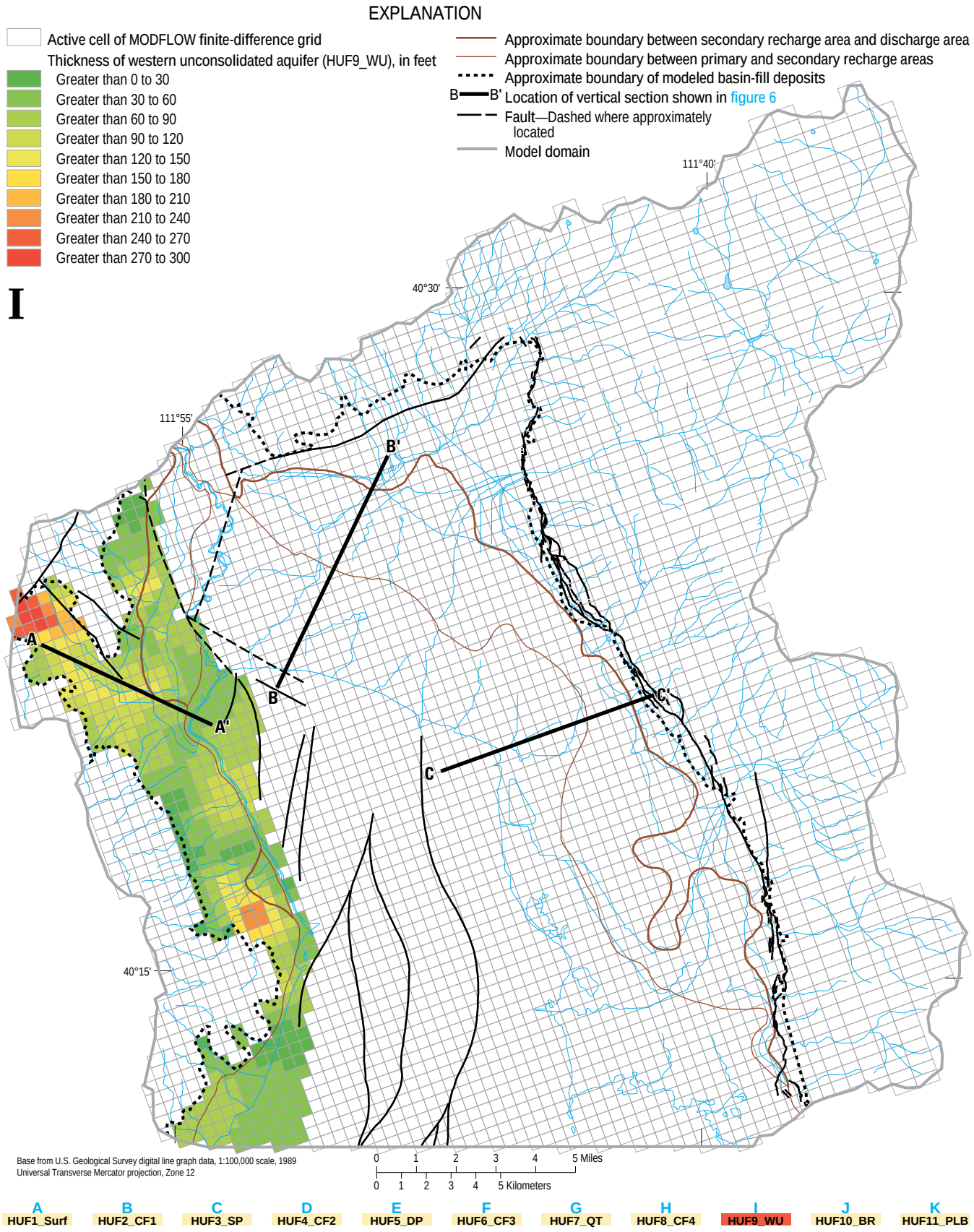

Figure 5i. Thickness and areal extent of the hydrogeologic unit HUF9_WU simulated with the Hydrogeologic Unit Flow Package in the ground-water flow model of northern Utah Valley, Utah.

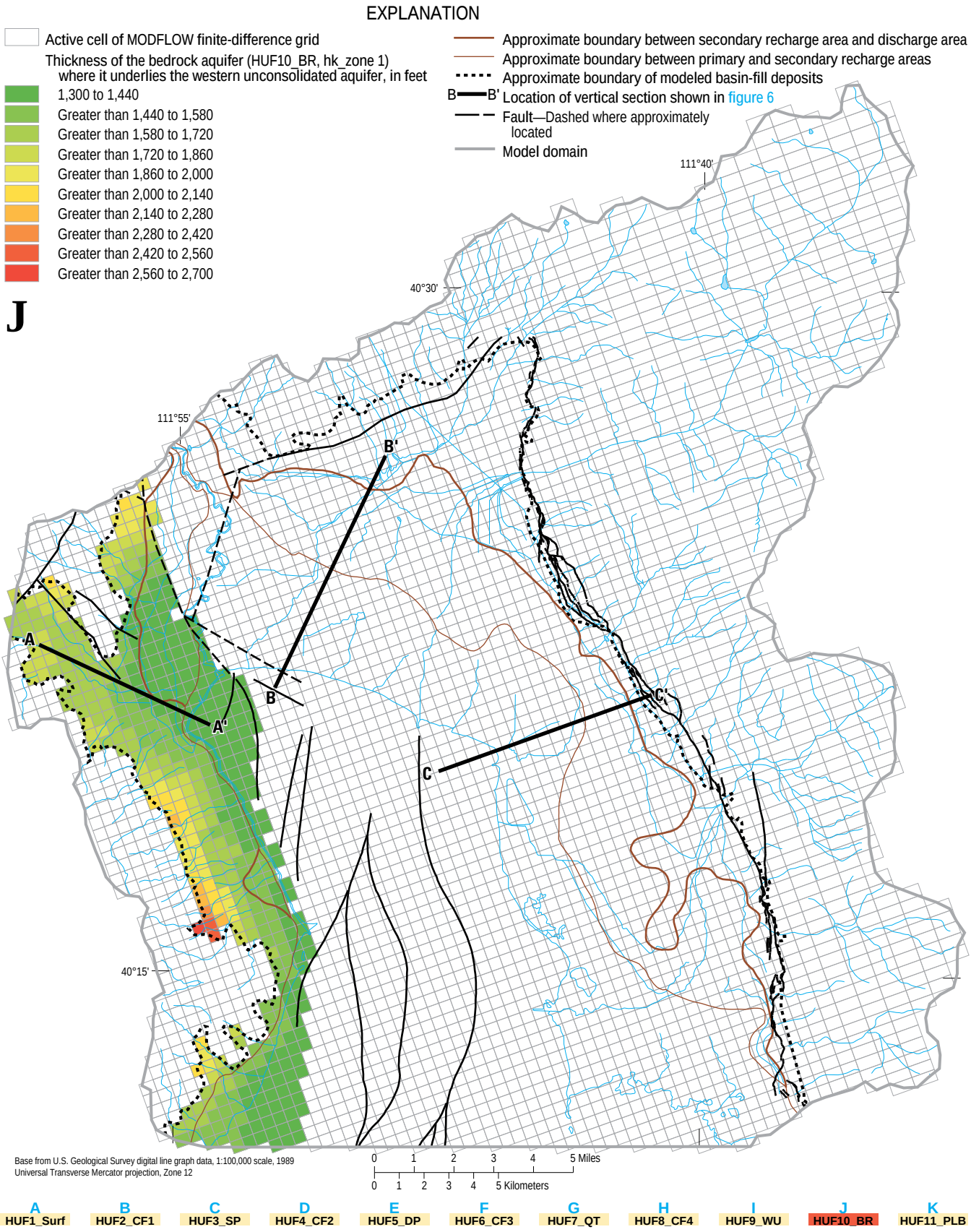

Figure 5j. Thickness and areal extent of the hydrogeologic unit HUF10_BR within the basin-fill boundary simulated with the Hydrogeologic Unit Flow Package in the ground-water flow model of northern Utah Valley, Utah.

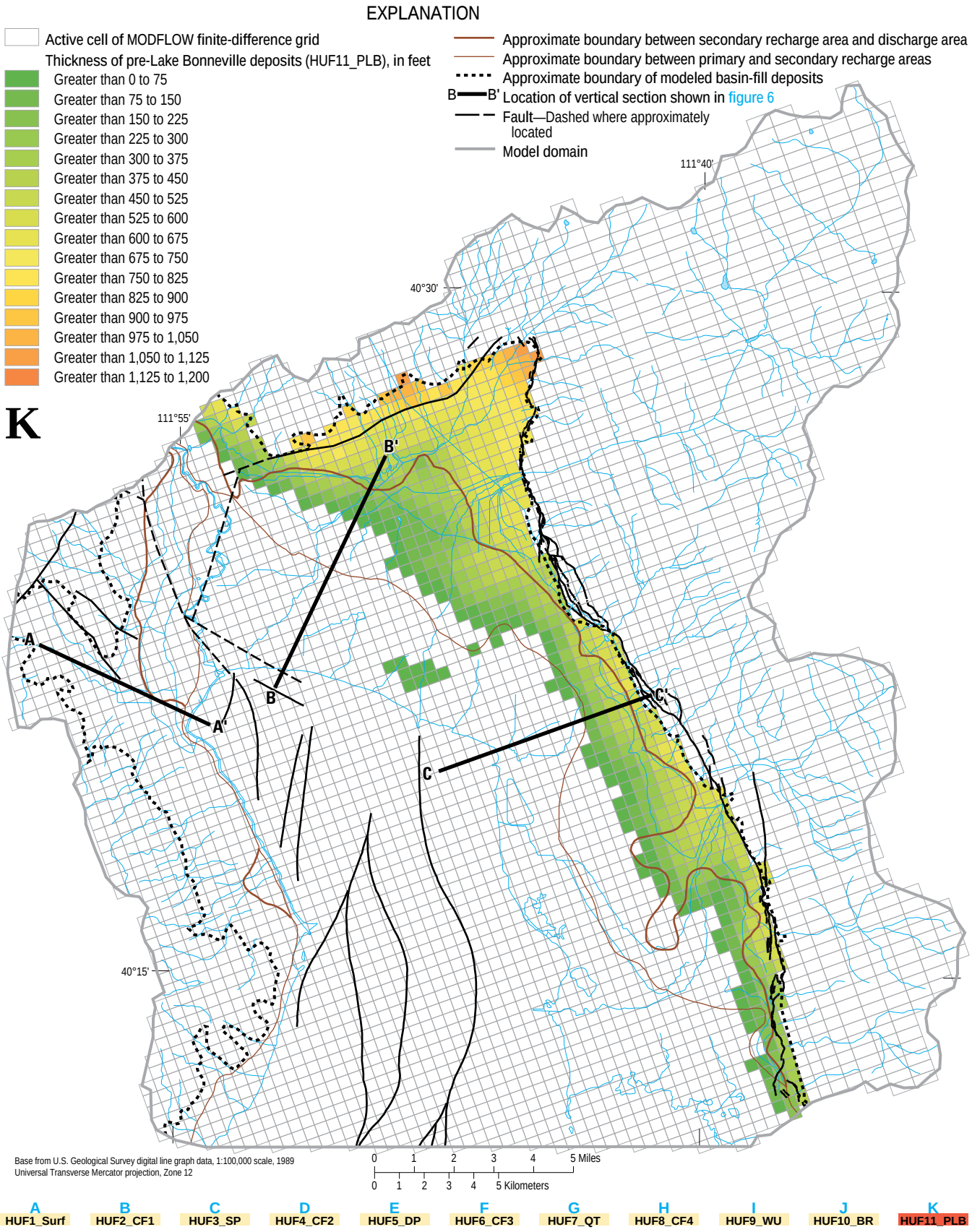

Figure 5k. Thickness and areal extent of the hydrogeologic unit HUF11_PLB simulated with the Hydrogeologic Unit Flow Package in the ground-water flow model of northern Utah Valley, Utah.

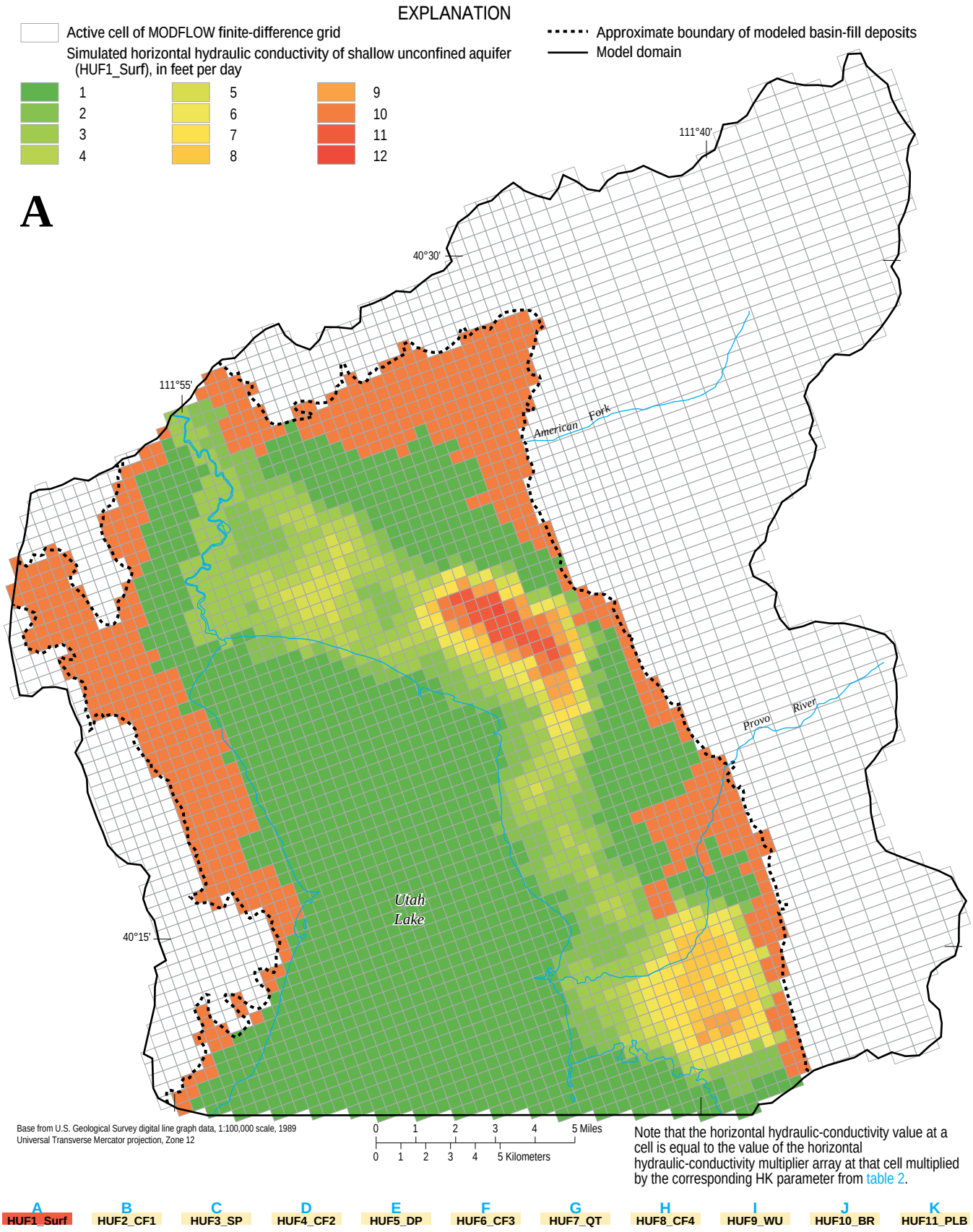

Figure 11a. Simulated horizontal hydraulic conductivity of the hydrogeologic unit HUF1_Surf simulated with the Hydrogeologic Unit Flow Package in the ground-water flow model of northern Utah Valley, Utah.

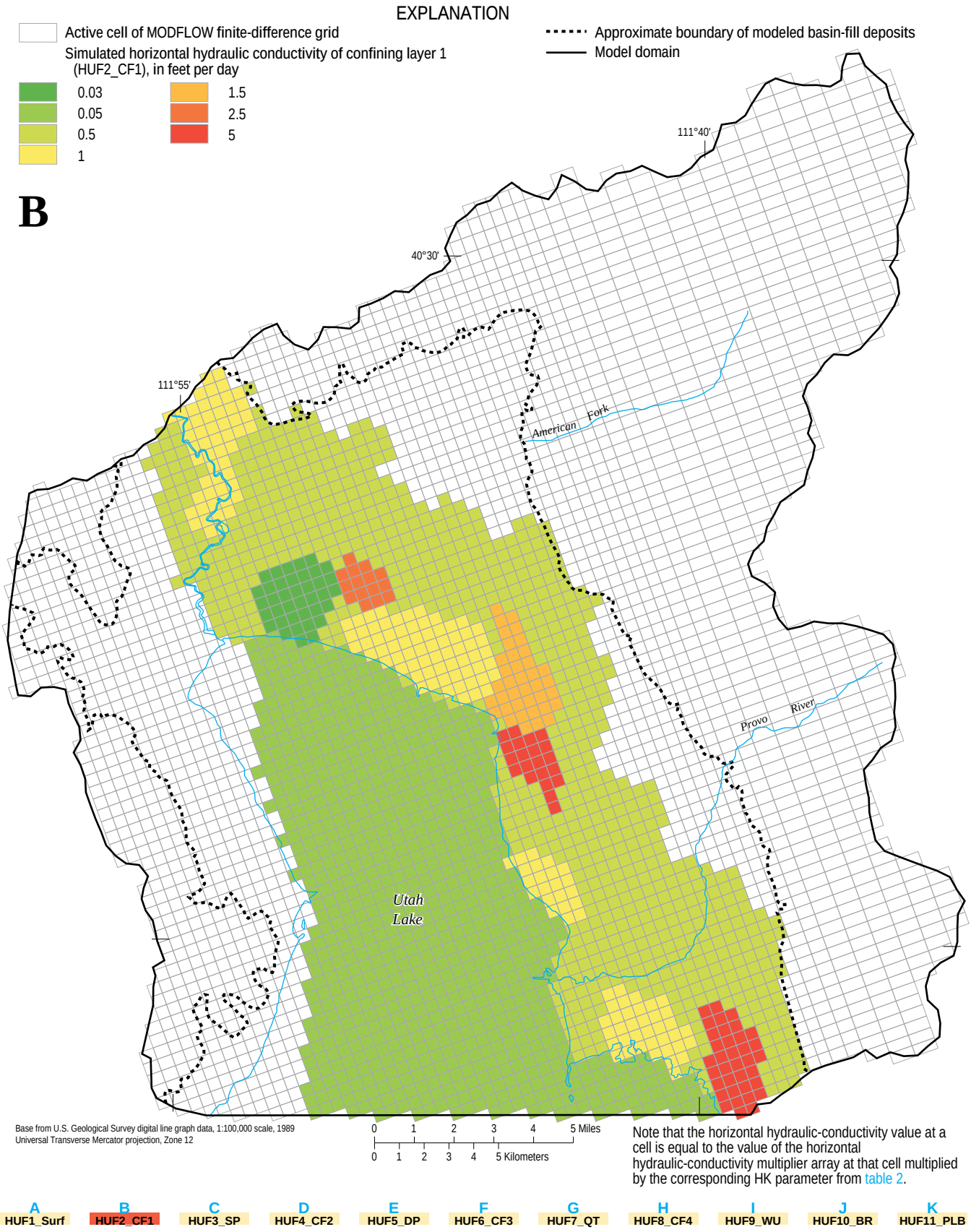

Figure 11b. Simulated horizontal hydraulic conductivity of the hydrogeologic unit HUF2_CF1 simulated with the Hydrogeologic Unit Flow Package in the ground-water flow model of northern Utah Valley, Utah.

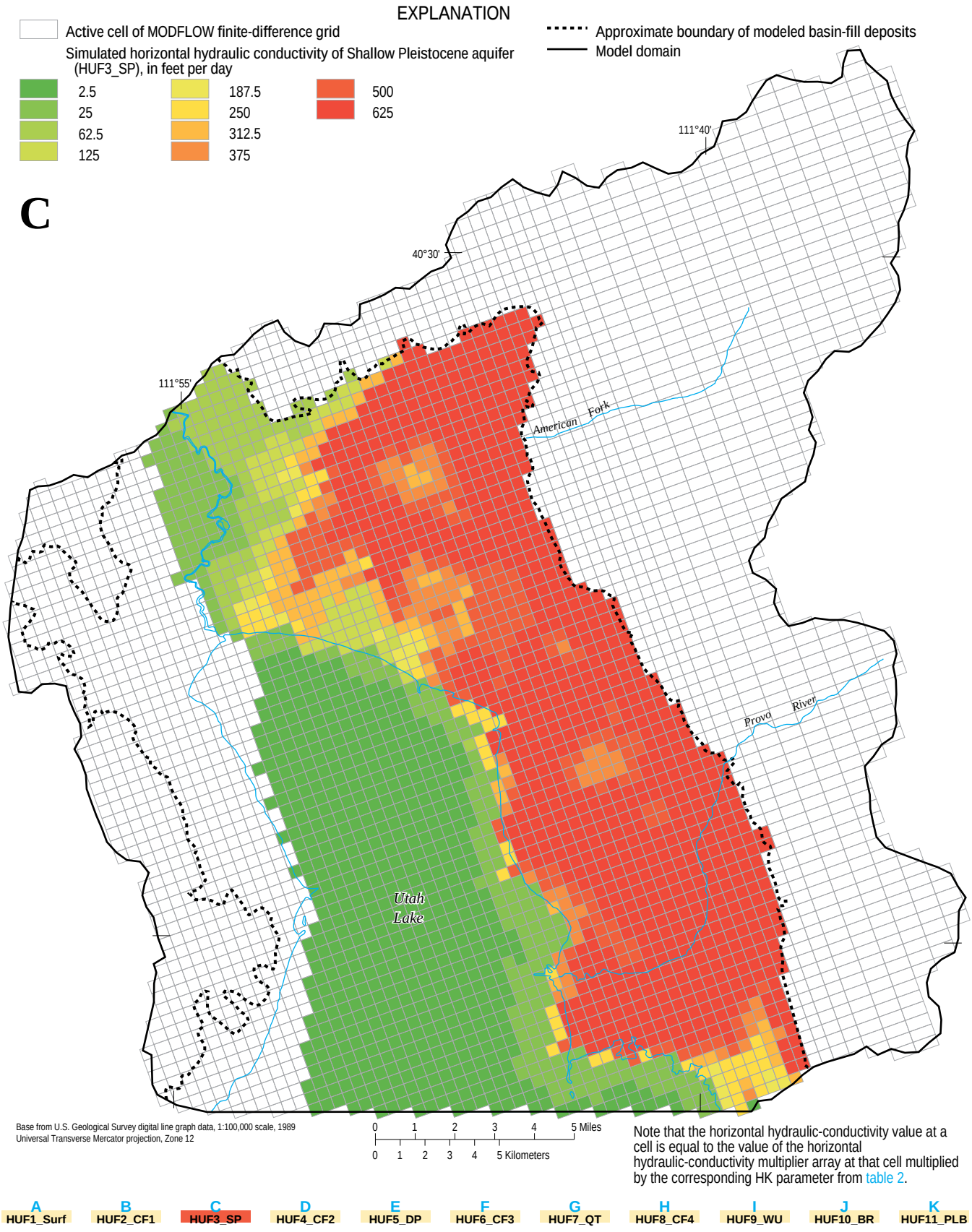

Figure 11c. Simulated horizontal hydraulic conductivity of the hydrogeologic unit HUF3_SP simulated with the Hydrogeologic Unit Flow Package in the ground-water flow model of northern Utah Valley, Utah.

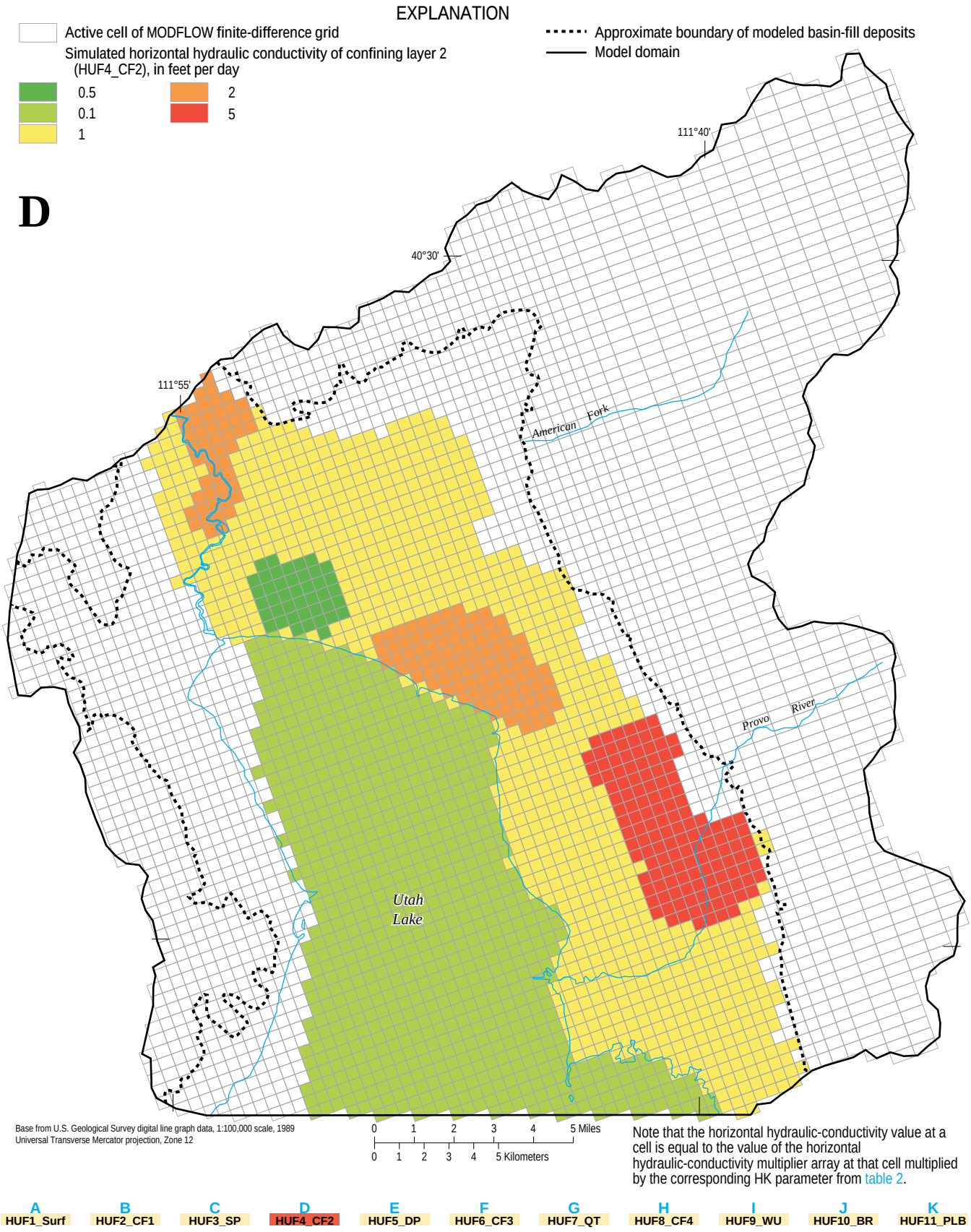

Figure 11d. Simulated horizontal hydraulic conductivity of the hydrogeologic unit HUF4_CF2 simulated with the Hydrogeologic Unit Flow Package in the ground-water flow model of northern Utah Valley, Utah.

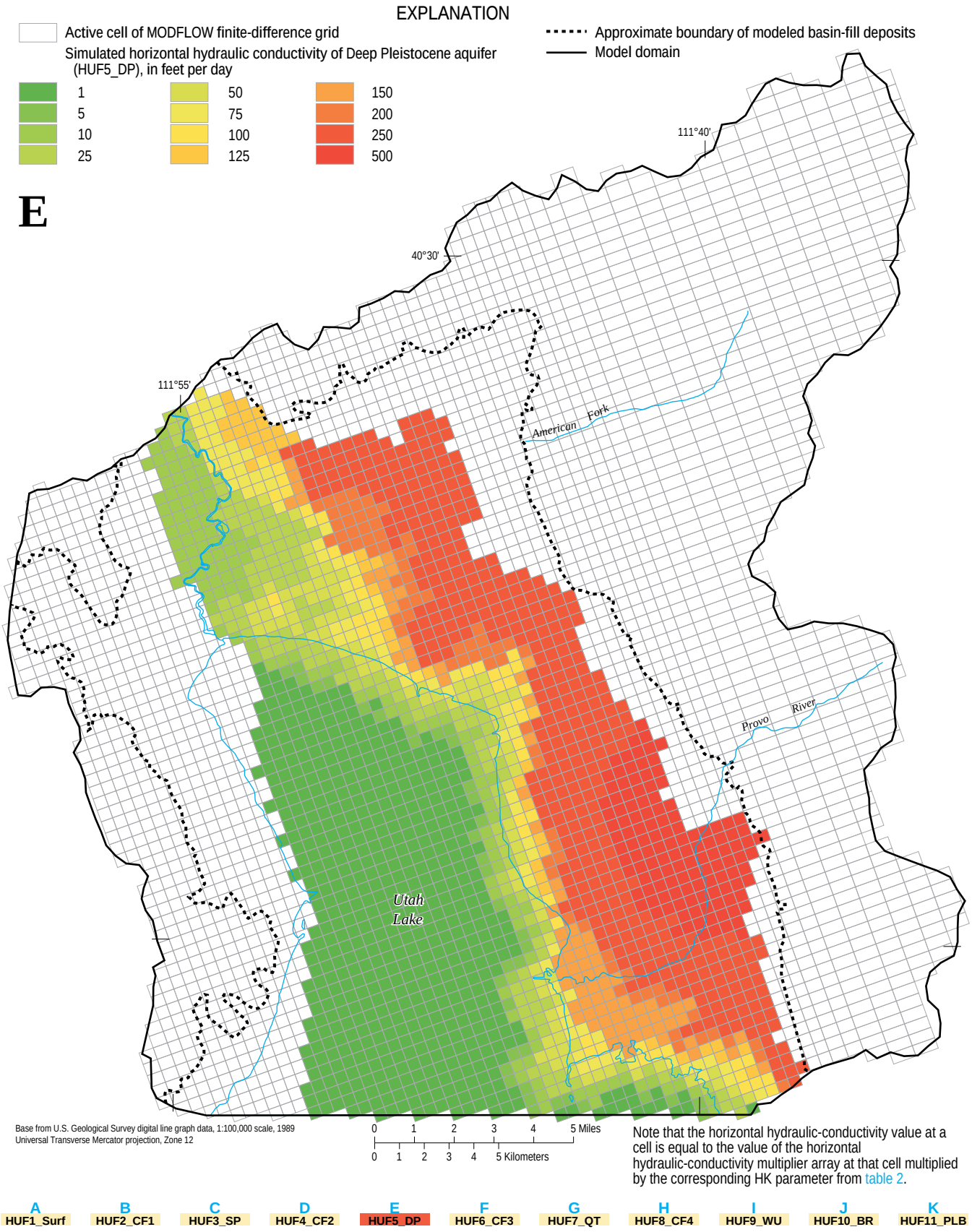

Figure 11e. Simulated horizontal hydraulic conductivity of the hydrogeologic unit HUF5_DP simulated with the Hydrogeologic Unit Flow Package in the ground-water flow model of northern Utah Valley, Utah.

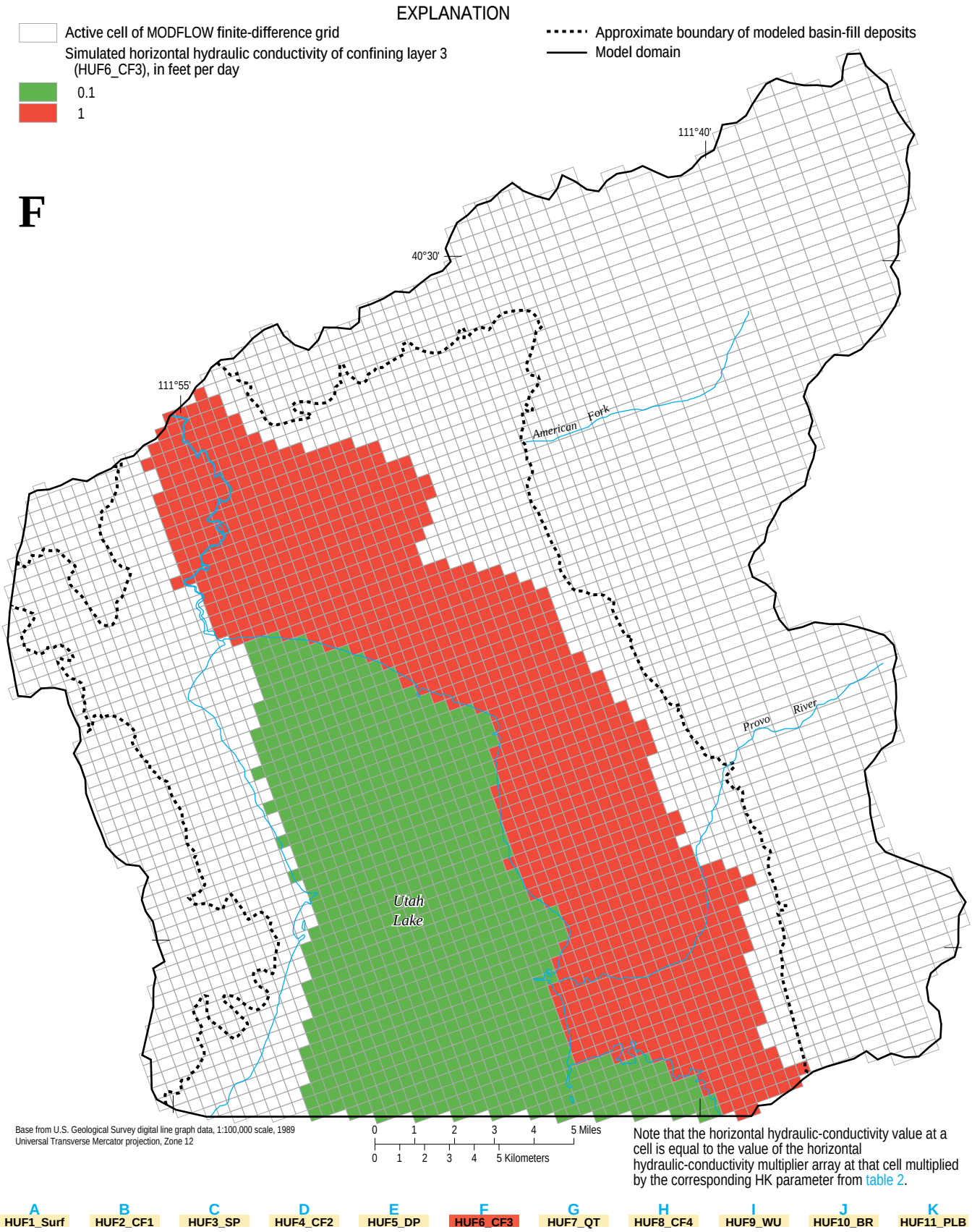

Figure 11f. Simulated horizontal hydraulic conductivity of the hydrogeologic unit HUF6_CF3 simulated with the Hydrogeologic Unit Flow Package in the ground-water flow model of northern Utah Valley, Utah.

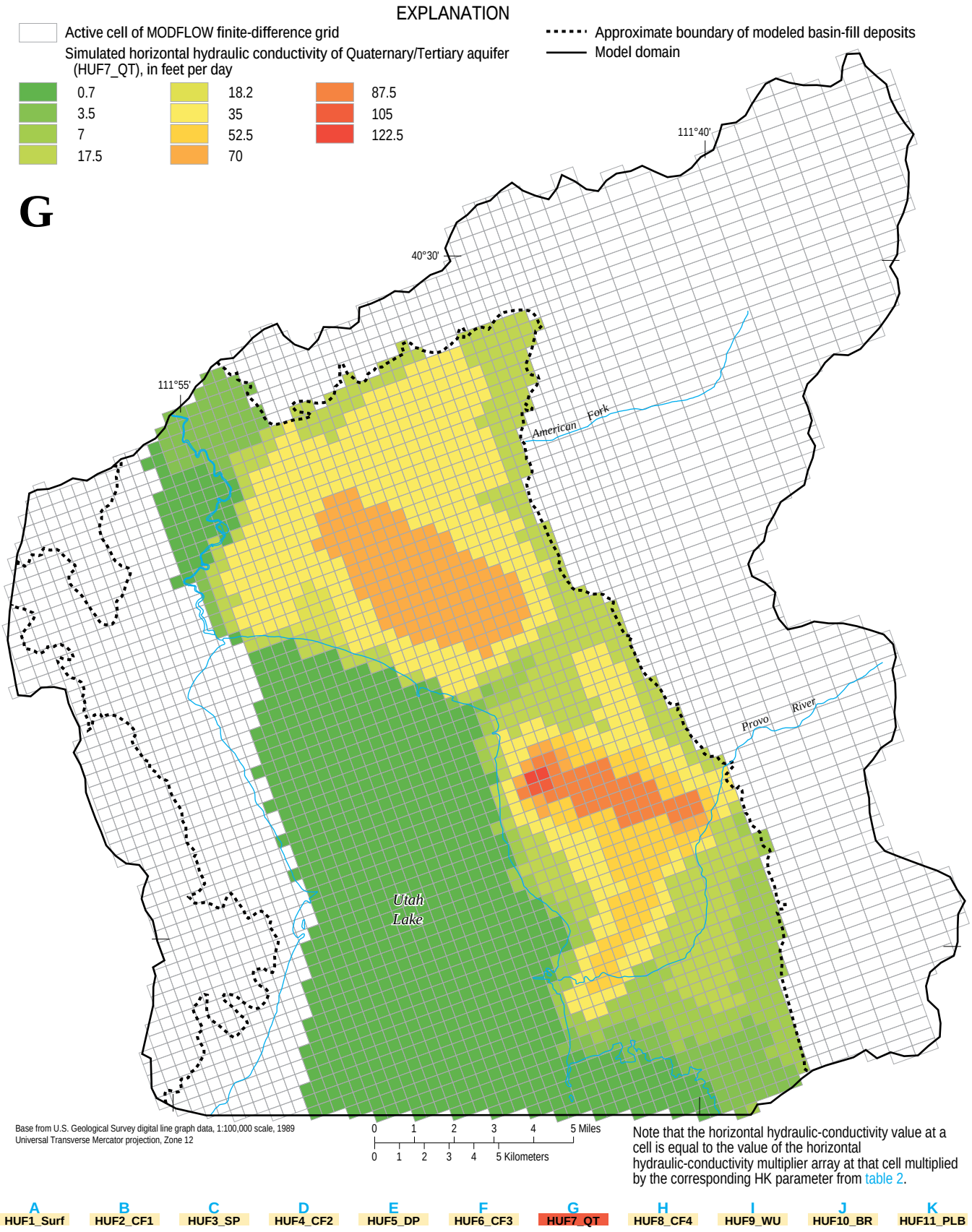

Figure 11g. Simulated horizontal hydraulic conductivity of the hydrogeologic unit HUF7_QT simulated with the Hydrogeologic Unit Flow Package in the ground-water flow model of northern Utah Valley, Utah.

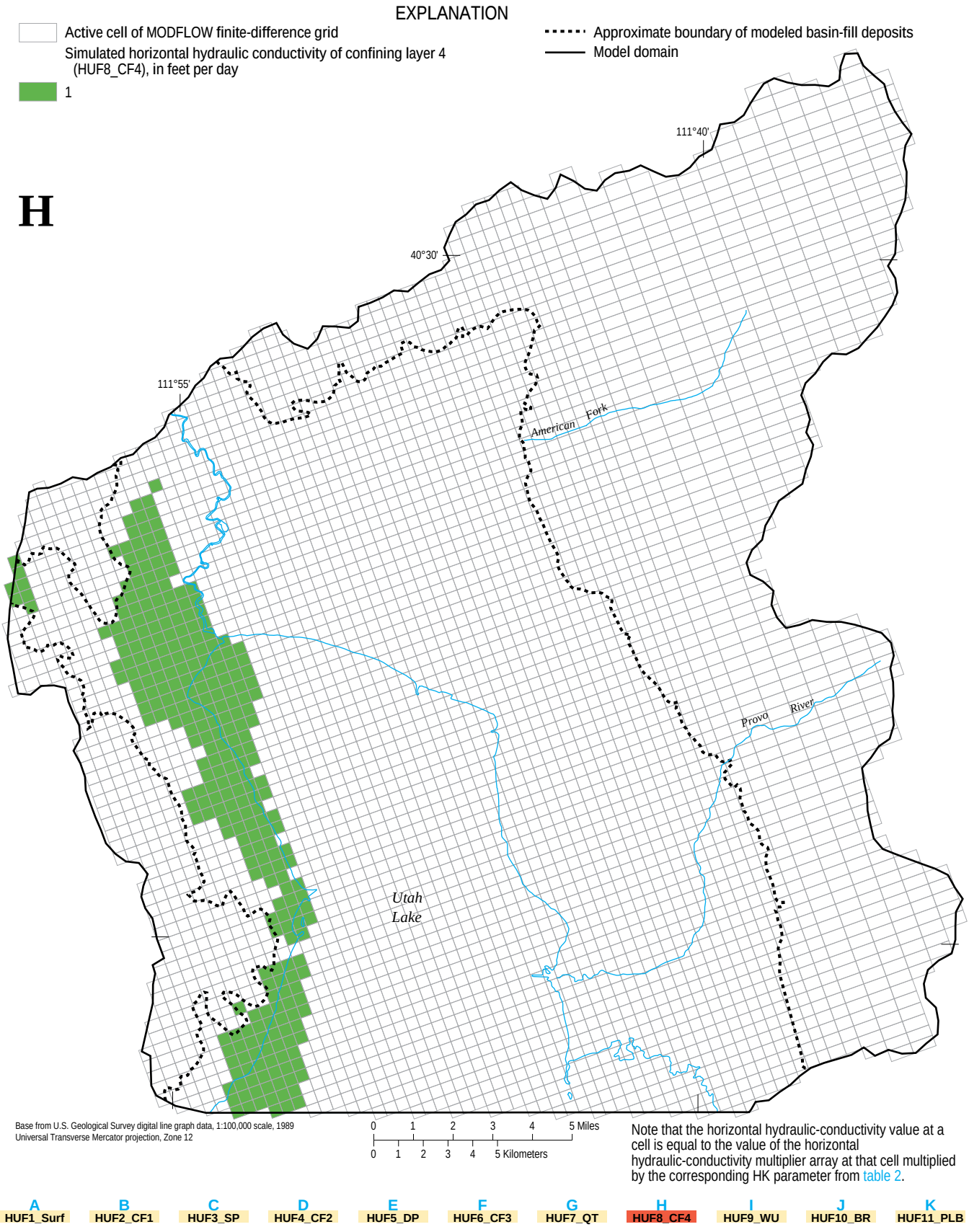

Figure 11h. Simulated horizontal hydraulic conductivity of the hydrogeologic unit HUF8_CF4 simulated with the Hydrogeologic Unit Flow Package in the ground-water flow model of northern Utah Valley, Utah.

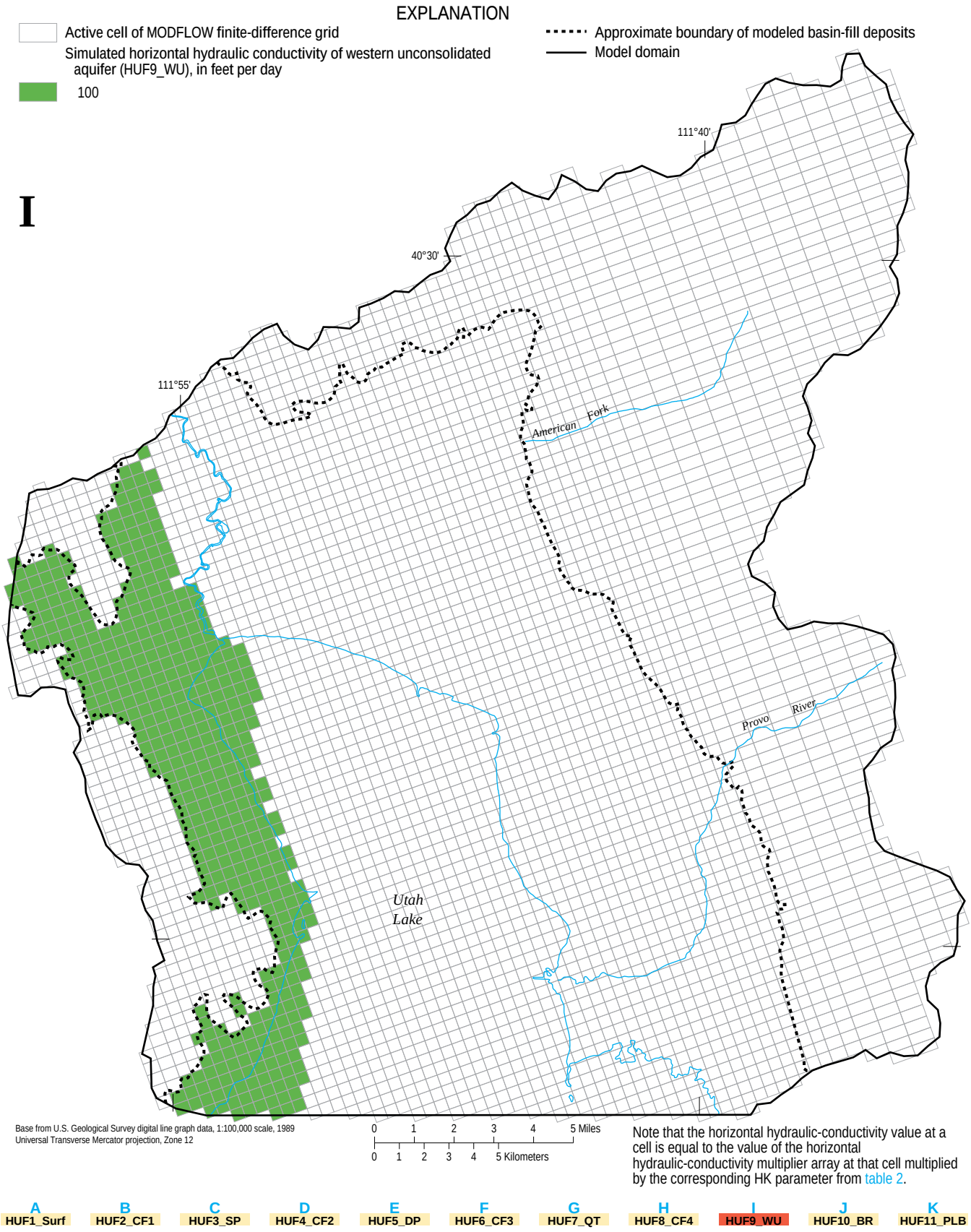

Figure 11i. Simulated horizontal hydraulic conductivity of the hydrogeologic unit HUF9_WU simulated with the Hydrogeologic Unit Flow Package in the ground-water flow model of northern Utah Valley, Utah.

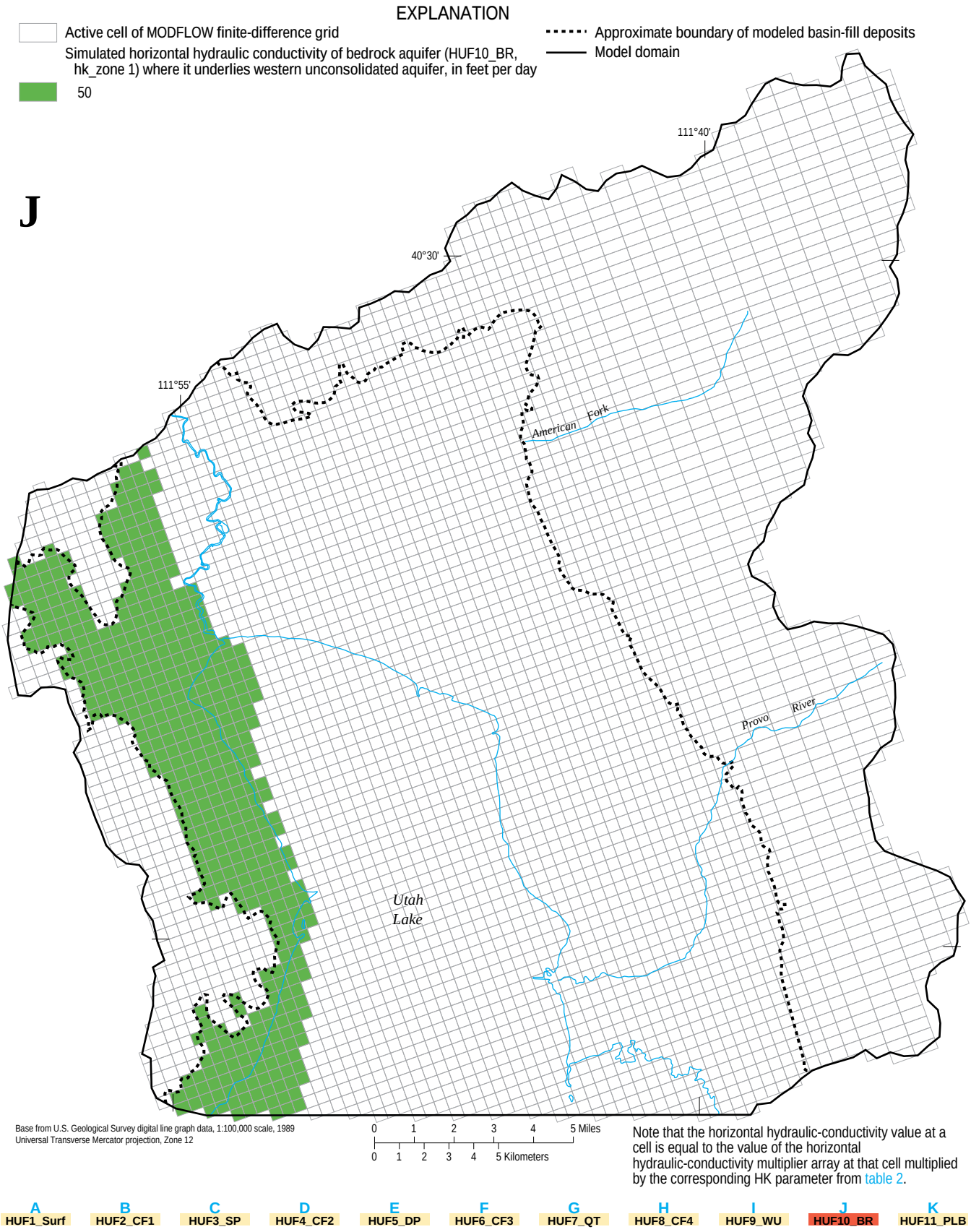

Figure 11j. Simulated horizontal hydraulic conductivity of the hydrogeologic unit HUF10_BR within the basin-fill boundary simulated with the Hydrogeologic Unit Flow Package in the ground-water flow model of northern Utah Valley, Utah.

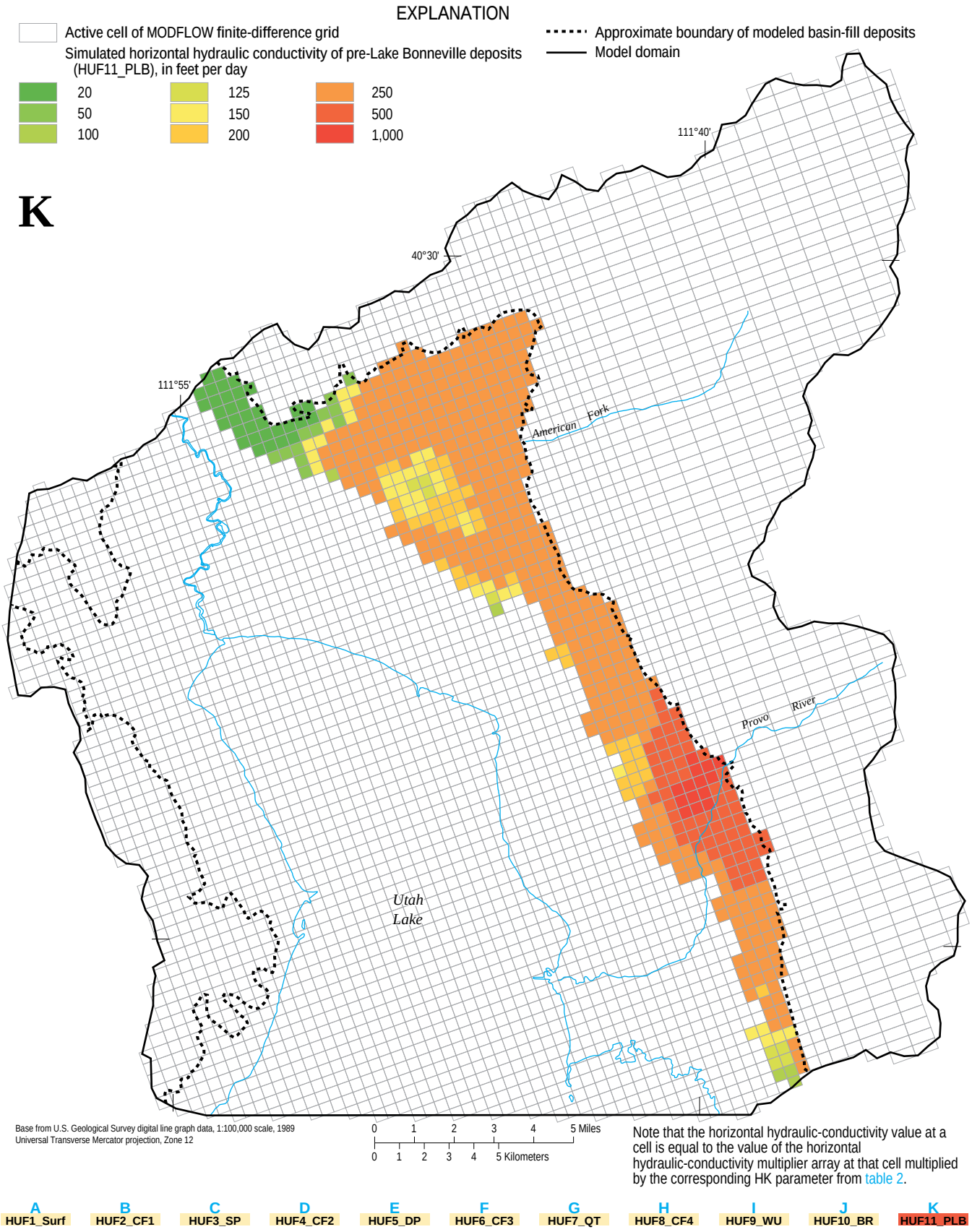

Figure 11k. Simulated horizontal hydraulic conductivity of the hydrogeologic unit HUF11_PLB simulated with the Hydrogeologic Unit Flow Package in the ground-water flow model of northern Utah Valley, Utah.

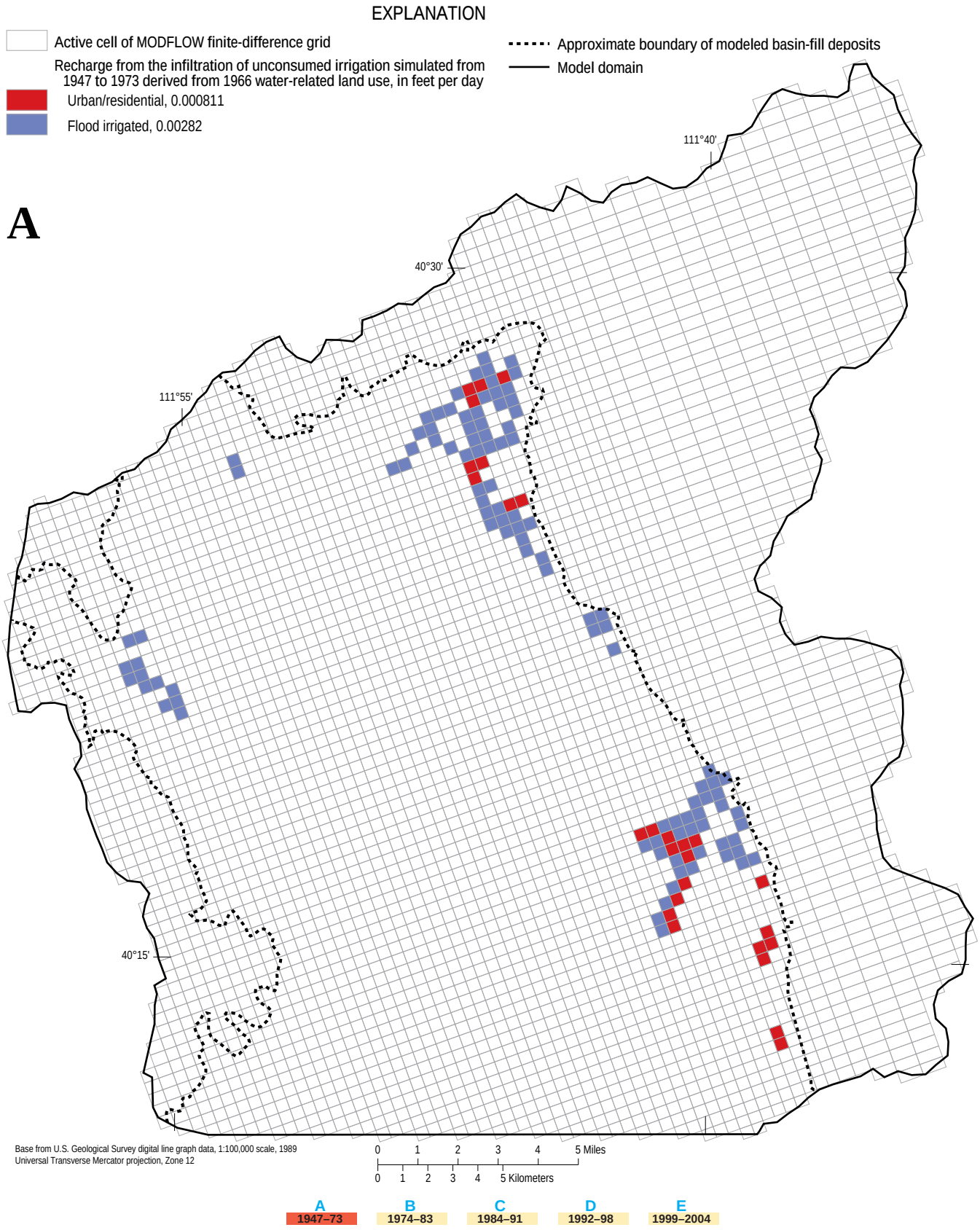

Figure 15a. Simulated recharge as seepage from irrigated fields, lawns, and gardens over the primary valley recharge area during 1947–73 in the ground-water flow model of northern Utah Valley, Utah.

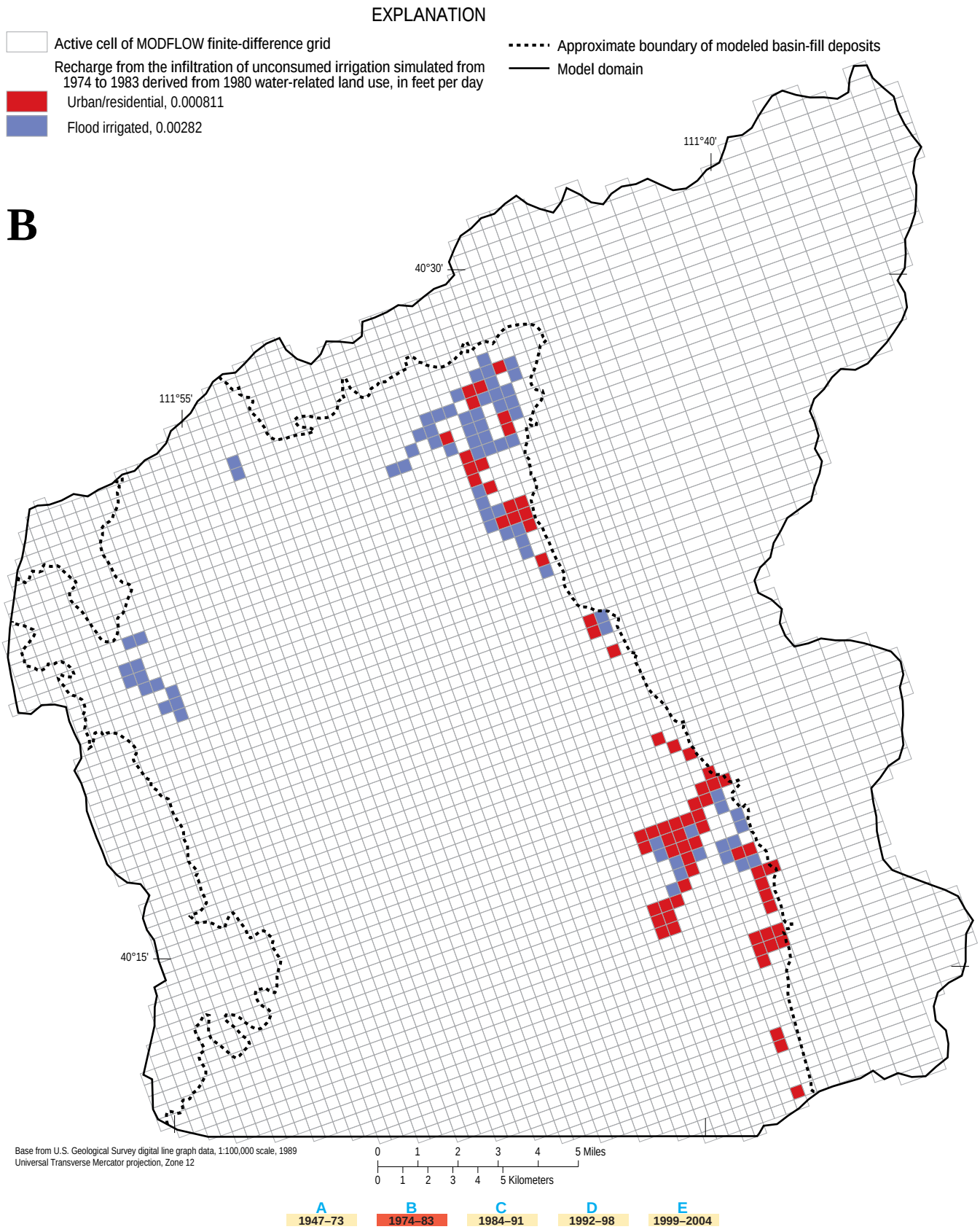

Figure 15b. Simulated recharge as seepage from irrigated fields, lawns, and gardens over the primary valley recharge area during 1974–83 in the ground-water flow model of northern Utah Valley, Utah.

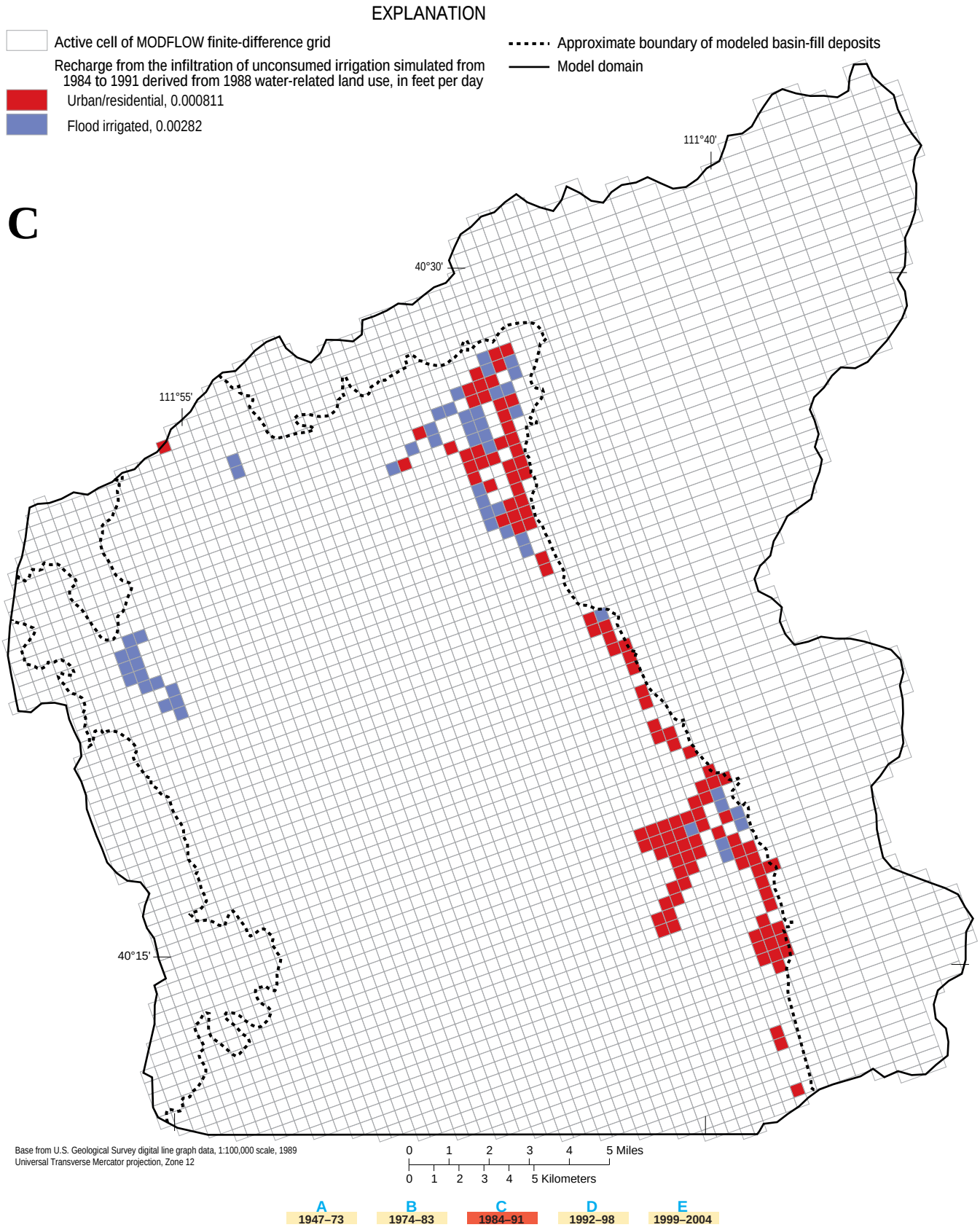

Figure 15c. Simulated recharge as seepage from irrigated fields, lawns, and gardens over the primary valley recharge area during 1984–91 in the ground-water flow model of northern Utah Valley, Utah.

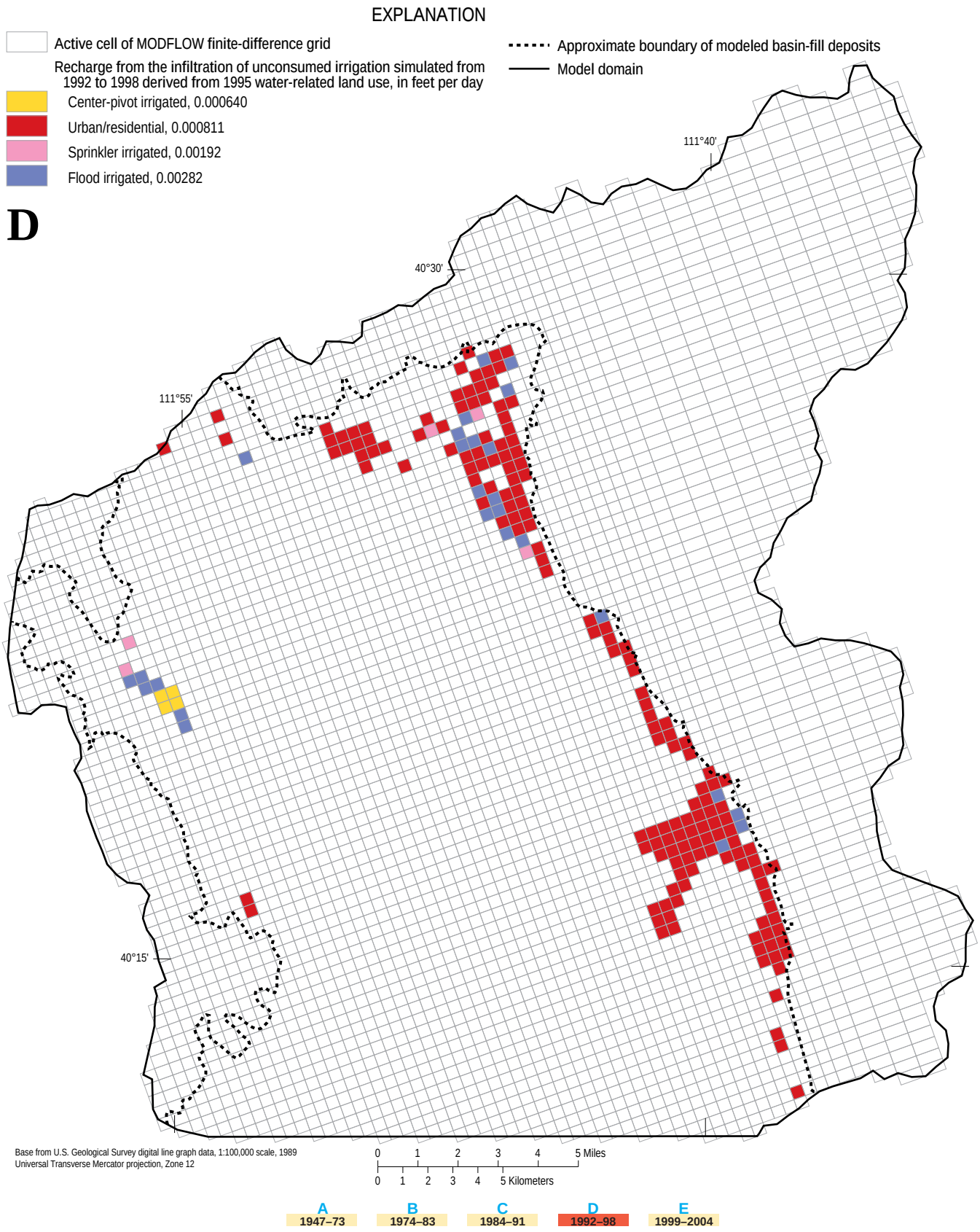

Figure 15d. Simulated recharge as seepage from irrigated fields, lawns, and gardens over the primary valley recharge area during 1992–98 in the ground-water flow model of northern Utah Valley, Utah.

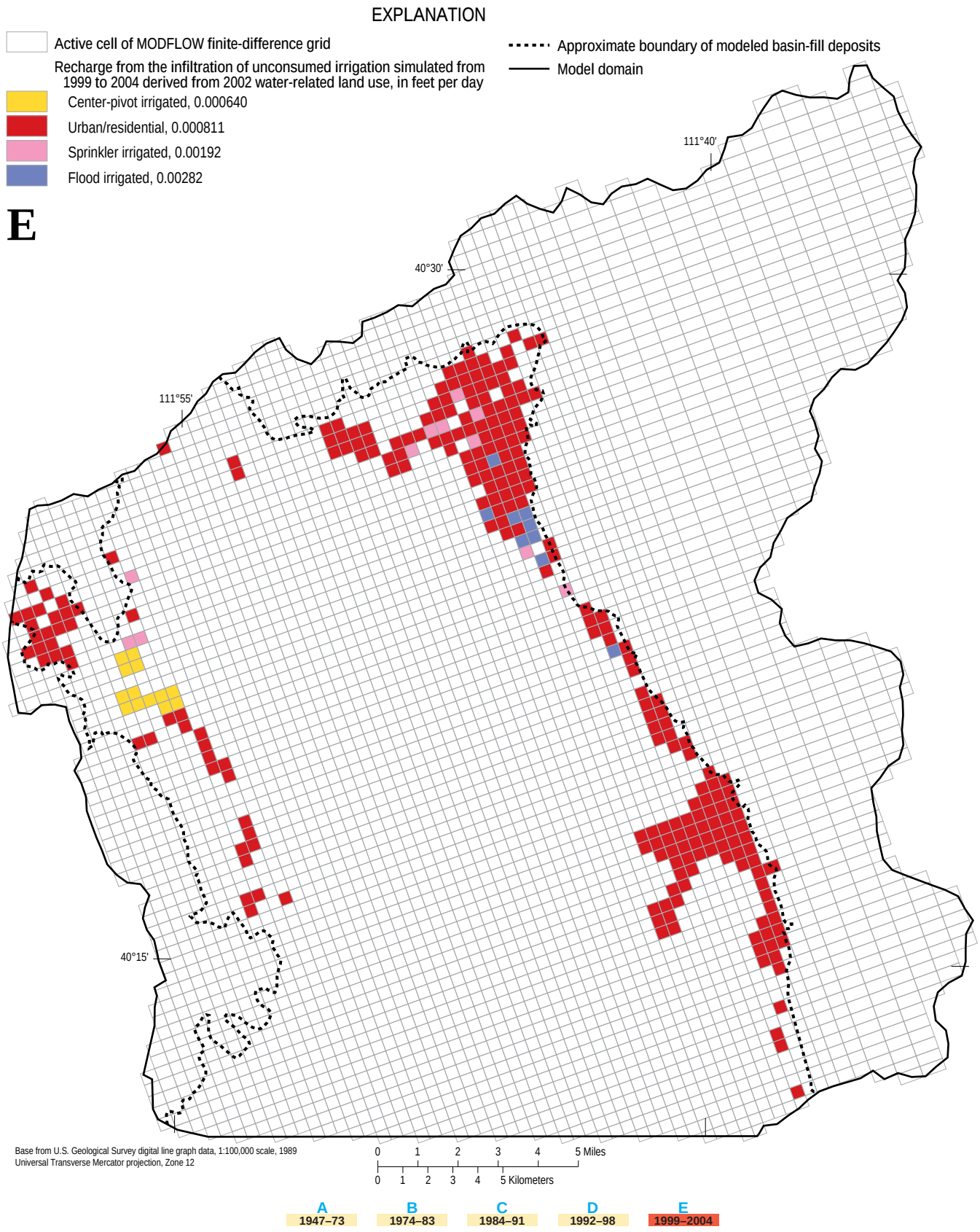

Figure 15e. Simulated recharge as seepage from irrigated fields, lawns, and gardens over the primary valley recharge area during 1999–2004 in the ground-water flow model of northern Utah Valley, Utah.